Klonierung und Expressionsanalyse des BMP-Antagonisten ‘Chordin’ in Amphioxus

Dem Fachbereich für Biologie, Chemie und Pharmazie der Freien Universität Berlin vorgelegt als

DIPLOMARBEIT

von Christoph Wiegreffe

Berlin, Dezember 2005

Die vorliegende Arbeit wurde in der Arbeitsgruppe „Evolution and Development“ der Abteilung „Vertebrate Genome Analysis“ des Max-Planck-Instituts für Molekulare Genetik, Berlin in der Zeit vom 13. April 2005 bis 13. Dezember 2005 angefertigt.

Gutachter: Prof. Dr. Hans Lehrach
Department Vertebrate Genome Analysis
Max-Planck-Institut für Molekulare Genetik, Berlin

Prof. Dr. Horst Kreß
Institut für Genetik
Fachbereich Biologie, Chemie und Pharmazie, Freie Universität Berlin

DANKSAGUNG

Ich möchte mich für die Möglichkeit der Durchführung meiner Diplomarbeit am Max-Planck-Institut für Molekulare Genetik sowie für die Begutachtung meiner Arbeit bei Herrn Prof. Dr. Hans Lehrach bedanken. Ebenso bedanke ich mich Herrn Prof. Dr. Horst Kreß für die Begutachtung der Arbeit.

Besonderer Dank geht an Dr. Georgia Panopoulou für die Betreuung meiner Diplomarbeit und die Verbesserungsvorschläge während der Schreibphase.

Für ihre Hilfsbereitschaft und die angenehme Arbeitsatmosphäre möchte ich allen anderen Mitgliedern der "Evolution and Development" Gruppe danken: Dr. Albert J. Poustka, Dr. Detlef Groth, Alexander Kühn, Vesna Weise, Maryam Zadeh-Khorasani, Christoph Seifert, Clemens Kühn und Andreas Hirsch.

Ich möchte mich außerdem bei meiner Familie und meinen Freuden für die Unterstützung bedanken, die Sie mir während des gesamten Studiums entgegengebracht haben. Am allermeisten danke ich Juliane für Ihr großes Verständnis, ohne daß ich diese Arbeit nicht überstanden hätte.

Für Emma

ZUSAMMENFASSUNG

Wir haben ein Amphioxus-Gen kloniert, das für Chordin kodiert. Die isolierte cDNA wurde mit mittels vergleichender Analyse der Proteinarchitektur und phylogenetischen Analysen als eindeutig ortholog zu Chordin erkannt. Die genomischen Organisation des Amphioxus-Gen ähnelt der des Wirbeltier-Chordin stärker als der des Chordin aus *Ciona intestinalis* oder *Drosophila melanogaster*. Amphioxus-Chordin ist im Organisator, in der Chorda und in der Neuralplatte exprimiert. Ich postuliere, daß diese neurale Expression ursprünglich in allen Chordaten vorhanden war und in der Wirbeltierlinie verloren gegangen ist. Wirbeltiere haben demnach die neural-spezifische Expression von Chordin abgeleitet und gebrauchen dieses Gen lediglich um neurales Gewebe zu induzieren. Maternales β-catenin ist in Wirbeltieren notwendig für die Induktion von Chordin, und Lithium ist bekannt dafür Wnt/β-catenin Signale zu verstärken. Wir haben Lithium dazu verwendet um herauszufinden, ob Chordin durch denselben Signaltransduktionsweg in Amphioxus reguliert wird und um den Effekt zu beschreiben, den Lithiumchlorid auf die Entwicklung von Amphioxus hat. Ich konnte feststellen, daß in mit Lithium behandelten Amphioxus Embryonen die Expression von Chordin verringert wurde, und sich am animalen Pol in einer noch undifferenzierten Zellschicht befindet. Daher schien die neurale Differenzierung durch die Behandlung gehemmt worden zu sein. Die Expressionsanalyse einer Reihe Organisator-spezifischer Gene mittels „whole mount“ *in situ* Hybridisierung zeigte, daß sich in Amphioxus eine Organisator-ähnliche Struktur während der Gastrulation ausbildet. Dieser Struktur scheint jedoch während der Gastrulation eher eine Toleranzfunktion als eine instruktive Rolle zuzukommen, weil Organisator-spezifische Gene auch schon vor ihrer Bildung aktiv sind. Der Effekt von Lithium auf die Expressionslevel von Organisator-spezifischen Genen und solchen, die an die Ausbildung der dorsoventralen Achse beteiligt sind, wird diskutiert.

Cloning and Expression Analysis of the BMP Antagonist ‚Chordin' in Amphioxus

ABSTRACT

We have isolated a cDNA for the amphioxus ortholog of Chordin. This cDNA codes for a true Chordin ortholog as verified by domain structure comparisons and phylogenetic analysis. The genomic organisation of the amphioxus Chordin resembles that of the vertebrate Chordins more than the Ciona intestinalis or the Drosophila Chordin. The amphioxus Chordin is expressed in the organizer, the notochord and at the neural plate. This neural expression of Chordin, which cannot be found in vertebrates, is proposed to be ancestral for the chordates. Vertebrates have lost this neural-specific expression of Chordin and only use it to induce neural tissue. In vertebrates maternal beta-catenin is necessary for the induction of Chordin. We have used lithium, which is known to upregulate Wnt/β-catenin signaling, to analyze whether Chordin is regulated through the same pathway in amphioxus but also to define the effect that lithium chloride has on the amphioxus embryonic development. I observed that in lithium treated amphioxus embryos the Chordin expression became reduced and localized at the animal pole in an undifferentiated outer layer. Neural differentiation seemed to become delayed by the treatment. The expression analysis via whole mount *in situ* expression patterns of a number of organiser genes showed that amphioxus possesses an organizer-equivalent structure during gastrulation. However, it seems this region has more of a permissive than an instructive role because organizer-specific genes are expressed before the organiser domain is actually formed. The effect of lithium on the level of expression of organizer-specific genes and those involved in dorsoventral axis specification is discussed.

TABLE OF CONTENTS

INDEX OF FIGURES

INDEX OF TABLES

1 INTRODUCTION

The cephalochordates, also known as lancelets or as amphioxus (the meaning of the name being: both ends pointed), are small marine chordates of up to 6 cm in length. This small branch of the animal kingdom comprises about 22 species (Poss and Boschung 1996) grouped into two taxa, *Branchiostoma* and *Epigonichthys*, that burrow in the sands of subtropical and temperate oceans in depths of 3 to 8 m worldwide. The synonym Acrania (animals without a cranium) demarcates them from the Craniota (animals with a cranium or vertebrates) with who they share close similarities such as in the musculature, the vascular system, and the position of a liver. Since their first description by Pallas (1774), lancelets have been studied extensively since the 1900s at the morphological, embryological, physiological, and ecological level (Kowalevski 1867; Conklin 1932). Because of its phylogenetic position and basic chordate morphology, its fast and simple mode of embryonic development, and because of its small genome, amphioxus has emerged as an important model organism for the study of vertebrate origins and evolution (Stokes and Holland 1998; Holland et al. 2004). Being so similar to lower vertebrates and having fewer genes (each amphioxus gene being the single ortholog of multiple vertebrate genes), studying the amphioxus genes will enable us to understand faster the function of vertebrate genes.

1.1 The morphology and phylogenetic position of amphioxus

Amphioxus, the closest living invertebrate relative of the vertebrates (Wada and Satoh 1994), closely resembles the vertebrate body plan as it possesses a notochord, a hollow dorsal neural tube, segmented muscle blocks (called myomeres), a perforated pharyngeal region, and a muscular post anal tail. An unpaired median fin runs from the anterior tip of the notochord dorsally over the tip of the tail to the ventral atrioporus, the opening of the atrial cavity (Figure 1-1). The obvious

notochord ends at the anterior and posterior tips of the body and consists of a longitudinal series of disc-shaped cells or plates, each having unusually thick myosin filaments running transversely from left to right (Flood et al. 1969). This unique differentiation makes contractions of the notochord possible contributing as an antagonist to the lateral muscles when amphioxus swims or burrows.

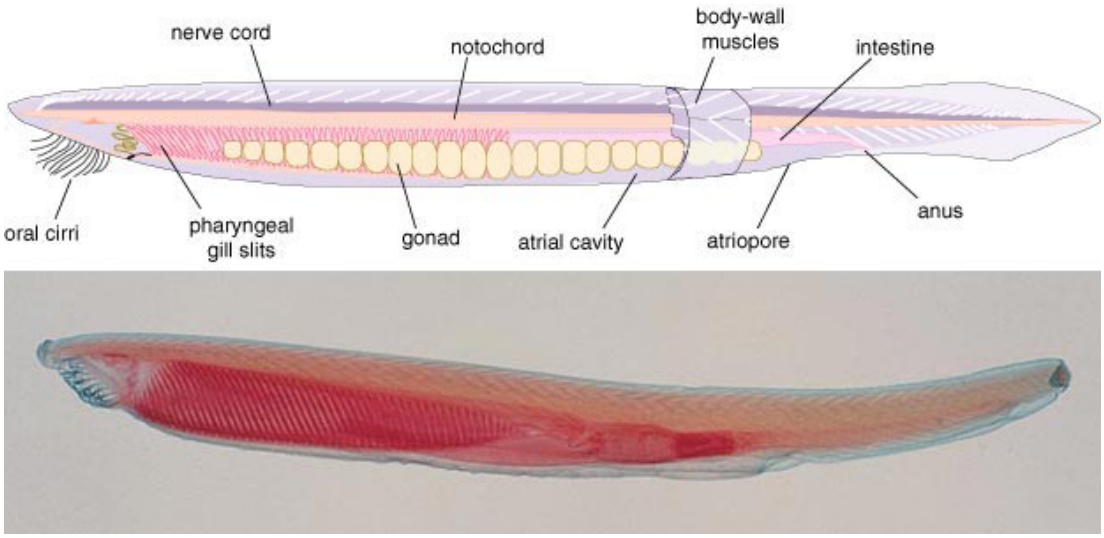

Figure 1-1. The general appearance of the cephalochordate *Branchiostoma floridae*.
Anterior is at left. In the drawing the muscle segments (violet) have been removed from most of the animal's surface to reveal internal organs. The photograph shows a fixed and stained adult (from Stokes and Holland 1998).

1.1.1 Current deuterostome phylogeny

The Cephalochordata belong to the phylum Chordata, together with the Tunicata and the Vertebrata. Several distinctive morphological characters are shared between cephalochordates, tunicates, and vertebrates at some point during their life time. The most important chordate features are a notochord, a dorsal hollow nerve cord, pharyngeal gill slits, and a muscular post anal tail. The vertebrates comprise the hagfish (Myxinoidea), the lampreys (Petromyzontoidae), and the jawed vertebrates (Gnathostomata). A cranium, a tripartite brain, and a neural crest are the most important innovations of vertebrate evolution. Morphological and physiological data have supported that lampreys are more closely related to gnathostomes. These include among other things the presence of true vertebrae, a lateral line system, radial muscles in the fins, and hyperosmoregulation (Forey 1984; Maisey 1986; Forey and

Janvier 1993). However, most molecular studies have supported a closer relationship between hagfish and lampreys (Stock and Whitt 1992; Mallat and Sullivan 1998; Kuraku et al. 1999; Furlong and Holland 2002, Takezaki 2003) which together form the Cyclostomata (Figure 1-2; Dumeril, 1806). Morphological characters that are uniquely shared by this taxon are the presence of single median nostril, a circular mouth, and pouch-like gills (Forey and Janvier 1993).

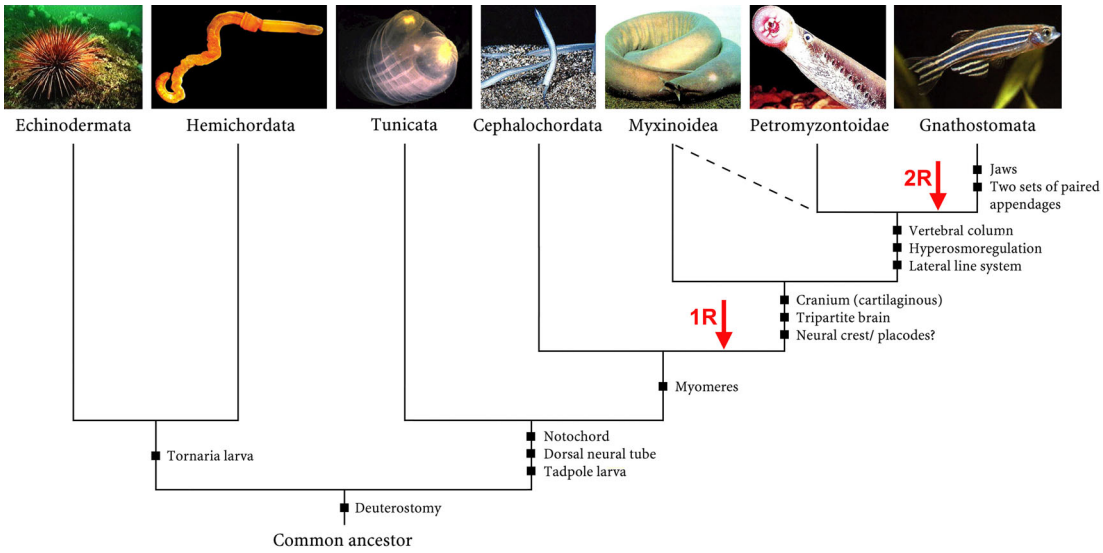

Figure 1-2. The evolution of the chordates.

The chordates comprise the tunicates, the cephalochordates, and the craniates (lampreys and jawed vertebrates). They are thought to have evolved from a common ancestor shared with the non-chordate deuterostomes (the echinoderms and the hemichordates). Recent molecular data support the original classification of hagfish and lampreys into a single taxon known as the Cyclostomata (see text). The red arrows indicate where whole genome duplication events have occurred (see section 1.3).

Traditionally, a closer relationship between the vertebrates and the cephalochordates, to the exclusion of the tunicates, has been supported by the presence of myomeres (Schaeffer 1987), and molecular data have corroborated this view (Turbeville et al. 1994; Wada and Satoh 1994; Cameron et al. 2000; Whinchell et al. 2002). More recent molecular studies suggest a closer relationship between the vertebrates and the tunicates, to the exclusion of the cephalochordates (Zrzavy et al. 1998; Giribet 2000; Oda et al. 2002; Blair and Hedges 2005; Philippe et al. 2005). Because tunicates are regarded as genetically highly divergent organisms (Dehal et al. 2002) and molecular studies might be the result of long-branch attraction biases, the relationships among the three chordate groups (tunicates, cephalochordates, and vertebrates) based on

molecular data remain controversial. The other two non-chordate deuterostome taxa, the Hemichordata and the Echinodermata, are grouped into a single taxon referred to as the Ambulacraria (Metschnikoff, 1869). This pairing has resulted from the recognition of shared tornaria larval characteristics (Nielsen 1997) but also been supported by molecular sequence data (Turbeville et al. 1994; Wada and Satoh 1994; Castresana 1998; Cameron et al. 2000; Furlong and Holland 2002; Winchell et al. 2002). *Xenoturbella* might be a fourth taxon belonging to the supertaxon of deuterostomes. Bourlat et al. propose that *Xenoturbella* is closely related to the echinoderms and hemichordates (Bourlat et al. 2003). Deuterostomes generally develop only the anus from the blastopore, the mouth forming as a secondary opening (deuterostome = "second mouth").

1.1.2 Body part homologies between amphioxus and vertebrates

One of the best-known examples of homologous structures between vertebrates and amphioxus is the homology between the vertebrate thyroid gland and the endostyle of amphioxus. The endostyle is a glandular portion of the endoderm on the right side of the pharynx that, during metamorphosis, is remodelled into a mid-ventral groove running along the floor of the pharynx. Its homology with the vertebrate thyroid gland was first proposed by Müller (1873) and has gained additional support ever since. Both structures derive from the pharynx, metabolize iodine to form iodothyronines, and synthesize similar thyroglobulins (see references in Holland 1999). In addition, homologs of vertebrate genes involved in thyroid development can also be found in amphioxus. For example, *Pax8* is a thyroid marker in vertebrates (Plachov et al. 1990), and its amphioxus homolog (*AmphiPax-2/5/8*) is an endostyle marker in amphioxus (Kozmik et al. 1999). Similarly, the vertebrate thyroid marker *Nk2.1* has an amphioxus homolog (*AmphiNk2.1*) that is expressed in the developing endostyle (Venkatesh et al. 1999). Together, these data strengthen the previously proposed homology between the endostyle in amphioxus and the vertebrate thyroid.

As a second example of homologous structures, I want to mention the homology of the vertebrate brain and the central nervous system (CNS) of amphioxus, which is based on conflicting ideas that arose during the 19th century (Steida 1873; Huxley 1874; Schäfer 1880). In more recent years, studies of amphioxus neuroanatomy and developmental genetics have supported each other and presented a more consistent picture that suggests that the dorsal hollow nerve cord of amphioxus, from anterior to posterior, comprises a diencephalic forebrain, a midbrain, a hindbrain, and a spinal cord. Therefore, the telencephalic forebrain appears to be an evolutionary novelty of the vertebrates (Shimeld and Holland 2005) that evolved most probably with the first appearance of mobile predators during the Cambrian Period (Wicht and Lacalli 2005).

A third example concerns the evolutionary origin of the definite neural crest. During vertebrate development, the neural crest arises from cells between the neural plate and the non-neural ectoderm. After these cells are internalized by neurulation they migrate, mostly as individuals, within the embryo and differentiate into a wide variety of cell types, including peripheral nervous system neurons and pigment cells. Although amphioxus lacks a definite neural crest, a cell population with properties corresponding at least in part to those of neural crest cells do exist in amphioxus, possibly representing an evolutionary source of the vertebrate definite neural crest. During amphioxus development, cells that are located at the edges of the neural plate migrate over it and subsequently fuse at the dorsal side resembling superficially the migratory behaviour of neural crest cells. Most importantly, these cells express genes whose homologs in vertebrates are key markers of premigratory and migratory neural crest cells (reviewed in Holland and Holland 2001).

1.1.3 Early chordate fossils

The oldest chordate fossils that have been found to date are from deposits of the Cambrian Period (545-490 million years ago). The fossil records of two famous fossil Lagerstätten (assemblages of extraordinarily preserved fossil organisms) - the Burgess Shale of Western Canada and the Chengjiang deposits in Southwestern China - have yielded important information on the evolution of chordates during the

Cambrian Period, a time when most of the major groups of animals first appear in the fossil record.

The Middle Cambrian *Pikaia* of the Burgess Shale is generally accepted as a primitive chordate with cephalochordate affinities (Figure 1-3A; Conway Morris 1982). Another cephalochordate, the Lower Cambrian *Cathaymyrus* of the Chengjiang fauna, predates *Pikaia* by another ten million years (Figure 1-3C; Shu et al. 1996). The chordate affinities of the lower Cambrian *Yunnanozoon* and *Haikouella* are being discussed controversially. Although originally interpreted as the immediate sister groups of the vertebrates (Chen et al. 1995), these animals from the Chengjiang fauna have been described as craniates (Chen et al. 1999; Holland and Chen 2001; Mallat and Chen 2003), as hemichordates (Shu et al. 1996), or as members of a deuterostome stem-group (Shu et al. 2003a). At present two main views predominate: *Yunnanozoon* and *Haikouella* may be more closely allied with vetulicolians, which may be stem deuterostomes, or they may be more closely related to craniates and represent an intermediate form between craniates and cephalochordates.

Fossils of agnathan origin have also been found in Chengjiang deposits (Janvier 1999; Shu et al. 1999). *Haikouichthys* (Fig. 1-3B) is a hagfish-like creature with anterior eyes, zig-zag-shaped muscle blocks, a cartilaginous skull, gill arches, a heart, fin support, and metameric gonads. Initially, it has been identified as being closely related to lampreys (Shu et al. 1999b), and later as a stem-group vertebrate or as the sister-group to all other vertebrates except hagfishes, depending on whether the character "metameric gonads" was included in the analysis (Shu et al. 2003). Finally, the segmented vetulicolians with putative gill slits are another enigmatic taxon of the Early Cambrian which Shu et al. proposed to be the most primitive deuterostomes (Shu et al. 2001) together with the yunnanozoans.

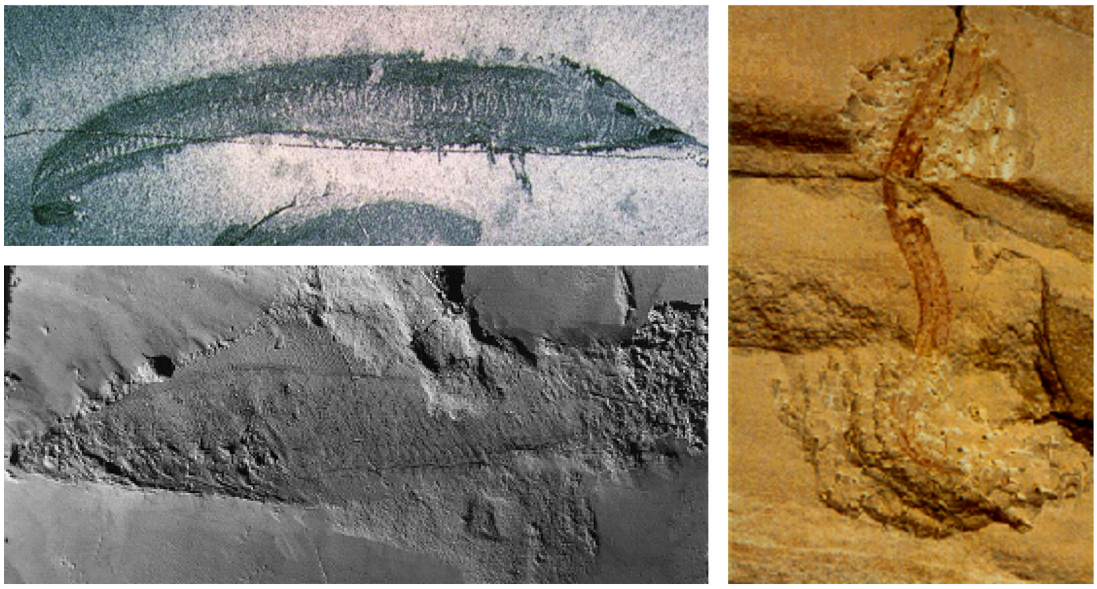

Figure 1-3. Chordate fossils from the Lower and Middle Cambrian Period.

In (a) and (b) anterior is to the left and the dorsal site up; in (c) anterior is up. (a) *Pikaia*, a primitive chordate from the Middle Cambrian Burgess Shale fauna (515 million years ago). (b) *Haikouichthys*, an agnathan vertebrate from the Lower Cambrian Chengjiang fauna (530 million years ago). (c) *Cathaymyrus*, a primitive chordate from the Lower Cambrian Chengjiang fauna (530 million years ago). (Pictures taken from Shu et al. 1999, John 1995, and Shu et al. 1996 for (a), (b), and (c), respectively)

These findings imply that the evolution of vertebrates had been well advanced by the early Cambrian with the chordates arising from more primitive deuterostomes in even earlier times (Ediacaran Period: 630-542 million years ago). This viewpoint is corroborated by a putative fossil tunicate (Shu et al. 2001) and two primitive ancestral echinoderm forms (Shu et al. 2004) from Chengjiang that imply the contemporary existence of all deuterostome forms, as we know them from extant taxa, during the Early Cambrian.

1.2 The embryology of amphioxus

The early development in amphioxus resembles that of echinoderms, while later the development is close to that of vertebrates. In natural populations of *B. floridae* the females spawn about once every two weeks from May until September. Before spawning, the eggs undergo meiotic maturation and arrest at second meiotic metaphase, with the first polar body attached to the animal pole surface of the egg.

The spawning generally occurs during the evening of that same day (Holland and Yu 2004). Each sex of *B. floridae* has 26 gonads on each side of the animal. The ripe gametes are freed from the gonads by rupture of their wall and are flushed out via the atrioporus. The females spawn 500 to several thousand eggs, depending on the size of the animal. The eggs are fertilized externally, and develop into free-swimming, fishlike larvae.

1.2.1 Fertilization and early cleavages

Within one minute after sperm entry, a cortical granule exocytosis occurs around the whole egg surface to create a fertilization envelope, which lifts away the first polar body. After the male and female pronuclei have fused to form the 2n zygote, the second polar body is being extruded from the egg and replaces the first polar body, marking approximately the animal pole of the animal-vegetal embryo axis (Whittaker 1997).

After fertilization, the alecithal eggs of amphioxus show a perfect demonstration of holoblastic cleavage. The first two cleavages in amphioxus are meridional but at right angles to each other resulting in four adjacent blastomeres of equal volume. The third cleavage is equatorial and divides the blastomeres unequally into two sets of blastomeres - an animal quartet of micromeres and a vegetal quartet of macromeres (Figure 1-4b). The micromeres contain about one-third and the macromeres two-thirds of the cytoplasm of the mother blastomere (Conklin 1932). The following cleavages are roughly synchronous in time up through the seventh cleavage. At the 32-cell stage (fifth cleavage) the developing embryo is a solid ball of cells consisting of four stacked, discernable octets of cells (Figure 1-4c). The blastocoel appears after the sixth cleavage as a small cavity in the center of the cell mass and enlarges during the next two cleavages (Figure 1-4d). The eight cleavage marks the beginning of the blastula stage. The cells of the animal hemisphere are flagellated and the blastula rotates within the fertilization membrane. The amphioxus development up to the blastula stage is ordinarily deuterostomal, superficially resembling the early development of echinoderms. The chordate affinities first become apparent through gastrulation and neurulation.

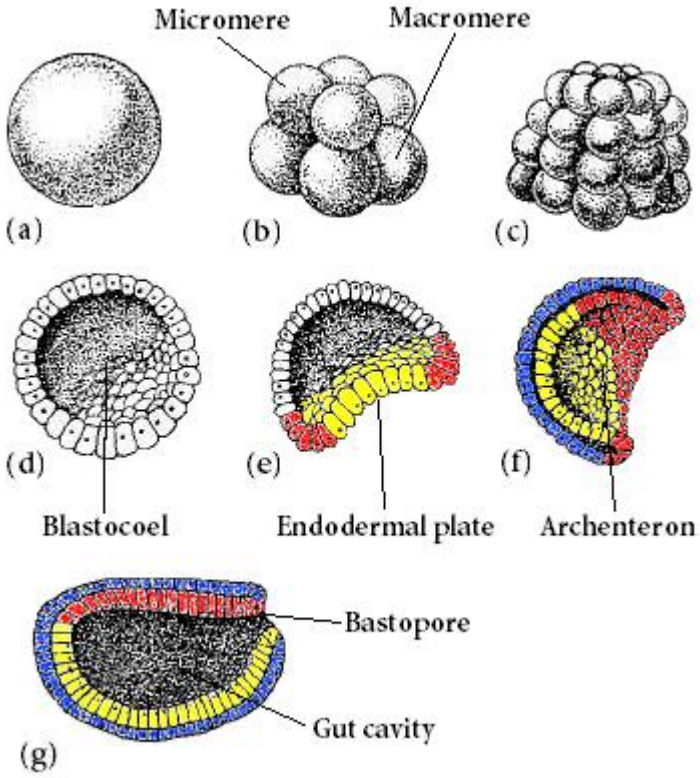

Figure 1-4. The early development of amphioxus up to late gastrula stage.

The germ layers are marked in different colours. The endoderm is yellow, the mesoderm is red and the ectoderm is blue (modified from Benton 2004).

1.2.2 The gastrula stage

At the beginning of the gastrulation the cells of vegetal zone of the blastula flatten into an endodermal plate (Figure 1-4e). This plate soon invaginates gradually eliminating the blastocoel and forming the embryonic gut cavity, called the archenteron (Figure 1-4f). The archenteron is surrounded by endoderm and opens to the exterior via the blastopore. The cells of the outer layer will differentiate into ectoderm. During further invagination of the dorsal and lateral lips of the blastopore presumptive notochord cells and mesodermal precursors give rise to the chordamesodermal plate in the roof of the archenteron. By the late gastrula stage the embryo has become ovoid and slightly flattened with a small posteriodorsal blastopore (Figure 1-4g). The flattened dorsal side of the embryo marks the neural plate, which will develop into a neural tube.

1.2.3 The neurula stage

The neurulation begins with the enclosure of the neural plate. The non-neural ectoderm detaches from the edges of the neural plate and begins to migrate from the caudal end forwards over the dorsal side of the embryo (Figure 1-5a). The neural plate begins to round up as the overlying ectoderm migrates over it. By the mid-neurula stage the non-neural ectoderm has fused dorsally over the embryo and covered the blastopore creating a closed neural tube that opens anteriorly at the neuropore and posteriorly by the neurenteric canal connecting with the gut cavity. However, unlike in vertebrates the neural plate has not rounded up completely at this point. The presomitic grooves, from which the somites will arise, are forming dorsolaterally as outpocketings from the roof of the archenteron (Figure 1-5b). The notochord is also forming axially as an outpocketing from the embryonic gut (Firgure 1-5c). At the late neurula stage the neural plate has completely rounded up to form the proper nerve cord and the somites and notochord have pinched off from the embryonic gut (Figure 1-5d). This is the time of hatching when the young larva with two formed somites begins to swim by ciliary movements in the water column.

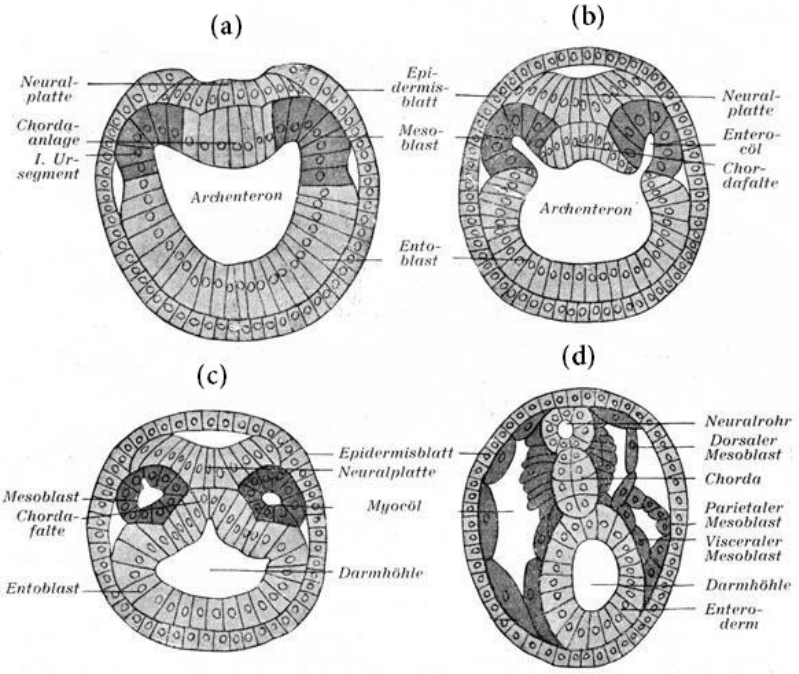

Figure 1-5. Hatschek's depiction of the amphioxus neurulae (1888).

Cross-sections through amphioxus larvae (modified from Brauckmann and Gilbert 2004, originally in Hatschek 1888).

1.2.4 The larval stage and metamorphosis

The larva undergoes major changes in its tissue and organ structure. Only a few of those will be described in the following. The one-day old larva already has approximately 15 somites (for development schedule see Table 3-1). At this time the intersomitic boundaries shift a half-segment between the right and left sides creating an asymmetry that persists into the adult. The larval mouth develops from an endodermal thickening in the left wall of the archenteron and opens laterally by a fusion of the endoderm and the ectoderm. It will eventually migrate during metamorphosis to the velar region as the adult mouth. Similarly, the club-shaped gland develops on the right side of the anterior pharynx but will disappear at metamorphosis. The first left gill slit forms on the ventral midline and migrates to the right side where it fuses with the ectoderm and breaks through the body wall. Several other left gill slits develop similarly, although some remain at the ventral midline. The first right gill slits develop at the proper right side. While the "left" gill slits are migrating to the left, the anus, which initially develops at the right, also migrates to the left side of the midline during metamorphosis. The adult amphioxus has approximately 180 gill slits.

1.3 The amphioxus genome

The amphioxus genome has a haploid content of approximately 570 megabases which is only slightly larger than one of the smallest known vertebrate genomes (*Tetraodon negroviridis*) and about one sixth the size of the human or mouse genome with 3,400 megabases (Gregory 2005). The gene number in amphioxus is about the same as in other invertebrates, such as *Drosophila* (about 15,000 genes). Although a number of cephalochordate lineage-specific gene duplications have been identified, the amphioxus genome lacks the large-scale gene duplications characteristic of vertebrates (e.g. only one Hox cluster). It has been suggested that two genome duplications have occurred at the origin of the vertebrate lineage (known as the 2R hypothesis). According to the 2R hypothesis one genome duplication occurred in the period following the split of the cephalochordate and vertebrate lineages and another

one before the emergence of gnathostomes (see figure 1-3; Holland et al. 1994). Therefore, each invertebrate gene is expected to have at least four vertebrate orthologs. However, the estimation that the human genome might contain as few as 25,000 genes (Venter et al. 2001; IHGSC 2004) has led to the assumption that if there had been whole genome duplications, they must have been followed by extensive gene loss. The analysis of the complete human genome sequence revealed the presence of short genomic segments that exist in duplicates or quadruplicates (termed as paralogous). While it is difficult to date the origin of all segments with the existing methods (e.g. molecular clock) the majority of segments that can be dated were duplicated at the origin of vertebrates at 500-700 million years ago (for a review of the alternative scenarios and evidence for the 2R see Panopoulou and Poustka 2005). Given its phylogenetic position at the root of the vertebrate lineage and the archetypical, unduplicated condition of its genome the amphioxus genome serves as an invaluable source for studying the origin of vertebrate genes and the evolution of the chordate genome.

1.4 Axis formation

The two main axes of bilaterians, the anterior-posterior (A-P) and the dorsal-ventral (D-V) axis, are defined early in embryonic development. Different gene networks are responsible for patterning each axis. For example, the *Hox* genes play an evolutionary conserved role in patterning the A-P axis of all bilaterians (Slack et al. 1993). *Hox* genes represent a subset of the larger family of homeobox containing transcription factors (Duboule 1994). In flies, nematodes, vertebrates, and in the basal chordate amphioxus, *Hox* genes are expressed in ordered domains from the head to the tail and instruct appropriate patterns of cell differentiation (Holland and Garcia-Fernandez 1996; Finnerty and Martindale 1998, De Rosa 1999). Patterning of the D-V axis in both vertebrates and insects depends on the activities of *decapentaplegic* (*dpp*) and *short gastrulation* (*sog*) homologs (Holley et al. 1995; Ferguson 1996). Although both the *Hox* code and the *dpp/sog* system seem to be evolutionary conserved the axis of gene expression of the latter system has been inverted between protostomes and deuterostomes. Gene expression data from the

Nematostella vectensis, a bilateral member of the phylum Cnidaria, provide evidence that both systems were already present before the split of protostomes and deuterostomes (Ferrier and Holland 2001; Finnerty et al. 2004) suggesting that bilateral symmetry may be more ancient than the last common bilateral ancestor.

1.4.1 Molecular players that define the D-V axis in the early embryo

As a result of fertilization cytoplasmic rotation occurs. The Dishevelled protein, a component of the Wnt signaling pathway (Figure 1-6), translocates from the bottom of the egg towards the dorsal side and inhibits glycogen synthase kinase-3-β (GSK3β), that in a multiprotein complex causes phosphorylation mediated degradation of β-catenin, a transcription factor that activates transcription factor genes critical for D-V axis formation (Yost et al. 1996; Larabell et al. 1997; Miller et al. 1999). β-catenin is degraded in ventral cells where Dishevelled is absent. β-catenin forms a complex with Tcf3 which activates *siamois* through binding to its promoter region (Moon and Kimelman 1998). *siamois* is expressed in the Nieuwkoop center immediately after mid-blastula transition (Lemaire et al. 1995). In the absence of β-catenin, Tcf3 inhibits *siamois* expression (Brannon 1997). Siamois activates the expression of *goosecoid* (Laurent et al. 1997), an organizer-specific gene that affects movement of cells that affects movement properties of cells at the dorsal blastopore lip, autonomously determines the dorsal mesodermal fates of the cells expressing it, and recruits neighboring cells into the dorsal axis. However, maximum *goosecoid* expression occurs as a result of a dorsal to ventral gradient of Nodal related proteins (Xnr1, Xnr2, and Xnr4) which is the result of the interaction between VegT and Vg1 signals from the vegetal pole with the dorsally located β-catenin (Germain et. al 2000). Nodal related proteins specify mesoderm so that regions with a high amount of Nodal proteins will become the organizer.

Two signaling centers form simultaneously on the dorsal side soon after zygotic transcription starts both as a result of β-catenin. The Nieuwkoop center expresses mesoderm inducers, such as Xnr1, 2, 4, 5, and 6 (Agius et al. 2000; Takahashi et al. 2000). High levels of Nodals at the gastrula induce dorsal mesoderm (Spemann

oragnizer) in overlying cells while the Nieuwkoop center cells, themselves, form anterior endoderm. In cells above the Nieuwkoop center, the β-catenin signal induces the expression of BMP antagonists, such as *Chordin* and *Noggin*. This region is recently renamed from preorganizer region to BCNE center (blastula Chordin and Noggin expression center). BCNE cells give rise to all of the forebrain, most of the mid and hindbrain, floor plate, and notochord. The BCNE center is involved in neural induction (Kuroda et al. 2004).

The selective localization of β-catenin at one pole of the early embryo has been remarkably conserved among metazoans. After a uniform distribution throughout the cnidarian embryo, β-catenin preferentially accumulates at the oral pole (Wikramanayake 2003). During sea urchin development, β-catenin accumulates in the nuclei of endoderm and mesoderm precursors suggesting that it plays a role in vegetal specification. Prior to the invagination of the archenteron the only cells that remain nuclear β-catenin form a ring peripheral to the archenteron (Logan et al. 1999). Similarly, in amphioxus β-catenin localizes in ectodermal cells with a peak of signaling around the blastopore. As neurulation begins β-catenin also clears from the neural plate suggesting that its down-regulation may be necessary for neural development in amphioxus (Holland et al. 2005).

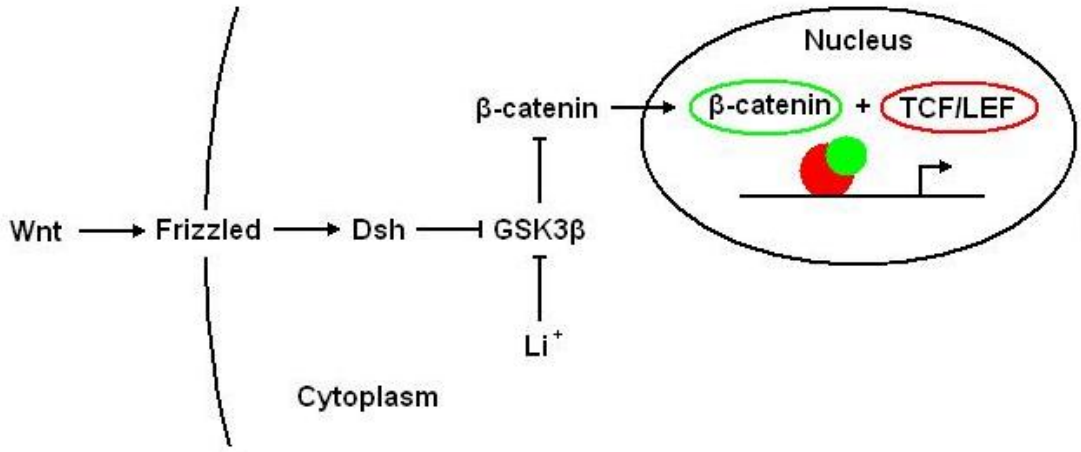

Figure 1-6. The Wnt signaling pathway.

Only the central components of the Wnt signaling pathway are shown. Lithium is thought to inhibit the action of GSK3β.

The molecular players involved in D-V patterning have been characterized by ectopic overexpression (gain of function) or selective knockout (loss of function) of target molecules. In addition, lithium treatment has been used in all species examined so far, to address the role of genes involved in axis formation. Lithium is thought to block the activity GSK3β, thereby releasing β-catenin from the degradation complex and allowing its translocation to the nucleus (Klein and Melton 1996). In vertebrates lithium chloride treatment can lead to a dorsalized/anteriorized or posteriorized phenotype depending on whether the treatment is applied before or after the mid-blastula transition, respectively (Yamaguchi and Shinagawa 1989; Stachel 1993; Roeser 1999).

1.4.1 D-V pattering of the ectoderm is evolutionary conserved

Around the time of gastrulation the embryos of both insects and vertebrates are patterned by two opposed gradients of homologous morphogens from the anti-neural side. The *decapentaplecgic* (*dpp*) gene is expressed dorsally in *Drosophila* and its vertebrate homologs *bone morphogenetic protein (Bmp) 4* and *Bmp2* are localized at the ventral side in vertebrates. These factors are antagonized by the secreted products of the homologous genes *short gastrulation* (*sog*) in *Drosophila* and *Chordin* in vertebrates from the neural side (De Robertis and Sasai 1996; Holley and Ferguson 1997). The site of action where *sog*/*Chordin* expression inhibits *dpp*/*Bmp2/4* corresponds in the fly and in vertebrates to the region of the dorsoventral axis that gives rise to the neuroectoderm. Most strikingly, *sog* and *Chordin* can functionally substitute for each other, which has been shown experimentally by RNA injections in *Xenopus* and *Drosophila* (Holley et al. 1995). Thus, in insects and vertebrates the anti-neural function of Dpp/BMP2/4 and the antagonizing neurogenic potential of Sog/Chordin seem to be conserved with respect to the dorsoventral body axis. Although this molecular system is limited to the ectoderm of *Drosophila* it occurs in both the ectoderm and the mesoderm of vertebrates.

AmphiBmp2/4, the amphioxus gene homolog to *decapentaplegic* of *Drosophila* and *Bmp2* and *Bmp4* of vertebrates, is first expressed in the regions of the hypoblast

where the paraxial mesoderm will form indicating that it might be involved in the earliest stages of somite formation, but not the patterning of the mesoderm at a whole (in fact, until late neurula amphioxus lacks any ventral mesoderm which remains paraxially along the dorsal side). At the early neurula stage, *AmphiBMP2/4* is expressed in the ectoderm except dorsally in the neural plate and adjacent ectoderm (Panopoulou et al. 1998). This pattern indicates that the morphogenetic system establishing the dorsoventral axis of amphioxus acts within the ectoderm. When the ventral side is defined by the location of the mouth, hemichordates express *Bmp2/4* in an ectodermal stripe at the dorsal midline. In a ventral midline ectodermal stripe, *Chordin* is expressed (Gerhard et al. 2005). Thus, hemichordates have a BMP-Chordin axis that is oriented like that of *Drosophila* and the inverse of chordates. While the antineural mechanism involving Dpp/BMP2/4 has been shown to limit the nervous system to one side as in vertebrates and *Drosophila*, it is apparently not acting on the nervous system of the enteropneust hemichordate, which possesses a basi-epithelial nerve net encircling the whole body, as well as a concentration of axon bundles in dorsal and ventral cords. The asymmetric expression of a *dpp* homolog in the cnidarian *Nematostella* (Finnerty et al. 2004) shows that, here too, the anti-neural mechanism does not prevent the formation of a diffuse base-epithelial nerve and suggests that in addition to Dpp/BMP inhibition by Sog/Chordin other factors are involved in the specification of neural fate. In conclusion, the inversion of the Bmp-Chordin axis must have occurred after the split of the ambulacrarians from the chordate lineage and before the split of the cephalochordates from the vertebrate lineage. Developmental genetic studies from amphioxus, tunicates (Miya et al. 1997), and *Drosophila* (Biehs et al. 1996) suggest that only the ectoderm has been patterned by BMP-like morphogens during most of bilaterian evolution, and that vertebrates have evolved a parallel BMP-based system in the mesoderm. In sea urchins the situation is more complex, as BMP signaling occurs in cells of the oral ectoderm, a signaling center with many similarities to the vertebrate organizer, to specify aboral fates (mesendoderm) by means of diffusion (Duboc et al. 2004).

1.4.2 The D-V axis in inverted between arthropods and vertebrates

As an alternative to an inversion of the BMP-Chordin axis during evolution, an inversion of the body itself could explain the inverse relationship between the two morphogen gradients in the early embryos of arthropods and vertebrates. In general, the ventral side of all Bilateria is marked by the position of the mouth and dorsal is on the opposite side of the animal. This arrangement makes direct comparisons of the dorsal sides between bilateral animals possible. The French naturalist E. Geoffroy Saint-Hilaire was the first to propose that the ventral side of the arthropods was homologous to the dorsal side of the chordates (Saint-Hilaire 1822). He dissected a lobster and turned it upside down to its usual orientation to the ground (Figure 1-7). In this orientation the lobster's CNS was located above the digestive tract, which in turn was located above the heart.

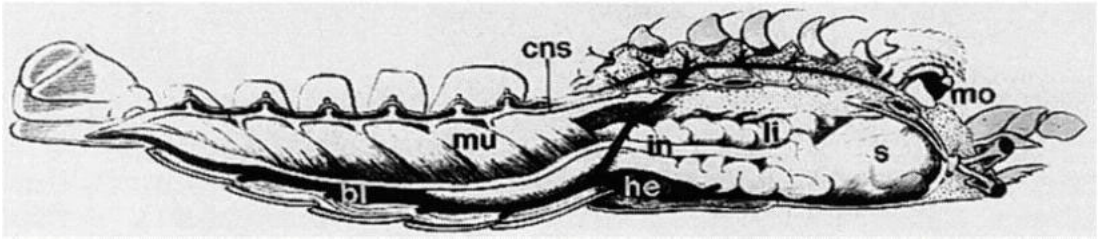

Figure 1-7. Geoffrey Saint-Hilaire's famous lobster
The animal is represented in an orientation opposite to that it would normally have with respect to the ground. The central nervous system (cns) lies above the digestive tract with the stromach (s), the liver (li), and the intestine (in). Below the gut are the heart (he) and the main blood vessels (bl). Muscles (mu) flank the CNS. In this orientation the body plan of the arthropods resembles that of the vertebrates (adapted from De Robertis and Sasai 1996).

In 1875 Dohrn proposed that the last common ancestor of arthropods and chordates was an annelid worm-like animal with a ventral nerve cord, a dorsal heart, and a circulatory system with blood flowing anteriorly in dorsal vessels. This orientation was retained among the evolving members of the protostome lineage but became inverted in the deuterostome lineage, as an ancestor of the chordates inverted its body, sideways over, but retained the same relative organ placements. The nerve cord was now dorsal, the heart ventral, and the blood flowed anteriorly in ventral vessels. The mouth eventually formed on the new ventral side and vanished from the

old location (Nübler-Jung and Arendt 1994). The inversion theory was denounced by Cuvier in 1830 but the idea has been discussed several times since then (Arendt and Nübler-Jung 1994; De Robertis and Sasai 1996).

1.4.3 Alternatives for an inversion of the chordate body axis

Different scenarios for the evolution of a centralized nervous system that do not involve an inversion of the chordate body plan have been proposed (reviewed in Gerhart 2000; Holland 2003; Lacalli 2003). These alternatives have usually favoured a less complex common ancestor of protostomes and deuterostomes. Recently, two hypotheses have gained support from molecular genetic studies on hemichordates, a basal group of the deuterostomes (Figure 1-8) that possess a basi-epithelial nerve net encircling the whole body, as well as a concentration of axon bundles in dorsal and ventral cords.

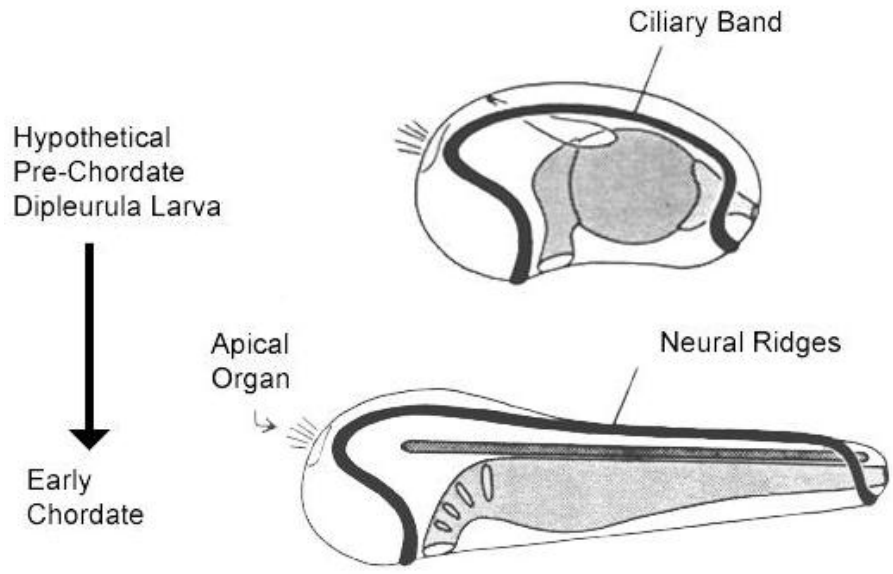

Figure 1-8. Garstang's Auricularia Hypothesis.

The bilateral ciliary bands of an ancestral deuterostome dipleurula-type larva moved dorsally, fused at the midline, and eventually gave rise to the modern chordate CNS (adapted from http://scaa.usask.ca/gallery/lacalli/tutorial/).

In the Auricularia Hypothesis (Garstang 1894, 1928) the origin of the chordate CNS may be found within the ciliary bands of a deuterostome dipleurula-type larval ancestor. Garstang proposed that through a series of evolutionary intermediates the bilateral ciliary rows and the associated nerve net moved dorsally, fused at the midline, and sank inside to form a new dorsal cord, without an inversion (Fig 1-9). Molecular evidence comes from a number of genes that are involved in the development of the chordate CNS and are expressed in the ciliary bands of sea urchins and/or the hemichordate *Ptychodera flava* larvae, including *Otx*, *NK2.1*, and *SoxB3* (Harada et al. 2000; Takacs et al. 2002; Taguchi et al. 2002). However, it has not been shown that the ciliary band derivatives give rise to cells of the adult nervous system after metamorphosis.

The other hypothesis states that the nervous system of the last common ancestor of chordates, hemichordates, and protostomes was organized in a diffuse, body-encircling, basi-epithelial way and became centralized independently in the protostome and deuterostome lines. Lowe et al. (2003) describe the expression pattern of genes in the direct developing hemichordate *Saccoglossus kowalevski* that are responsible for axial patterning of the nervous system in chordates and arthropods. Most surprisingly, the axial patterning genes in *Saccoglossus* are expressed throughout the ectoderm, in a series of domains that encircle the whole body, and their expression patterns are nearly identical to that in vertebrates. A diffuse nervous system can also be found in putative outgroups to the bilateral animals, the cnidarians and ctenophores, and could therefore be an ancient condition of Bilateria. On the other hand an internal ancestral nervous system could have been reverted to the surface in hemichordates due to an adaptation to a burrowing life style (Lacalli 2003).

1.5 BMP-signaling during embryology

BMP morphogen gradients in the gastrulating embryo are interpreted to generate a diverse array of cell fates in all three germ layers. The role of BMPs as ventral/epidermal inducers in the ectoderm has been well established. According to the widely accepted default model of neural induction BMP-inhibition is sufficient to

maintain the 'default state' of the epidermal cells to adopt a neural fate (Figure 1-9; Hemmati-Brivanlou and Melton 1997; Weinstein and Hemmati-Brivanlou 1999; Munoz-Sanjuan and Brivanlou 2002). Despite a vast amount of evidence that extracellular BMP antagonists are sufficient to induce neural tissue in a variety of assays (e.g. Sasai et al. 1995; Xu et al. 1995; Hawley et al. 1995), genetic evidence suggests that neural induction occurs in the absence of extracellular BMP antagonists (reviewed by Stern 2005). The most compelling evidence comes from findings in the chick (Steit and Stern 1999a), where the patterns of gene expression of components of the BMP pathway do not agree with the default model of neural induction (Streit et al. 1998) and misexpression of BMP antagonists in competent epiblast explants does not cause tissues to neuralize (Streit and Stern 1999b). Mice that are double mutant for *Chordin* and *Noggin* still develop a nervous system with anterior neural truncations (Bachiller et al. 2000), suggesting that antagonising BMP signaling by Chordin and related molecules is one key mechanism of neural induction, but that additional signaling events are at work.

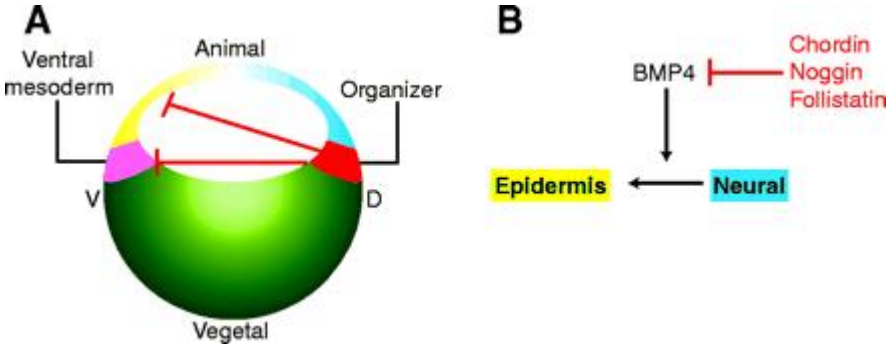

Figure 1-9. The 'default model' of neural induction in *Xenopus*.
(A) A rough fate map of blastula-stage embryo. Prospective territories are organizer in red, ventral mesoderm in pink, neural tissue in blue, epidermis in yellow and yolky endoderm in green. The red lines represent BMP antagonist activity emanating from the organizer. (B) A 'genetic' diagram of the inductive interaction proposed by the model (from Stern 2004).

In ascidians the inhibition of BMP is not involved in neural specification (Darras and Nishida 2001), but instead FGF plays an essential role as a direct neural inducer (Hudson et al. 2003; Bertrand et al. 2003). Here, FGF induces a GATA transcription factor that accounts for the distinct response of animal cells to FGF signaling and targets the neural program to the ectoderm. The involvement of FGF in neural induction has also been suggested in chick and *Xenopus* (Streit et al. 2000; Wilson et

al. 2000; Linker and Stern 2004; Delaune et al. 2005). In the chick the slow induction by FGF of the *Churchill* (*ChCh*) transcription factor in the neural plate in turn directly induces the expression of *Sip1* (*Smad interacting protein 1*), which inhibits mesodermal genes and sensitizes cells to later neural inducing factors (Sheng et al. 2003). Sheng and colleagues demonstrate that the expression of *ChCh* arrests movements of cells through the streak, while loss of *ChCh* leads to continued gastrulation. The authors therefore suggest that neural induction not only involves a decision between neural and epidermal fates but also involves a major fate decision between neural and mesodermal fates, by establishing the boundary that limits cell ingression during gastrulation (Sheng et al. 2003).

As part of a 4-signal model which has been proposed to pattern the vertebrate neural tube dorsoventrally involving FGF, RA, and Shh signaling, the inductive activities of BMPs produced in the ectoderm, overlying the spinal cord, and in the roof plate, pattern the dorsal half of the spinal cord (Wilson and Maden 2005). BMPs in the roof plate can induce dorsal markers and dorsal neuronal subtypes when cultured with intermediate neural plate (Liem et al. 1995; 1997). In zebrafish mutants that have varying degrees of compromised BMP signaling activity, there are corresponding changes in D-V patterning such as loss of dorsal sensory neurons and expansion of interneurons (Barth et al. 1999; Nguyen et al. 2000). These mutants provide good evidence for a concentration-dependent mechanism of BMP action.

BMPs have also been identified as ventrolateral mesoderm inducers in both *Xenopus* and zebrafish embryos (Munoz-Sanjuan and Brivanlou 2001), and there are abundant genetic data to support the notion that BMP signaling is the major determinant of ventral mesendodermal fates during gastrulation. Although the role of BMPs in endodermal patterning is less strong, recent evidence suggests that BMP signaling also promotes ventroposterior fates in the endoderm (Tiso et al. 2002). Therefore, the activities of BMPs appear to act to pattern all three germ layers, the ectoderm, the mesoderm, and the endoderm in vertebrates.

1.5.1 The BMP signaling pathway

BMPs signal through a defined molecular pathway (Attisano and Wrana 2002). Extracellular BMPs bind with weak affinity to type I and type II ligand-specific receptors alone, but with high affinity to typeI/typeII heteromeric complexes (Figure 1-10). Upon BMP-induced heteromeric complex formation, the constitutively active serine/threonine kinase of the type II receptor phosphorylates the type I receptor. The intracellular messenger downstream from the activated receptors are the Smad proteins, which can be divided into three classes: receptor-mediated Smads (R-Smads), that are phosphorylated in a ligand-specific manner by activated receptor complexes, the common mediator Smad (Co-Smad), Smad4, and the inhibitory Smads (I-Smads), Smad6 and Smad7, that negatively regulate the Smad signal transduction pathway. The BMP R-Smads are Smad 1, 5 and 8, and upon phosphorylation by the activated type-I receptor form a complex with Smad4. The heteromeric BMP-regulated Smad complex then translocates to the nucleus where it can bind directly, or through transcriptional partners to specific sequences in the promoters of BMP target genes to regulate transcription.

Smads have been shown to bind directly to GC-rich Smad binding elements within target gene promoters to control gene expression (Karaunalov et al. 2004) and to distinct sequences that can be found as repeated copies in the BMP response elements of the gene promoters of several genes, such as *xVent2*, *xVent2B*, *Msx1*, *Msx2*, *Hex*, and *Smad7* (Hari et al. 2000; Henningfeld et al. 2000; Alvarez Martinez et al. 2002; Zhang et al. 2002; Benchanabe and Wrana 2003; Brugger et al. 2004). Finally, the transcription of BMP genes has shown to be maintained by the activity of BMP protein itself (Biehs et al. 1996; Schulte-Merker et al. 1997)

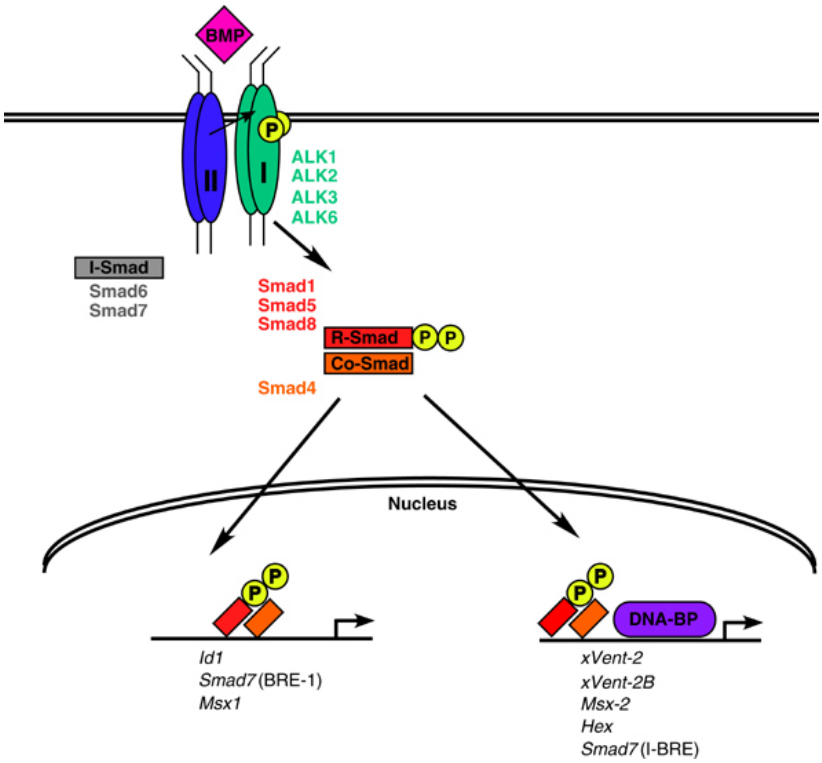

Figure 1-10. The BMP signaling pathway activates two classes of regulatory elements.

BMPs regulate transcription of target elements through direct Smad interaction (left side), and through a canonical pathway including DNA-binding partner proteins (right side). I-Smad, inhibitory Smad; R-Smad, receptor-regulated Smad; Co-Smad, common-mediator Smad; DNA-BP, DNA-binding protein (from Varga and Wrana 2005).

1.5.2 Extracellular modulation of BMP signals by Chordin

The extracellular modulation of BMP signaling is extremely complex (Pearce et al. 1999; Garcia Abreu et al. 2002; Munoz-Sanjuan and Brivanlou 2002) with a network of secreted proteins that set up a graded activation of the bone morphogenetic pathway. The robustness of this morphogen gradient arises from a tight regulation in the extracellular space. A number of secreted BMP inhibitors act to bind BMPs and prevent receptor activation. The majority of the secreted inhibitors, which include Noggin (Smith and Harland 1992; Zimmerman et al. 1996), Chordin (Sasai et al. 1994; Piccolo et al. 1996), Follistatin (Hemmati-Brivanlou et al. 1994; Fainsod et al. 1997), Cerberus (Bouwmeester et al. 1996; Belo et al. 1997), and Xnr3 (Smith et al. 1995; Hansen et al. 1997), have restricted expression domains in dorsal tissues in

vertebrates, and they are thought to act locally to eliminate BMP signals. There are many molecules with Chordin-like repeats (CR-repeats), which supposedly also bind BMPs and are likely to play important roles in the generation of BMP graded signals (Garcia Abreu et al. 2002).

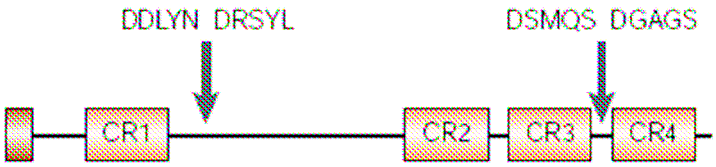

Figure 1-11. Chordin contains cysteine-rich domains and is cleaved by Tolloid/Xolloid.
Chordin is secreted protein of 120 kDa containing four internal cysteine-rich domains (CR1-4), each about 70 amino acids, which bind to BMP molecules and prevent them from binding to their cognate receptors. The signal peptide is indicated by the brown box. The specific zinc metalloprotease Xolloid cleaves Chordin at in two specific sites (indicated by arrows) (from De Robertis et al. 2000).

Chordin (Figure 1-11) is a BMP-antagonist that contains four cysteine-rich domains that bind BMP, blocking its binding to the receptor (Piccolo et al. 1996). The individual CR domains bind to BMPs, although with a tenfold lower affinity than the full-length Chordin (Larrain et al. 2000). This can be explained by the action of Twisted Gastrulation (Tsg) that facilitates the binding of intact Chordin to BMPs (Figure 1-12; Oelgeschläger et al. 2000; Chang 2001; Ross et al. 2001). After a metalloproteinase, called Xolloid, cleaves Chordin at two specific sites restoring the ability of BMP to signal (Marques et al. 1997; Piccolo et al. 1997), Tsg competes the residual activity of the cleaved Chordin fragments to bind to BMPs and facilitates their degradation (Larrain et al. 2000, 2001; Oelgeschläger et al. 2000). Tsg also facilitates the cleavage of Chordin by Xolloid (Scott et al. 2001; Larrain et al. 2001). This molecular pathway, in which Xolloid switches the activity of Tsg from a BMP antagonist to a pro-BMP signal once all endogenous full-length Chordin is degraded, is also acting in *Drosophila* and helps explain how sharp borders between embryonic territories are generated during development (De Robertis et al. 2000).

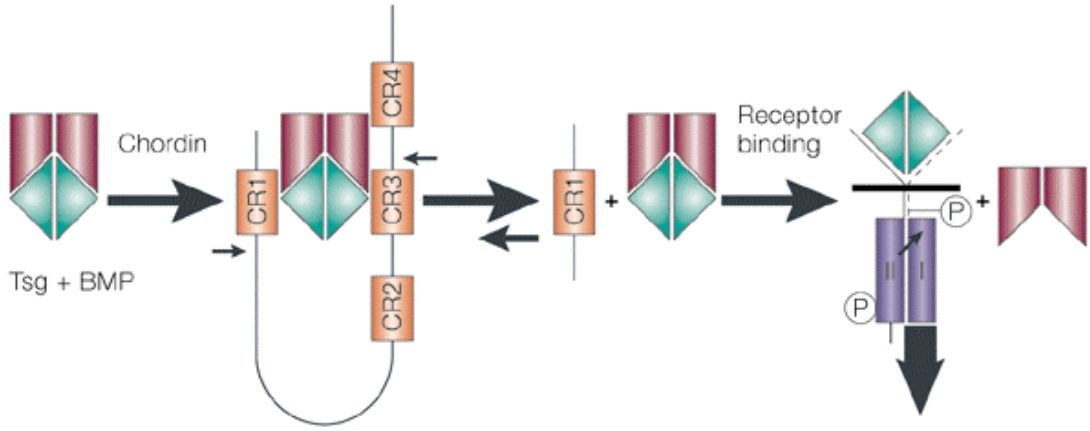

Figure 1-12. A molecular pathway involving BMP, Chordin, Tolloid/Xolloid and Twisted gastrulation

Chordin binds BMP through cysteine-rich domains CR1 and CR3. Twisted gastrulation forms a ternary complex with Chordin and BMP making Chordin a better BMP antagonist. After cleavage of Chordin by Xolloid, residual binding of CR modules to BMP is readily competed by Tsg. The binary complex of BMP and Tsg does not interfere with the BMP receptor. The thick arrows indicate the effects of Tsg on this molecular pathway (from De Robertis et al. 2000).

Recent evidence from studies in the fly by the use of mathematical modeling suggests an additional role for the Dpp/BMP inhibitor Sog/Chordin. Eldar et al. (2002) present a model, in which soluble Dpp or Sog does not diffuse, although Dpp/Sog complexes can diffuse greatly. Therefore, a second role for Sog/Chordin would be to act as a carrier of inactive dpp/BMP molecules to a distant site of action, following cleavage by Tolloid-like proteases. In this model, Tolloid can only cleave Sog/Chordin as part of a complex with Dpp/BMP and Tsg. The degradation of Chordin by the Tolloid protease would allow a peak of BMP signaling away from Chordin producing cells (and not simply a smooth gradient) as is the case for the dorsal midline cells of the *Drosophila* embryo. Consistently, the diffusion of Dpp was dependent on the expression of *sog/Chordin* or *Tsg*, as there was little diffusion of Dpp in flies, mutant for either one of these genes (Eldar et al. 2002). After all, the regulation of BMP signaling likely involves controlling the rates of synthesis, diffusion, degradation, and differential affinity for distinct receptor complexes (Munoz-Sanjuan and Brivanlou 2004).

1.6 The aim of this thesis

Growth factor antagonists have not been described in amphioxus so far. I will isolate the amphioxus ortholog of the BMP-antagonist Chordin and describe its role during embryogenesis via whole mount *in situ* hybridization. As lithium chloride can be used to enhance Wnt/β-catenin signaling by blocking GSK3β the change in expression domain and level of Chordin expression will be investigated in lithium treated embryos. I will also analyze the spatial expression of genes that are downstream of β-catenin and/or are involved in D-V axis specification during early stages of development and study their respond to lithium treatment.

2 MATERIAL

2.1 Technical equipment

Table 2-1. Technical equipment

Name	Company	Model
24 well cell culture microplates	Corning Inc., Corning, NY, USA	Costar® 24 Well TC-Treated Microplate
autoradiography cassettes	Amersham Biosciences Europe GmbH, Freiburg	Hypercassette™ (35 × 43 cm)
bench top centrifuge, small (refrigerated)	Eppendorf AG, Hamburg	Centrifuge 5417 R
bench top centrifuge, large (refrigerated)	Eppendorf AG, Hamburg	Centrifuge 5810 R
blotting membranes	Amersham Biosciences Europe GmbH, Freiburg	Hybond™-N+ (22.2 × 22.2 cm)
centrifugal vacuum concentrator	Thermo Electron Corporation, Milford, MA, USA	SC210A SpeedVac®
cover glasses	Menzel-Gläser GmbH & Co. KG, Braunschweig	Microscope Cover Slips
diamond knife	Delaware Diamond Knives, Wilmington, DE, USA	Diamond Histo Knife
digital microscope camera	Carl Zeiss AG, Oberkochen	AxioCam HR
filter tips	Biozym Scientific GmbH, Oldendorf	SafeSeal-Tips® "Premium"
fixed-angle rotor	Eppendorf AG, Hamburg	FA-45-24-11
gelatine capsules	Carl Roth GmbH + Co. KG, Karlsruhe	Gelatine Capsules
gel documentation	Alpha Innotech Corporation, San Leandro, CA, USA	AlphaImager®
hybridization oven	Binder GmbH, Tuttlingen	BFED 53
image eraser	Amersham Biosciences Europe GmbH, Freiburg	ImageEraser

Name	Company	Model
incubator	Kendro Laboratory Products GmbH, Langenselbold	B6200
incubator shaker	New Brunswick Scientific Co., Inc., Edison, NJ, USA	Innova®44
laser scanning microscope	Carl Zeiss AG, Oberkochen	LSM 510
light microscope	Leica Mikrosysteme Vertrieb GmbH, Bensheim	MZ 8
magnetic stirrer, small	Heidolph Instruments GmbH & Co. KG, Schwabach	MR 3001
magnetic stirrer, large	IKA® Werke GmbH & Co. KG, Staufen	Midi MR 1 digital IKAMAG®
microcentrifuge	Sigma Laborzentrifugen GmbH, Osterode am Harz	Sigma 112
microscope slides	Menzel-Gläser GmbH & Co. KG, Braunschweig	Microscope Slides, Cut Edges
mini centrifuge	LMS Co. Ltd, Tokyo, Japan	GMC 060
optical adhesive covers	Applied Biosystems, Foster City, CA, USA	ABI PRISM® Optical Adhesive Cover
optical reaction plate	PE Applied Biosystems, Foster City, CA, USA	ABI PRISM® Optical 96-Well Reaction Plate
pH meter	Mettler-Toledo GmbH, Giessen	MP220
phosphor imager	Amersham Biosciences Europe GmbH, Freiburg	Storm™820
phosphor screen	Amersham Biosciences Europe GmbH, Freiburg	Mounted, GP (35 × 43 cm)
pipettes	Gilson, Inc., Middleton, WI, USA	Pipetman®P
polyethyleneimine-cellulose sheets	Macherey-Nagel GmbH & Co. KG, Düren	801052
power supply	Bio-Rad Laboratories GmbH, München	PowerPac Basic Power Supply
precision scale	Mettler-Toledo GmbH, Giessen	PB1501
real-time PCR system	PE Applied Biosystems, Foster City, CA, USA	ABI 7900HT

Name	Company	Model
rotor for deepwell microplates	Thermo Savant, Holbrook, NY, USA	MPTR12-210
shacking water bath	Julabo Labortechnik GmbH, Seelbach	SW20-D
spectrophotometer	NanoDrop Technologies, Wilmington, DE, USA	ND-1000
swing-bucket rotors	Eppendorf AG, Hamburg	A-4-62 A-4-81-MTP
thermal cycler	MJ Research, Inc., Watertown, MA, USA	PTC-100™
thermomixer	Eppendorf AG, Hamburg	Thermomixer comfort
thermostat	VLM GmbH, Leopoldshöhe	LS-2V-130
touch mixer	Scientific Industries, Inc., Bohemia, NY, USA	Vortex-Genie®2
ultramicrotome	Reichert-Jung (Leica Mikrosysteme Vertrieb GmbH), Bensheim	Ultracut E
UV transilluminator	Herolab GmbH Laborgeräte, Wiesloch	UVT-28M
video printer	SEIKO Precision GmbH, Hamburg	DVP 1200
water bath	Grant Instruments Ltd, Cambridgeshire, UK	SUB14

2.2 Chemicals, enzymes, and cells

Table 2-2. Chemicals

Name	Company	Catalog no.
2-mercaptoethanol	Merck KgaA, Darmstadt	805740
2-propanol	Merck KgaA, Darmstadt	818766
[α32P]dCTP	Amersham Buchler GmbH & Co KG, Braunschweig	-
agar	BD, Franklin Lakes, NJ, USA	214030
agarose	Invitrogen GmbH, Karlsruhe	15510
ampicillin	Sigma-Aldrich Chemie GmbH, Taufkirchen	A9393
anti-digoxigenin-AP	Roche Diagnostics GmbH, Mannheim	1093274
BCIP	Sigma-Aldrich Chemie GmbH, Taufkirchen	B8503
benzil	London Resin Company, Reading, UK	-
betaine	Sigma-Aldrich Chemie GmbH, Taufkirchen	B2629
blocking reagent	Roche Diagnostics GmbH, Mannheim	1096176
bromphenol blue	Merck KgaA, Darmstadt	108122
BSA	Carl Roth GmbH + Co. KG, Karlsruhe	8076
CHAPS	Sigma-Aldrich Chemie GmbH, Taufkirchen	C5070
chloroform	Merck KgaA, Darmstadt	102431
DEPC	Sigma-Aldrich Chemie GmbH, Taufkirchen	D5758
DIG RNA Labeling Mix	Roche Diagnostics GmbH, Mannheim	1277073
dATP	Sigma-Aldrich Chemie GmbH, Taufkirchen	D4788
dCTP	Sigma-Aldrich Chemie GmbH, Taufkirchen	D4913
dGTP	Sigma-Aldrich Chemie GmbH, Taufkirchen	D5038
dodecyl sulfate sodium salt	Merck KgaA, Darmstadt	822050
DTT	Sigma-Aldrich Chemie GmbH, Taufkirchen	D9779
dTTP	Sigma-Aldrich Chemie GmbH, Taufkirchen	T9656
EDTA	Sigma-Aldrich Chemie GmbH, Taufkirchen	E4378
ethanol	Merck KgaA, Darmstadt	100983
ethidium bromide	Sigma-Aldrich Chemie GmbH, Taufkirchen	E1510
formamide	Sigma-Aldrich Chemie GmbH, Taufkirchen	47671
glucose	Merck KgaA, Darmstadt	108342

Name	Company	Catalog no.
glycerol	Merck KgaA, Darmstadt	104093
Heparin	Sigma-Aldrich Chemie GmbH, Taufkirchen	H9399
HEPES	Merck KgaA, Darmstadt	115231
hydrochloric acid	Merck KgaA, Darmstadt	109057
kanamycin A	Sigma-Aldrich Chemie GmbH, Taufkirchen	K4000
lithium chloride	Merck KgaA, Darmstadt	105679
low melting point agarose	Carl Roth GmbH + Co. KG, Karlsruhe	6351
LR-Gold Resin®	London Resin Company, Reading, UK	-
magnesium chloride	Merck KgaA, Darmstadt	105833
magenesium sulfate	Merck KgaA, Darmstadt	105886
NBT	Sigma-Aldrich Chemie GmbH, Taufkirchen	N6876
NE Buffer 3	New England Biolabs, Beverly, MA, USA	B7003S
NE Buffer *EcoR*1	New England Biolabs, Beverly, MA, USA	B0101S
paraformaldehyde	Sigma-Aldrich Chemie GmbH, Taufkirchen	P6148
PCI	Invitrogen GmbH, Karlsruhe	15593
phenol	Merck KgaA, Darmstadt	100200
potassium chloride	Merck KgaA, Darmstadt	104936
potassium phosphate	Merck KgaA, Darmstadt	104877
random hexamers	Applied Biosystems, Foster City, CA, USA	N8080127
Rnase inhibitor	Applied Biosystems, Foster City, CA, USA	N8080119
RNA Storage Solution	Ambion, Inc., Austin, TX, USA	7000
sheep serum	Sigma-Aldrich Chemie GmbH, Taufkirchen	S2263
sodium acetate	Merck KgaA, Darmstadt	106268
sodium chloride	Merck KgaA, Darmstadt	106400
sodium phosphate	Merck KgaA, Darmstadt	106347
sodium hydroxide solution	Merck KgaA, Darmstadt	109137
Torula yeast RNA	Sigma-Aldrich Chemie GmbH, Taufkirchen	R6625
TRIS	Merck KgaA, Darmstadt	108382
TRIS acetate salt	Sigma-Aldrich Chemie GmbH, Taufkirchen	T1258
TRIS-HCl	Merck KgaA, Darmstadt	108219
trisodium citrate	Sigma-Aldrich Chemie GmbH, Taufkirchen	106448
TRIZOL® reagent	Invitrogen GmbH, Karlsruhe	15596018
tryptone	BD, Franklin Lakes, NJ, USA	211699

Name	Company	Catalog no.
Tween®20	Sigma-Aldrich Chemie GmbH, Taufkirchen	P9416
water	Sigma-Aldrich Chemie GmbH, Taufkirchen	W4502
X-Gal	Sigma-Aldrich Chemie GmbH, Taufkirchen	B9146
yeast extract	BD, Franklin Lakes, NJ, USA	210941

Table 2-3. Enzymes

Name	Company	Catalog no.
DNA polymerase I, Large (Klenow) Fragment	New England Biolabs, Beverly, MA, USA	M0210S
*EcoR*1	New England Biolabs, Beverly, MA, USA	R0101S
M-MLV Reverse Transcriptase, RNase H Minus	Promega GmbH, Mannheim	M5301
*Not*1	New England Biolabs, Beverly, MA, USA	R0189S
Pfu DNA polymerase	Stratagene, La Jolla, CA, USA	600135
Proteinase K	Ambion, Inc., Austin, TX, USA	2548
SP6 RNA polymerase	Roche Diagnostics GmbH, Mannheim	810274
Taq DNA polymerase	MPIMG	stock

Table 2-4. Cells

Name	Genotype	Company
One Shot® TOP10 Chemically Competent *E. coli*	F-, mcrA, Δ(mrr-hsdRMS-mcrBC), Φ80lacZΔM15, ΔlacX74, recA1, araD139, Δ(ara-leu)7697, galU, galK, rpsL(StrR), endA1, nupG	Invitrogen GmbH, Karlsruhe
XL1-Blue Subcloning-grade Competent Cells	recA1, endA1, gyrA96, thi-1, hsdR17, supE44, relA1, lac [F′, proAB, $lacI^qZ\Delta M15$, *Tn*10 (Tet^r)]	Stratagene, La Jolla, CA, USA

2.3 DNA-markers, vectors, and primers

Table 2-5. DNA-markers

Name	Company	Catalog no.
1 kb DNA ladder	Stratagene, La Jolla, CA, USA	201115
100 bp DNA ladder	New England Biolabs, Beverly, MA, USA	N3231S

Table 2-6. Vectors

Name	Company	Catalog no.
pCR®II-TOPO®	Invitrogen GmbH, Karlsruhe	K460001
pSPORT1	Invitrogen GmbH, Karlsruhe	-

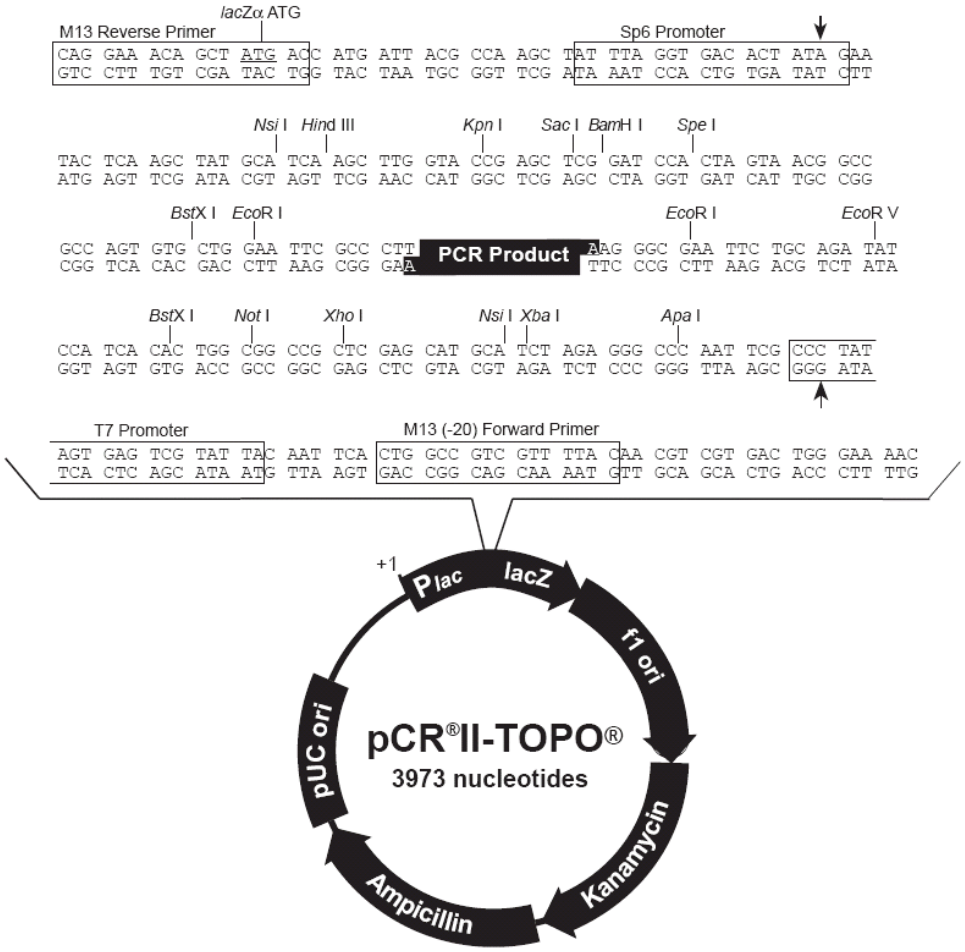

Figure 2-1. Vector map and multiple cloning site of pCR®II-TOPO®

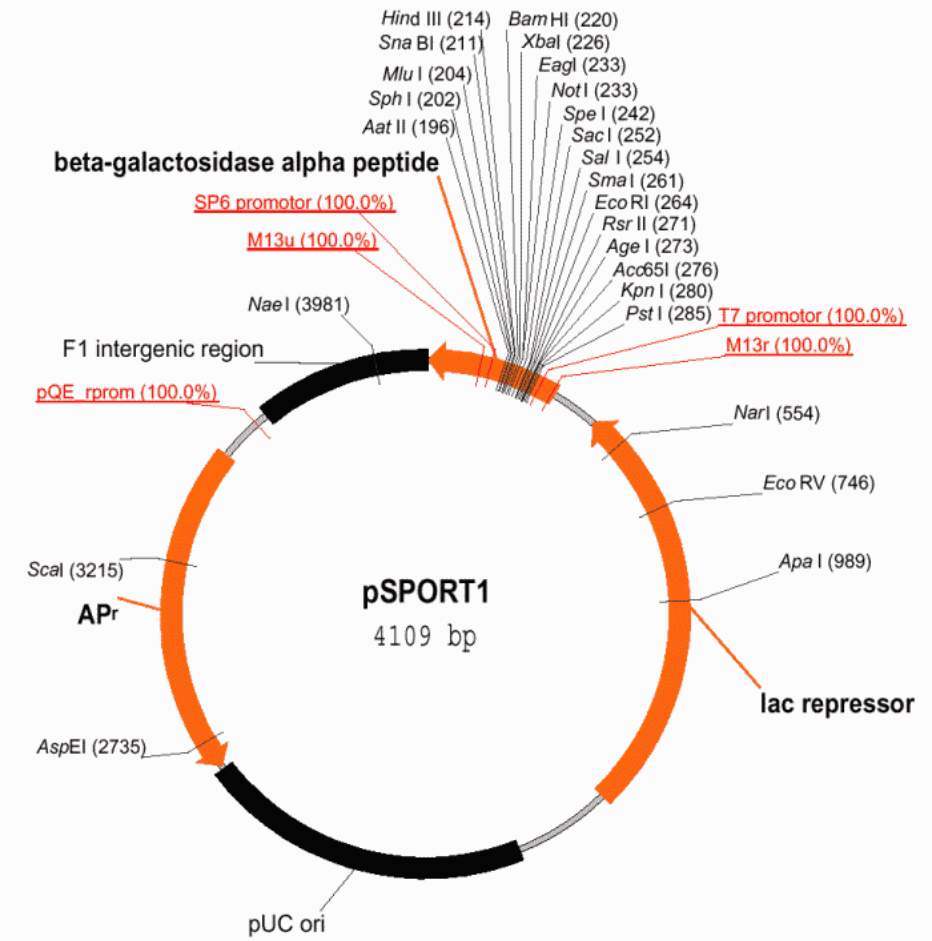

Figure 2-2. Vector map of pSPORT1

Table 2-7. Primers for RACE-PCR

Name	Sequence (5'→ 3')	Tm (°C)
5'_GSP1	GTTGAGCCCCGCCACCAGGATCTCATAG	69.3
5'_NGSP1	GCAGTCCCCGTCTATGGACAACCACGC	69.6
3'_GSP2	AGAGGAGGCCATTCGGAGAGATTCG	71.5
3'_NGSP2	CATGGCACAGGAGCGGGAGTACGAGCG	71.1

Table 2-8. Primers used for sequencing

Name	Sequence (5'→ 3')	Tm (°C)
M13_FSP	GCTATTACGCCAGCTGGCGAAAGGGGGATGTG	68.7
M13_RSP	CCCCAGGCTTTACACTTTATGCTTCCGGCTCG	67.4
BFCHD_FW_1	TCTTATCCCGATCAGCTCCG	59.9
BFCHD_FW_2	GCAAGTCAGAGGACGGATAG	59.9

Name	Sequence (5'→ 3')	Tm (°C)
BFCHD_FW_3	GTACGAGCGGGTGAAGGAAG	61.9
BFCHD_FW_4	ATGTGCCATCTGCGTCTGC	59.7
BFCHD_FW_5	ATCCTCAAACCTGCACCTCTGC	65.0
BFCHD_FW_6	CGTACAGTCCGTTCTACCAGACG	63.2
BFCHD_FW_7	ATCATCGTGCAACAAGAGACG	61.3
BFCHD_FW_8	ATCAGAGTCAACCCGACAGACTGC	66.2
BFCHD_REV_1	CTGACGCCCGTGTGATATTC	59,9
BFCHD_REV_2	GTCATTTCTCCGATCTCTGCG	60.0
BFCHD_REV_3	AGCTGAGTTCCGTTGCGGAG	61.9
BFCHD_REV_5	GTCCCACAGTCCCTTAAACATGAC	63.0
BFCHD_REV_6	ATGACATCTGTTGGGGATTTGC	63.2
BFCHD_REV_8	GCATGGCACGCATAAAGGTGAC	66.9
BFCHD_REV_A	GCAGGTACTACATTTCTCGTCG	60.1
BFCHD_REV_B	CGCAGATGGCACATTTGATGTAG	60.2

Table 2-9. Primers used for PCR on cDNA

Name	Sequence (5'→ 3')	Tm (°C)
ExonB_FW	CTCCCTGCACTATGAGATCC	59.9
BFCHD_REV_C	GCAGTCTGTCGGGTTGACTC	61.9
BFCHD_FW_10	GCACGGTCGGTACAACTCG	62.7
BFCHD_REV_7	CGCTTGTCATTTGTCATCATTG	61.4

Table 2-10. Primers used quantitative real-time PCR

Name	Sequence (5'→ 3')	Tm (°C)
QPCR_AmphiACTIN1_FW	TGCCCCGAGTCTCTCTTCC	50.0
QPCR_AmphiACTIN1_REV	CCTTCCTGATATCGATGTCGC	49.0
QPCR_AmphiBETACAT1_FW	TGCCGTCATCCGCAGTCTA	48.0
QPCR_AmphiBETACAT1_REV	TCTCCTTGTCCTGTGCCAGTT	49.0
QPCR_AmphiBMP1_FW	TCGTCGTGGGAATCCTTTG	46.0
QPCR_AmphiBMP1_REV	GCGCTTTGGAGACACCACTT	49.0
QPCR_AmphiCHD1_FW	GAGGAAGAGCAGCACTCCGT	51.0
QPCR_AmphiCHD1_REV	AGCCATGCCCGTGGTACTC	50.0

Name	Sequence (5'→ 3')	Tm (°C)
QPCR_AmphiFOXQ_FW	AACTTCCCGTTCTACCGCAAC	49.0
QPCR_AmphiFOXQ_REV	TGCCCTTACCGTCCTGAGAC	51.0
QPCR_AmphiGSC1_FW	CATCTTCGGAGTTCGAGTCGA	49.0
QPCR_AmphiGSC1_REV	TGCTGAAGACAGACGGGCT	48.0
QPCR_AmphiNOG1_FW	CCTGTAGCATTGAGCCATGGA	49.0
QPCR_AmphiNOG1_REV	GGTGTAGAAACGGCTGACCG	51.0
QPCR_AmphiSOXB1-1_FW	GCCCAGGAGGAAGACAAAAAC	49.0
QPCR_AmphiSOXB1-1_REV	TGGCGATGGTACGCTGAAC	48.0
QPCR_AmphiWNT8-1_FW	CCTCTGGTCTCTGTCGGTCC	53.0
QPCR_AmphiWNT8-1_REV	ACGACTTGGGTCCTGTGATC	51.0

2.4 Kits, solutions, and media

Table 2-11. Kits

Name	Company	Catalog no.
AccuPrime™ *Taq* DNA Polymerase High Fidelity	Invitrogen GmbH, Karlsruhe	12346086
BigDye® Terminator v3.1Cycle Sequencing Kit	Applied Biosystems, Foster City, CA, USA	4337455
QIAEX II Gel Extraction Kit	QIAGEN GmbH, Hilden	20021
QIAprep® Spin Miniprep Kit	QIAGEN GmbH, Hilden	27106
QIAquick® PCR Purification Kit	QIAGEN GmbH, Hilden	28106
Smart™ Race cDNA Amplification Kit	BD Biosciences Clontech, Palo Alto, CA, USA	634914
TURBO DNA-free® Kit	Ambion, Inc., Austin, TX, USA	1907
TOPO TA Cloning® Kit	Invitrogen GmbH, Karlsruhe	K4600-40
SYBR®Green PCR Master Mix	Applied Biosystems, Foster City, CA, USA	4309155

Table 2-12. Solutions for WMISH

Name	Composition
1× PBT	1× PBS; 0.1% Tween®20
4% PFA pH 7.0	4% paraformaldehyde; 0.8× PBS; 0.01% Tween®20
APT	2 M $MgCl_2$; 5 M NaCl; 2 M Tris pH 9.0; 10% Tween®20
blocking solution	1% blocking reagent; 2 mg/ml BSA; 1× PBT
hybridization buffer	0.5% CHAPS; 5 mM EDTA; 50 % formamide; 100 µg/ml Heparin; 2× SSC pH 4.5; 500 µg/ml *Torula* yeast RNA; 0.2% Tween®20
stain solution	APT; 9.0 µl/ml BCIP; 7.0 µl/ml NBT

Table 2-13. Solutions for filter hybridization

Name	Composition
2× RP mix	0.26 mg/mL BSA; 439 mM HEPES pH 6.6; 43.9% TM; 0.04 mM dATP; 0.04 mM dGTP; 0.04 mM dTTP; 0.06 OD/mL random hexamers
Church buffer	1 mM EDTA; 250 mM Na_2HPO4 pH 7.2; 5% SDS
stripping solution	20 mM Na_2HPO4; 0.1% SDS
TM	250 mM TRIS-HCl pH 8.0; 25 mM $MgCl_2$; 50 mM 2-mercaptoethanol
washing solution	1 mM EDTA; 20 mM Na_2HPO4; 0.1% SDS

Table 2-14. Other solutions

Name	Composition
1× TAE	40 mM TRIS acetate pH 7.5; 0.01 M EDTA
1× TE	10 mM TRIS-HCl pH 8.0; 1 mM EDTA
10× PBS	27 mM KCl; 1.37 M NaCl; 0.1 M phosphate buffer pH 7.4
10× PCR buffer	0.35 M TRIS acetate pH 9.0; 0.15 M TRIS-HCl pH 9.0; 0.5 M KCl; 15 mM $MgCl_2$; 1% Tween®20
20× SSC pH ~7.0	3 M NaCl; 0.3 M trisodium citrate dihydrate
gel loading buffer	4 mM TRIS acetate pH 8.0; 0.2 mM EDTA; 0.25% bromphenol blue; 50% glycerol

Table 2-15. Media

Name	Composition
2YT	0.5% NaCl; 1.6% tryptone; 1.0% yeast extract
LB	1.0% NaCl; 1.0% tryptone; 0.5% yeast extract
LB agar	1.5% agar; 1.0% NaCl; 1.0% tryptone; 0.5% yeast extract
S.O.C.	2.0% tryptone; 0.5% yeast extract; 10 mM NaCl; 2.5 mM KCl; 10 mM $MgCl_2$; 10 mM $MgSO_4$; 20 mM glucose

2.5 Database accession numbers

Table 2-16. Nucleotides

Name	Accession no.
AmphiBMP2/4	AF068750
AmphiFoxQ2	AY163864
AmphiWnt8	AF190470
amphioxus *goosecoid*	AF281674
AmphiBetaCat	DQ013259
BfCA1	D87406.

Table 2-17. Proteins

Name	Accession no.
DmSog	Q24025
DrChd	O57472
GgChd	Q90ZD5
HrChd	Q964I1
HsCHD	Q9H2X0
MmChd	Q9Z0E2
XlChd	Q91713

3 METHODS

3.1 Collection, treatment, and fixation of amphioxus embryos

The embryos of *B. floridae* were collected in Old Tampa Bay, Florida, in the summers of the years between 2000 and 2002. Ripe adults were dug out from sandy bottom within the bay by means of shovel and sieve. After enough animals had been collected (generally, more than 400) they were transferred to the laboratory and induced to spawn. For this purpose, each animal was transferred into a separate plastic container and electro-shocked for 1-3 sec with pulses of 50 V DC. The gametes that emerge from the atriopore of the adult were collected with a pipet and transferred into petri dishes containing filtered sea water. For fertilization, several drops of concentrated sperm were added to several thousand eggs and the fertilization envelopes began to form around the fertilized eggs.

Table 3-1. Development schedule (at 25°C) for *Branchiostoma floridae* (from Holland and Holland 1993)

Time	Stage
55 min	2-cell
75 min	4-cell
95 min	8-cell
3.5 h	Blastula
5.5 h	Gastrula
10.0 h	Neurula hatches
38.0 h	Larval mouth opens
18 d	Metamorphosis begins
23 d	Metamorphosis complete

The embryos were raised in petri dishes at a concentration so that no more than a monolayer was covering the bottom of the dish. Feeding was not necessary until the embryos became older than 30 to 36 hrs. At hatching which occurs at 10 hrs of development (see Table 3-1) the embryos swim towards the surface and towards the light. The water was exchanged once before 20 hrs of development. For this the embryos were pipetted from the surface of the dish and transferred into a new dish with fresh seawater, removing them from abnormally developing embryos and dead eggs, which tend to remain at the bottom. For the generation of lithium mutants, embryos were either raised continuously in seawater containing lithium at a concentration of 50 mM or only for a short amount of time at higher concentrations (300 mM or 500 mM) before they were transferred to normal seawater again. The pulse of higher lithium concentrations was applied in the 20 minutes before the onset of gastrulation. Embryos were fixed at frequent intervals in 4% PFA, and the water was removed by treating the embryos in an ethanol series (25%, 50%, 2× 70%). Finally, the embryos were stored in 70% ethanol at -20°C.

3.2 Agarose gel electrophoresis

Agarose gel electrophoresis is used to separate nucleic acid strands by size, and to determine the size of the separated strands by comparison to strands of known length. An electric field is used to drag the negatively charged nucleic acid molecules through a gel matrix. The shorter molecules move faster than the longer ones since they slip through the gel more easily. The purpose of the gel is to identify DNA or RNA, to quantify it or to isolate a particular band. Ethidium bromide can be used to visualize the nucleic acids in the gel. This fluorescent dye binds strongly to nucleic acids by intercalating between the stacked bases. It absorbs invisible UV light and transmits the energy as visible orange light.

0.7 g of agarose and 70 mL of 1× TAE buffer were boiled in a microwave oven until the agarose was completely dissolved. After the solution had cooled down to approximately 60°C, 5 µL of ethidium bromide (0.5 µg/mL) were added and the solution was filled into a gel chamber. A comb was inserted at one side of the chamber. When the gel had completely cooled down and become solid, the comb

was removed and the gel was covered with 1 × TAE buffer. The DNA or RNA samples were mixed with loading buffer and injected into the slots. A current of 30 V was applied to the chamber, while the nucleic acids were migrating towards the anode. Gels were exposed to UV light, photographed, and printed on an AlphaImager® gel documentation system (Alpha Innotech Corporation). For DNA extraction from agarose gels (see section 3.11) 100 mL instead of 70 mL 1 × TAE buffer were used.

3.3 DNA concentration determination

With the aid of spectroscopy, nucleic acids and proteins can be quantitatively analyzed. Nucleic acids absorb ultraviolet with an absorbance maximum at 260 nm. The absorption of 1 OD (A) is equivalent to approximately 50 µg/mL dsDNA or 40 µg/mL for RNA. Proteins absorb ultraviolet light with an absorbance maximum at 280 nm. The ratio $A_{260}/_{280}$ is used to estimate the purity of nucleic acid. Pure DNA should have a ratio of approximately 1.8, whereas pure RNA should have a value of approximately 2.0. Absorption at 230 nm reflects contamination of the sample by substances such as carbohydrates, peptides, phenols or aromatic compounds. In the case of pure samples, the ration A_{260}/A_{230} should be approximately 2.2.
The concentration of DNA or RNA was determined with a Nanodrop® spectrophotometer (NanoDrop Technologies), which uses only 1 µL of sample for one measurement. If necessary, the samples were diluted up to 1: 1000 before measurement.

3.4 RNA isolation with TRIZOL® Reagent

The most widely used method for purifying total RNA from marine embryos is based on the single-step method of Chomczynski and Sacchi (1987). In this method the cells are homogenized in guanidinium isothiocyanate and extracted with acidified phenol and chloroform. Chomczynski (1993) modified the method using a patented TRI Reagent, which is commercially available from several sources. TRIZOL®

Reagent (Invitrogen) is a ready-to-use reagent for the isolation of total RNA from cells and tissues.

The anterior "heads" of 20 amphioxus embryos were cut and directly homogenized in liquid nitrogen using a prechilled mortar and pestle. After a fine powder was obtained 24 mL of TRIZOL® Reagent were added and the solution was further homogenized using a glass-Teflon® homogenizer. The sample was incubated for 5 min at RT to permit the complete dissociation of nucleoprotein complexes. Subsequently, 0.2 mL of chloroform was added per 1 mL of TRIZOL® Reagent. The tubes were shacked vigorously by hand for 15 sec and incubated at RT for 2-3 min. The samples were centrifuged at 10,000 × g for 15 min at 4°C. Following centrifugation the aqueous (upper) phase was transferred to a fresh tube and the RNA was precipitated from the aqueous phase by mixing with isopropyl alcohol. 0.5 mL of isopropyl alcohol was used per 1 mL of TRIZOL® Reagent used for the initial homogenization. The samples incubated at RT for 10 min before they were centrifuged at 12,000 × g for another 10 min at 4°C. The supernatant was carefully removed and the RNA pellet was washed with 75% ethanol by adding 1 mL of 75% ethanol per 1 mL of TRIZOL® Reagent used for the initial homogenization. The samples were mixed by vortexing and centrifuged at 7,500 × g for 5 min at 4°C. The supernatant was removed and the RNA pellet was briefly air-dried before it was finally dissolved in 1 mL of RNA Storage Solution. To determine if the RNA was intact, an aliquot was diluted and the RNA was analyzed on an agarose gel. Additionally, the RNA concentration was measured photometrically and stored at –80°C until usage.

3.5 cDNA synthesis

RNA can be transcribed to DNA with the aid of reverse transcriptase and suitable primers. The classical method of cDNA synthesis uses the oligo(dT) primer to prime first-strand synthesis. Random hexameric primers provide an alternative procedure by which first-strand cDNA synthesis is initiated from internal sites within the mRNA molecule. Total RNA was used as template in cDNA synthesis; the resulting

DNA/RNA hybrid molecules were used as template in subsequent PCR reactions. The procedure used was modified from Gerard et al. (1997).

For cDNA synthesis 2 µg of total RNA were brought up to a volume of 5 µL with dH_2O DEPC, and denatured at 70°C for 5 min. After denaturation, the RNA was allowed to cool down on ice for 5 min. The following components were added to the RNA: 4 µl of 10 mM dNTPs, 2 µL of 5× reverse transcriptase buffer, 2 µL of 50 µM random hexamers, 0.5 µL of RNase inhibitor (20 U/µl), and 0.5 µL of reverse transcriptase (200 U/µL). The reaction was filled up with DNase/RNase free water (Sigma) to a final volume of 20 µL and the following PCR program was used to drive cDNA synthesis: 37°C for 20 min, 42°C for 20 min, and 51°C for 20 min. The reaction product was diluted up to 100 µL with DNase/RNase free water (Sigma) and heated at 95°C for 2 min. The cDNA was stored at –20°C until usage.

3.6 Database analysis

The protein sequence of Chordin from *S. purpuratus* (Poustka et al. unpublished) was chosen for searching a database of raw sequence traces from JGI's *Branchiostoma floridae* sequencing project for matching reads. The tblastn search identified 59 reads that were assembled into 13 separate contigs. These contigs were in turn blasted against a non-redundant protein database and contigs matching Chordin from *Danio rerio* with a threshold expect value greater than 1e-04 were selected for further analysis. Five contigs above this cut off score were reassembled manually whereby two contigs were merged. The four resulting contigs (see Table 3-2) comprised 16 reads and were subsequently used for primer design.

Table 3-2. Contigs from raw sequence traces with BLAST hits for *D. rerio* Chordin.

contig	size (bp)	no. of reads	BLAST hits for D. rerio Chordin
3/4	1,695	6	768- 802; 805- 839
5	1,590	2	540- 606; 588- 647
6	1,479	3	630- 720
10	1,234	5	529- 608

3.7 Polymerase chain reaction

The polymerase chain reaction (Mullis et al. 1986; Saiki et al. 1988) is an *in vitro* method used for enzymatically synthesizing defined sequences of DNA. The reaction uses two oligonucleotide primers that hybridize to opposite strands and flank the target DNA sequence that is to be amplified. The elongation of the primers is catalyzed by a thermostable DNA polymerase. A repetitive series of cycles involving template denaturation, primer annealing, and extension of the annealed primers by the polymerase, results in exponential accumulation of a specific DNA fragment. Because the primer extension products synthesized in a given cycle can serve as a template in the next cycle, the number of target DNA copies approximately doubles every cycle.

During denaturation the hydrogen bonds between the complementary DNA strands are broken and the double stranded DNA separates into single strands. The annealing step ensures that the primers bind to the DNA and normally requires temperatures, which are 5°C below the lowest melting temperatures of the two primers. The elongation temperature depends on the DNA polymerase, and the time for elongation should be approximately one minute for every 1000 bp of the DNA template molecule. Typical values for DNA denaturation, primer annealing, and extension are 94-96°C, 50-65°C, and 65-80°C, respectively.

For amplifying DNA fragments from cDNA 40 ng of cDNA were used as template in a 50 µL reaction. The following components were mixed together in decreasing order of their volume:

25.63 µL	dH_2O
15.03 µL	5 M betaine
5.00 µL	10× PCR-buffer
1.67 µL	5 µM forward-primer
1.67 µL	5 µM reverse-primer
0.50 µL	10 mM dNTPs
0.50 µL	*Taq* DNA polymerase (10 U/µL)

The following program was performed to amplify DNA in a PTC-100™ (MJ Research) thermal cycler:

96°C 30 sec
65°C 3 min 30 sec
30 cycles:
    96°C 25 sec
    65°C 3 min 30 sec

When the initial PCR failed to give a product or only weakly amplified the desired fragment, a second PCR reaction was performed to amplify the fragment of interest in sufficient amount. Instead of using 2 µL of cDNA, 2 µL of PCR product were used in the second reaction.

3.8 RACE-PCR

Rapid amplification of cDNA ends (RACE) is a polymerase chain reaction-based technique, which facilitates the cloning of full-length cDNA sequences when only a partial cDNA sequence is available. Partial clones that lack sequences representative of the 5' end of the corresponding mRNA arise commonly in cDNA libraries when reverse transcriptase fails to extend first-strand cDNA along the full length of the mRNA template. Partial cDNA clones that lack the 3' regions occur infrequently in oligo(dT)-primed cDNA libraries but are common to random hexamer-primed cDNA libraries. Several methods were developed to overcome the procedure of re-screening cDNA libraries in greater depth. In the late 1980s Frohman et al. (Frohman et al. 1988) described a general method for the rapid amplification of cDNA ends. Several additional features including anchored PCR (Loh et al. 1989), antibody-mediated automatic hot-start PCR (Kellogg et al. 1994) and nested PCR were added to the procedure.

The SMART™ RACE cDNA Amplification Kit (BD Biosciences Clontech) was used to prepare cDNA for RACE-PCR. SMART™ RACE technology involves oligo(dT)-primed reverse transcription reaction, adding an adapter to the 3' end of the synthesized cDNA (the 5' end of the mRNA), and amplifying by PCR with a

gene specific primer and a primer that recognizes the adapter sequence. I recommend using primers with a length of 25-30 nt, GC-content of 50-70%, and a melting temperature of 69-72°C. When possible, these primers should include a "GC-clamp" at their very 3' end.

3.8.1 First-strand cDNA synthesis

Two different cDNA populations were synthesized from total RNA (five hours gastrula stage RNA). The cDNA for 5' RACE was synthesized using an adapter oligonucleotide and a modified oligo(dT) primer (5' CDS primer). The modified oligo(dT) primer has two degenerate nucleotide positions at the 3' end, that position the primer at the start of the poly-A tail and eliminate the 3' heterogeneity that can occur with conventional oligo(dT) priming (Borson et al. 1992). The M-MLV-RT used for cDNA synthesis exhibits terminal transferase activity upon reaching the end of a RNA template adding three to five dCTPs to the 3' end of the first strand. This short C-overhang serves as an annealing site for the adapter oligonucleotide, which possesses terminal stretches of G-residues and serves as an extended template for the reverse transcriptase. After the reverse transcriptase switches templates from the mRNA to the adapter molecule, a complete cDNA copy of the original RNA is synthesized with the additional adapter sequence at the end. The synthesis of cDNA for 3' RACE lacks the adapter oligonucleotide but employs a special oligo(dT) primer (3' CDS primer A), which includes the degenerate nucleotide positions at the 3' end and has a portion of the adapter sequence at its 5' end. By incorporating this adapter sequence into both cDNA populations, both RACE-PCR reactions can be primed using the same universal primer (UPM) that recognizes the adapter sequence, in conjunction with distinct gene-specific primers (GSPs).

For first-strand cDNA synthesis the following components were combined for 5' RACE and 3' RACE cDNA, respectively:

cDNA for 5' RACE	cDNA for 3' RACE
3 µL RNA sample (1 µg)	3 µL RNA sample (1 µg)
1 µL 5'-CDS primer	1 µL 3'-CDS primer A
1 µL SMART II™ A oligonucleotide	1 µL dH_2O

The samples were incubated at 70°C for 2 min. After cooling on ice for another two minutes, the following components were added to each sample:

2 µL 5× first-strand buffer
1 µL 20 mM DTT
1 µL 10 mM dNTPs
1 µL reverse transcriptase

---

10 µL total volume

The samples were incubated at 42°C for 90 min in an air incubator. The first-strand reaction products were diluted with 100 µL dH_2O, heated at 72°C for 7 min, and stored at –20°C until usage.

3.8.2 5' RACE and 3' RACE

5' RACE and 3' RACE fragments were amplified from the cDNA described in 3.8.1 with a high-fidelity *Taq* DNA polymerase from Invitrogen. This DNA polymerase amplifies nucleic acid templates using antibody-mediated hot-start, a blend of *Taq* DNA polymerase, and proofreading enzyme, and that possesses a 3' to 5' exonuclease activity.

The following components were combined for 5' RACE-PCR and 3' RACE-PCR, respectively:

5' RACE-PCR	3' RACE-PCR
32.5 µL dH_2O	32.5 µL dH_20
5.0 µL cDNA for 5' RACE	5.0 µL cDNA for 3' RACE
5.0 µL 10× PCR Buffer I	5.0 µL 10× PCR Buffer I
5.0 µL 10 mM UPM	5.0 µL 10 mM UPM
1.0 µL 10 mM 5'GSP	1.0 µL 10 mM 3'GSP
1.0 µL 10 mM dNTPs	1.0 µL 10 mM dNTPs
0.5µL high fidelity *Taq* DNA polymerase (5 U/µL)	0.5µL high fidelity *Taq* DNA polymerase (5 U/µL)
50 µL total volume	50 µL total volume

The following PCR-program was used for both 5' RACE-PCR and 3' RACE-PCR:

94°C 15 sec
30 cycles:
94°C 5 sec
68°C 3 min

After this first PCR a nested PCR reaction was performed using the nested universal primer (NUP) and a nested gene-specific primer (NGSP). 5 µL of the primary PCR product were diluted into 245 µL dH_2O (1:50). 5 µL of the diluted primary PCR product were used in place of the cDNA for nested RACE-PCR. 1 µL of 10 mM NUP and 1 µL of 10 mM NGSP were used and the volume of water was increased to 36.5 µL. The same PCR-program that was used for the primary amplification was used in the nested PCR reaction.

The high fidelity *Taq* DNA polymerase possesses a 3' to 5' exonuclease activity, which partially removes 3' A-overhangs necessary for TA- and TOPO TA-cloning (see section 3.13). To increase the yield of cloning efficiency, 3' A-overhangs were

added to these PCR products by mixing 1 µL of conventional *Taq* DNA polymerase (1 U/µL) to the freshly made PCR product and incubating at 65°C for 8-10 min.

3.9 Quantitative real-time RT-PCR

mRNA expression can be analysed by reverse transcription (RT) followed by the polymerase chain reaction (PCR). Quantitative real-time RT-PCR is highly sensitive and allows quantification of the initial amount of the template and detects even small changes in gene expression (Heid et al. 1996). The system is based on the detection and quantification of a flourescent reporter, whose signal increases in direct proportion to the amount of PCR product in the reaction. By recording the amount of flourescence emission at each cycle, it is possible to monitor the PCR reaction during exponential phase where the first significant increase in the amount of PCR product correlates to the initial amount of target template. The higher the starting copy number of the nucleic acid, the sooner a significant increase in flourescence is observed. A fixed fluorescence threshold is set significantly above the baseline. The parameter C_T (threshold cycle) is defined as the cycle number at which the fluorescence emission exceeds the fixed threshold.

Several "markers" are described by Pfaffl (Pfaffl 2004) that make up for a successful real-time RT-PCR: integrity of purified RNA, production of single-stranded complementary DNA copy of the RNA through reverse transcriptase (RT) and its dynamic range, sensitivity, and specificity, the right detection chemistry, quantification strategy, efficiency evaluation, data evaluation, and data normalization.

3.9.1 RT reaction for kinetic PCR

The RNA for cDNA synthesis was treated with TURBO DNA-free® Kit (Ambion), to remove any possible DNA-contaminations that might disturb the quantitative real-time PCR. 10 µg of total RNA were mixed with 5 µL of DNase buffer and 1 µL of DNase, the reaction was brought up to a volume of 50 µL with dH_2O DEPC, and incubated at 37°C for 30 min. After incubation, 5 µL of DNase Inactivation Reagent were added and the sample was incubated at RT for 2 min. The sample was

centrifuged at 13,000 × g for 5 min and the supernatant containing the RNA was transferred to a fresh tube. After determining the concentration, the RNA sample was stored at -80°C until usage.

For synthesis of cDNA 1 µg of total RNA (DNA-free), 1 µL of 50 µM random hexamers, and 2 µL of 10 mM dNTPs were mixed in a 0.2 mL microcentrifuge tube. The reaction was brought up to a volume of 10 µL with dH_2O DEPC and incubated at 65°C for 10 min. After the incubation, the sample was placed on ice and 4 µL of 5× reverse transcription buffer, 4 µL of 25 mM $MgCl_2$, 0.5 µL RNase-inhibitor (20 U/µL), and 1.5 µL reverse transcriptase (200 U/µL) were added. The reaction was incubated at 42°C for 60 min before adding 20 µL of DNase/RNase free water (Sigma). The cDNA was stored at -20°C until usage.

3.9.2 Sequence detection with SYBR® Green I dye chemistry

Two general methods for quantitative sequence detection in kinetic PCR have become established: sequence specific flourescent probes or non-sequence specific double strand binding agents based on flourescence resonance energy transfer (FRET). The simplest detection technique uses SYBR® Green I flourescence dye that binds specifically to double-stranded DNA (Morrison 1998) by intercalating between adjacent base pairs.

The following components were combined in one well of an ABI PRISM® Optical 96-Well Reaction Plate (PE Applied Biosystems):

5.0 µL SYBR®Green PCR Master Mix
2.0 µL cDNA
0.6 µL 5 µM Forward-Primer
0.6 µL 5 µM Reverse-Primer
1.8 µL dH_2O DEPC

Each cDNA was diluted 1:4 and 1:16. For each dilution and each primer pair triplicate samples were measured on one reaction plate. A second PCR run was carried out with an additional cDNA population to account for reverse transcription efficiency during the RT reaction step. The reaction plates were covered with ABI PRISM® Optical Adhesive Cover (PE Applied Biosystems) and placed in the real-time PCR system, ABI 7900HT (PE Applied Biosystems) to execute the following program:

50°C 2 min
95°C 10 min
40 cycles:
    96°C 15 sec
    65°C 1 min
95°C 15 sec
65°C 15 sec
95°C 15 sec

The data was analyzed with the SDS software version 2.1 (PE Applied Biosystems). Agarose gel electrophoresis and dissociation curve evaluation were used to check if the desired PCR product was amplified. Primers for quantitative real-time PCR were generated with the PrimerExpress software 2.0 (PE Applied Biosystems).

3.9.2 Relative quantification with the comparative C_T method

Relative quantification describes the change in gene expression of a target gene relative to some reference group such as an untreated control or a sample at time zero in a time-course study. The amount of expression of target genes in untreated, lithium- or zinc-treated embryos was analyzed by the comparative C_T method, also known as the $2^{-\Delta\Delta C_T}$ method.

An internal control gene was used to normalize the PCR data for the amount of RNA added to the reverse transcription reactions and the untreated control was used as the

calibrator. The data were calculated as the fold change in gene expression normalized to an endogenous reference gene and relative to the untreated control (the calibrator). The cycle threshold differences ($\Delta\Delta C_T$) were calculated as the normalized cycle threshold (ΔC_T) of the treated sample minus the normalized cycle threshold (ΔC_T) of the control sample. Since data from two different cDNA populations were obtained, treated samples of both cDNAs were compared to the control sample of the same and the other cDNA population resulting in four $\Delta\Delta C_T$ values for each target gene. Each PCR cycle was assumed to increase the product by 1.94 times (Hinman 2003), and, therefore, fold differences were calculated as $1.94^{-\Delta\Delta C_T}$. The final values were averaged and the error was expressed as the one times standard deviation. No errors from averaging the triplicates of both cDNAs were considered in the calculation because the error between the two cDNA populations was larger, so that the smaller error could be neglected.

3.10 PCR product purification

For further analysis, PCR products were purified from primers, salts, enzymes, unincorporated nucleotides, ethidium bromide, and detergents with the QIAquick® PCR Purification Kit (QIAGEN). Spin columns with immobilized silica beads that reversibly bind DNA are central to the procedure.

Five volumes of buffer PB were added to one volume of PCR sample and mixed. To bind DNA the sample was applied to a QIAquick® spin column, placed in a 2 mL collection tube, and centrifuged at 13,000 × g for 1 min. The flow-through was discarded, 0.75 mL buffer PE was added to the QIAquick® column, and the sample was again centrifuged at 13,000 × g for 1 min. After discarding the flow-through, the sample was centrifuged one more time. The QIAquick® column was placed in a clean 1.5 mL tube and 30 mL of buffer EB were added to the center of the QIAquick membrane. After incubating for one minute the samples were centrifuged at 13,000 × g for 1 min and the flow-through was stored at –20°C until usage.

3.11 DNA extraction from agarose gel

The QIAEX II Gel Extraction Kit (QIAGEN) was used to extract and purify individual DNA-bands from agarose gels. Non-nucleic acid impurities such as agarose, proteins, salts, and ethidium bromide are removed with this procedure. The method is based on reversible binding of DNA to silica beads in the QIAEX II suspension.

The DNA band of interest was excised under a UV transilluminator from the 0.7% agarose gel with a clean scalpel, and transferred into a 1.5 mL tube. The gel slice was weighed, put into a microcentrifuge tube, and mixed with three volumes of buffer QX1 for one volume of gel. The QIAEX II suspension was vortexed for 30 sec and 10 mL of it were added to the sample. The sample was incubated at 50°C for 10 min to dissolve the agarose and bind the DNA. Every two minutes the sample was mixed by vortexing to keep the QIAEX II in suspension. The sample was centrifuged at 13,000 × g for 30 sec and the supernatant carefully removed with a pipet. The pellet was washed once with buffer QX1 to remove residual agarose contaminants. 500 µL of buffer QX1 were added to the sample and the pellet was resuspended by vortexing. After centrifugation at 13,000 × g for 30 sec the supernatant was again carefully removed with a pipet. To remove residual salt contaminants the pellet was washed twice with 500 µL of buffer PE. The resulting pellet was air-dried for 15 minutes and 20 µL of water were added to elute the DNA. The sample was incubated for five minutes, centrifuged at 13,000 × g for 30 sec, and the supernatant transferred into a clean tube. The last step was repeated to increase the yield and the eluates were combined. The DNA was stored at –20°C until usage.

3.12 Filter hybridization

Numerous approaches can be used for hybridizing small or large filters containing arrayed bacterial clone colonies. The method described here uses plastic hybridization boxes and shaking incubators as hybridization equipment.

3.12.1 Probe labeling

Following PCR amplification, probes for filter hybridization were cleaned by PCR product purification (see section 3.10) or, if necessary, by extraction from agarose gel (see section 3.11). The PCR-derived probes were labeled by random primed labeling (Feinberg and Vogelstein 1983). During this procedure the DNA sample is denatured and small oligonucleotides which hybridize randomly to the template molecules are added. [α32P]dCTP becomes incorporated into the copied DNA by elongation of the random primers by Klenow fragment of DNA polymerase I.

Approximately 100 ng of DNA to be labeled was diluted in dH_2O in a final volume of 30 µL and denatured at 95°C for 5 min. After cooling on ice for five minutes, the DNA solution was again diluted up to 30 µL if necessary, and an equal volume of 2× RP mix was added. 1µL (10 Ci/µL) of [α32P]dCTP (3,000 Ci/mmol) and 2 µL of *E. coli* DNA polymerase I (Klenow fragment) (10 U/µL) were added and the above reaction incubated at 37°C for 2 hrs. The efficiency of the labeling reaction was checked by spotting 1 µL of labeling reaction onto a polyehtyleneimine (PEI) sheet (Macherey-Nagel). The chromatography paper was air-dried and vertically placed into a beaker with 0.75 M potassium di-hydrogenphosphate pH 3.5 (the running buffer should not cover the spots). After the solvent front was allowed to progress until approximately 15 cm of the start, the PEI sheet was air-dried, wrapped in Saran Wrap® and exposed on a phosphor imager screen for 20 minutes. The labeled probe should appear at the point where the sample was applied while the unincorporated nucleotides are migrating with the solvent front.

3.12.2 Hybridization

When filters are prepared target DNA is denatured and bound to a nylon or nitrocellulose filter. During hybridization the denatured labeled probe that is added to the filter can bind to the filter, only, if it base pairs with the DNA that was initially bound to the filter.

Prior to hybridization, DNA membranes were pre-hybridized at 65°C for 20 min in Church buffer. Maximally ten filters separated by mesh sheets were placed in hybridization boxes with approximately 100-200 mL of buffer and incubated in a

hybridization oven with a shaking unit. The buffer was exchanged for 50 mL of fresh Church buffer containing the denatured [α32P]dCTP labeled probe. The probe was denatured by adding 10 µL of 5 M NaOH solution. If necessary, additional buffer was added and the filters were hybridized at 65°C for at least 16 hrs in the hybridization oven. After hybridization excess probe was removed by washing the filters under high-stringency conditions in 1 mM EDTA, 20 mM Na_2HPO_4, 0.1% SDS initially briefly at RT and then twice at 65°C for 20 min.

The DNA filters were placed on a plastic support with the DNA side up, covered with Saran Wrap®, and exposed to a phosphor imager screens overnight. Screens were scanned with the phosphor imager Storm™820 (Amersham Biosciences) and analyzed with the ImageQuant™ software (Amersham Biosciences).

3.12.3 Stripping of probes

Probes were stripped from the nylon membranes by washing the filters twice in stripping solutions at 65°C. After the filters were cleaned from the radioactive probes, they were washed once with 1× TE pH 8.0 and finally stored in 1× TE at 4°C.

3.13 TOPO TA-Cloning®

The plasmid vector pCR®II-TOPO® (Invitrogen) is supplied linearized with single 3'-thymidine (T) overhangs and topoisomerase I covalently bound to the vector. *Taq* polymerase has a nontemplate-dependent terminal transferase activity that adds a single deoxyadenosine (A) to the 3' ends of PCR products allowing PCR inserts to ligate efficiently with the vector. Topoisomerase I from *Vaccinia* virus binds to dsDNA at specific sites and cleaves the phosphodiester backbone after 5'-CCCTT in one strand. The energy from the broken phosphodiester backbone is conserved by formation of a covalent bond between the 3' phosphate of the cleaved strand and a tyrosyl residue (Tyr-274) of topoisomerase I. The phosphotyrosyl bond between the DNA and enzyme can subsequently be attacked by the 5' hydroxyl of the PCR insert, reversing the reaction and releasing topoisomerase. The TOPO TA Cloning® Kit (Invitrogen) was used for cloning reactions.

For ligation, 4 µL of purified PCR product were added to 1 µL of salt solution (1.2 M NaCl; 0.06 M $MgCl_2$) and 1 µL of pCR®II-TOPO® vector (10 ng/µL), mixed gently, and incubated at RT for 30 min. 2 µL of the ligation reaction were added to one vial of chemically competent *E. coli* (TOP10), mixed gently by pipetting up and down, and incubated on ice for 30 minutes. The cells were heat-shocked for 30 sec at 42°C and immediately transferred to ice again. 250 µL of RT S.O.C. medium were added, and the cells were shacked horizontally (300 rpm) at 37°C for one hour for recovery. From each transformation 100 µL and 150 µL were spread on separate selective LB plates containing kanamycin (100 µg/mL) and X-Gal (128 µg/mL) and incubated at 37°C overnight. From each plate ten white colonies were picked for further analysis. Two primers, M13FW and M13REV, which bind on both sites of the multiple cloning site were used in colony PCR to check if the insert of expected size was correctly ligated into the vector. The same primers were used to determine the orientation of the insert and its DNA sequence.

3.14 Isolation of plasmid DNA

Bacteria were directly picked from cDNA libraries (BFL26 or BFLG) or from selective agar plates (blue/white screening). 5 mL cultures with LB or 2YT broth containing 0.2% of ampicillin were set up and left at 37°C overnight in a shacking incubator. The cultures were centrifuged at 2000 rpm for 20 min at 4°C and the supernatant was subsequently discarded.

Plasmid isolation was performed using the QIAprep® Spin Miniprep Kit (QIAGEN GmbH, Hilden). The pelleted bacteria were resuspended in 250 µL of Buffer P1 and transferred to a microcentrifuge tube. To allow cell lysis 250 µL of Buffer P2 were added and the tubes were gently inverted 4-6 times to mix. 350 µL of Buffer N3 were added and the tubes were immediately but gently inverted 4-6 times. The samples were centrifuged at 13,000 rpm for 10 min. The DNA was recovered from the supernatant by binding to a silica column. Therefore, the supernatant was applied to QIAprep spin column, placed on a 2 mL collection tube. The tubes were subsequently centrifuged at 13,000 rpm for 1 min and the flow-through was discarded. The spin column was washed with 750 µL of Buffer PE and centrifuged at

13,000 rpm 1 min. The flow-through was discarded and the column was centrifuged an additional minute to remove residual wash buffer. The column was placed in a clean 1.5 mL microcentrifuge tube and 50 µL of Buffer EB were added to the center of the QIAprep column to elute the DNA. The column was left for one minute and then centrifuged at 13,000 rpm for 1 min. The DNA concentration of the eluate was spectrophotometrically determined as described in section 3.3 and stored at -20°C until usage.

3.15 Sequencing of DNA

Two different methods for DNA sequencing were introduced in the late 1970s: The chain determination method (Sanger et al. 1977) and the chemical degradation method (Maxam and Gilbert 1977). The former method has gained more popularity, mainly, because it is easier to automate than the latter.

3.15.1 Thermal cycle sequencing and primer walking

While the chain determination method requires preparation of a single-stranded DNA molecule, cycle sequencing uses double-stranded DNA and requires only little amount of starting template. Thermal cycle sequencing (Sears et al. 1992) is much similar to conventional PCR but just one primer is used, and in addition to dNTPs a small amount of ddNTPs is used in the reaction. The template DNA is used to enzymatically generate DNA fragments *in vitro* by thermal cycling. The polymerase does not discriminate between dNTPs and ddNTPs, so every time a ddNTP becomes incorporated into the growing chain, elongation is blocked because it lacks the 3'-hydroxyl group needed to form a connection with the next nucleotide. The result is a set of new chains, all of different length, but each ending with a ddNTP. A different flourolabel is attached to the ddNTPs, with a different flourolabel used for each one. The ABI PRISM® 377 DNA sequencer (Applied Biosystems) automatically analyzes DNA molecules labeled with multiple flourescence dyes. After the samples are loaded onto the system's vertical gel, they undergo electrophoresis, laser detection, and computer analysis.

In primer walking, a specific primer that binds to a known sequence in the flanking DNA (e.g., vector sequence) is used to initiate a sequence run across the region of interest. Sequence data from the far end of the first run are used to prepare a second specific primer for a second run into the region of interest. This process can berepeated many times to sequence extensive tracts of DNA. For sequencing, 100-150 ng of purified plasmid DNA were used as template. The DNA was mixed with 2 µL of 10 µM primer and 2 µL of BigDye® Terminator Mix (Applied Biosystems) in a final volume of 10 µL. A thermal cycler was used to perform the following program:

96°C 1 min
35 cycles:
96°C 20 sec
X°C 10 sec , where X is the Tm of the primer minus 5°C
60°C 4 min

The synthesized DNA fragments were purified by adding 25 µL of 100% ethanol and incubating at RT for 10 min. The probes were centrifuged at 4000 rpm for 1 hr at RT. The supernatant was discarded and the DNA pellet was washed twice by adding 100 µL of ethanol and subsequent centrifugation at 4000 rpm for 30 min. Finally, the DNA pellet was vacuum-dried in a SpeedVac® (Thermo Electron Corporation) and handed to the service group for DNA sequencing at the MPIMG.

3.15.2 Analysis of sequences

The collection, editing, and assembly of the nucleotide sequences were performed using the Staden software package (Bonfield et al. 1995). The Staden package includes DNA sequence assembly, analysis, and comparison tools. Primers were generated with the primer selection algorithm OSP (Hillier and Green 1991), which is provided by the Staden package. Flanking vector sequences in DNA fragments were identified with the VecScreen program provided by the NCBI (http://www.ncbi.nlm.nih.gov/VecScreen/VecScreen.html). To corroborate the

linkage of a sequence to a specific gene, the data were analyzed with the Basic Local Alignment Search Tool (Altschul et al. 1990). The nucleotide sequences were translated to protein sequences using the Open Reading Frame Finder (http://www.ncbi.nlm.nih.gov/gorf/gorf.html) Finder provided by the NCBI. The ORF Finder is a graphical analysis tool that finds all possible open reading frames within a given sequence. The open reading frames were identified using the universal genetic code. Graphical presentation of nucleotide and deduced amino acid sequence was accomplished using the sequence editor package BioEdit (Hall 1999), which includes the PROTDIST program used for calculating distance matrices.

3.16 Phylogenetic analyses

The traditional objective of a phylogenetic tree is to represent the evolutionary relationship between species. In molecular phylogeny, an alignment of homologous genes usually is input into the tree reconstruction. The phylogeny of the species can be transferred from the gene tree, if the genes are orthologous. Methods for phylogeny reconstruction are classified according to their input data. Character based methods take as input a character state matrix. Examples for character based methods are Maximum-Parsimony (MP) and Maximum-Likelihood (ML). Distance based methods take as input a distance matrix, which is obtained by measuring the dissimilarities or the evolutionary distance between the taxa. Examples for distance based methods are UPGMA clustering and Neighbor-Joining (NJ).

For phylogenetic analysis the deduced amino acid sequence of amphioxus *Chordin* and further homologs of this gene family were selected from different organisms (see section 2.5). The amino acid sequences were then aligned using the progressive multiple sequence alignment program CLUSTAL W (Thompson et al. 1994). Protein domains and intermediate regions were separately re-aligned. The protein alignment was subjected to phylogenetic analysis using Neighbor-Joining (Saitou and Nei 1987) and quartet puzzling (Strimmer and von Haeseler 1996), a Maximum-Likelihood based tree reconstruction method.

To maximize the statistical significance of the phylogenetic trees generated by the character and the distance based methods, bootstrap analysis (Felsenstein 1992) was

performed using 1000 random replicates for each analysis. Bootstrapping is the most commonly used method to obtain a quantity telling us something about the uncertainty of tree reconstructions, but it provides no information about the reliability of the chosen tree estimation method. Given the tree estimation method the data is disturbed by sampling from the alignment and the stability of the outcome is checked. A new bootstrap replicate is generated by drawing columns from the original alignment at random with replacement. This is repeated until the bootstrap replicate contains as many columns as the original alignment. The tree estimation method is applied to all replicate in turn, yielding 1000 bootstrap trees each coming with a set of splits. Bootstrap values correspond to the relative frequency at which a split of the tree (estimated on the original alignment) occurred in the bootstrap replicates.

3.17 Riboprobe synthesis

RNA labeling can be done in several ways. *In vitro* transcription is a convenient method for labeling DNA fragments that are cloned into vectors with a MCS flanked by promoters for different RNA polymerases (e.g., SP6, T3, T7) with DIG-11-dUTP. The choice of the correct RNA polymerase is important for making anti-sense RNA probes (riboprobes) that can be used for *in situ* hybridization. Therefore, the correct orientation of the insert has to be known prior to selection of the enzyme for making RNA. To circumvent "run around" transcripts, the vector has to be linearized downstream of the sequence that is to be amplified.

3.17.1 Linearization of plasmid DNA

Plasmids were linearized by DNA digest with a restriction enzyme. The restriction site for the specific enzyme was chosen according to the vector maps in figure 2-1 and 2-2 in section 2.3. The pSPORT1 vector (Invitrogen) was digested with *EcoR*I: 2 µg of plasmid DNA were mixed with 1 µL of *EcoR*I (10 U/µL) and 2 µL of NE Buffer *EcoR*I. The pCR®II-TOPO® vector (Invitrogen) was digested with *Not*I: 2 µg of plasmid DNA were mixed with 1 µL of *Not*I (10 U/µL), 2 µL of NE Buffer 3,

and 2 µL of BSA (1 mg/mL). The solutions were made up to 20 µL with dH_2O and incubated at 37°C for at least 2 hrs.

3.17.2 Purification of digest

The linearized plasmid DNA was cleaned from the remaining enzyme and buffer with PCI, a mixture of phenol, chloroform, and isoamylalcohol (25:24:1). An equal volume of PCI was added and the sample was vortexed and subsequently centrifuged at 13,000 rpm for 1 min. The upper phase was transferred to a fresh microcentrifuge tube and DEPC-treated sodium acetate was added to a final concentration of 0.3 M. Two volumes of 100% ethanol were added and the DNA was allowed to precipitate at -20°C for at least two hours. After centrifugation at 13,000 rpm for 15 min, the supernatant was discarded and the DNA pellet was washed with 400 µL of 70% ethanol DEPC, and again centrifuged at 13,000 rpm for 15 min. The supernatant was discarded and the pellet was air-dried before it was finally dissolved in 20 µL of 1 mM sodium citrate solution pH 6.4.

3.17.3 In vitro transcription

To avoid RNase contamination, disposable plastic ware was used whenever possible. RNase-free water was prepared by stirring two times distilled water with 0.01% DEPC overnight, followed by autoclaving to break down the DEPC into H_2O and CO_2. All buffers and solutions used in the following were prepared using DEPC-treated water.

DIG-labeled anti-sense RNA probes were synthesized according to the following procedure: 1-2 µg of purified, linearized plasmid DNA was mixed with 2 µL of 10× DIG RNA Labeling Mix (Roche Diagnostics), 2 µL of 10× transcription buffer, 1 µL of RNasin (40 U/µL), and 1 µL of SP6 polymerase (20 U/µL). The mixture was made up to 20 µL with dH_2O DEPC, vortexed, centrifuged briefly, and incubated at 37°C for 2 hrs. The RNA was precipitated by adding 100 µL dH_2O DEPC, 10 µL of 4 M LiCl DEPC, 300 µL of pre-chilled 100% ethanol, and incubating at -20°C for at least two hours. The solution was then centrifuged at 13,000 rpm for 30 min at 4°C, the supernatant was discarded, and the RNA pellet was washed with 70% ethanol

DEPC. After centrifugation at 13,000 rpm for 30 min at 4°C, the pellet was briefly air-dried, and finally dissolved in 20 µL of 1 mM sodium citrate solution pH 6.4. The amount of RNA was estimated by agarose gel electrophoresis and diluted with hybridization buffer to a final concentration of 50 ng/µL. The diluted RNA was stored at -20°C until usage.

3.18 Whole-mount *in situ* hybridization

In situ hybridization is a significant method, which allows the localization of nucleic acids in tissues. In comparison to nucleic acid analysis using Southern or Northern blotting, the hybridization signal is not visualized on a membrane, but directly within a biological preparation sample. In whole-mount *in situ* hybridization a whole organism (e.g., an embryo) is used to detect the hybridization signal. Spatial and temporal expression of specific genes can be monitored in a sense *in vivo*. The visualization of patterns of gene expression in embryos is an essential technique for molecular analysis of development. Such patterns are revealed most accurately by *in situ* hybridization to mRNA (Holland et al. 1996). This technique has been used in cell and developmental biology since the early 1980s, and it has found widespread use because of its sensitivity and the speed with which specific probes can be produced from cloned cDNA or by the synthesis of oligonucleotides (Wilkinson and Nieto 1993).

Gene expression was studied by whole-mount *in situ* hybridization of developmental stages of *B. floridae* fixed at frequent intervals. The amphioxus embryos had been fixed in 4% paraformaldehyde and stored in 100% ethanol at -20°C to preserve tissue structure and terminate loss of target nucleic acids as describes in Holland et al. (1996). Fertilization envelopes of unhatched embryos were removed by gently pipetting up and down a few times to facilitate the penetration of reagents. All solutions were prepared with DEPC-treated, autoclaved water. All washes were done in 1.5 mL microcentrifuge tubes in a volume of 1 mL at RT for 5 min, if not stated otherwise.

3.18.1 Pre-hybridization

The embryos were transferred from 100% ethanol to PBT and washed twice with PBT. Proteinase K treatment was used to increase the permeability of the cells and to make them accessible for the riboprobe and the antibody. Proteinase K was added to a final concentration of 2 µg/mL and the embryos incubated at 37°C for 30 seconds to up to four minutes depending on the developmental stage of the embryos. Embryos fixed at earlier stages of development needed more incubation time than later fixed embryos. When the incubation time was very short and the embryos did not have enough time to sink to the tip of the tube, the sample was diluted with PBT and directly put on ice to prevent further activity of the enzyme. The embryos were washed twice with PBT and re-fixed in 4% PFA for one hour. The solution was subsequently exchanged with PBT three times. The embryos were washed once with 50% PBT/ 50% hybridization buffer and twice with 100% hybridization buffer. Following the washes the embryos were hybridized at 55°C for at least six hours to prevent unspecific binding of riboprobes.

3.18.2 Hybridization

Hybridization was done in a total volume of 150 µL. The DIG-labeled anti-sense RNA probe was added to the pre-hybridized embryos to a final concentration of 1 ng/µL. The tubes were mixed gently and the embryos hybridized overnight at 55°C.

3.18.3 Post-hybridization

The embryos were washed with 50% formamide/5× SSC/0.1% Tween®20, 50% formamide/2× SSC/0.1% Tween®20, and 50% formamide/1× SSC/0.1% Tween®20 in order to remove unspecifically bound probe. Each wash was done twice with prewarmed solutions at 55°C for 30 min. The solution was exchanged with PBT three times and the reaction was stopped by the addition of blocking solution and incubating overnight at 4°C. Blocking solution was prepared by dissolving 0.5 g of blocking reagent in 50 mL of PBT at 70°C. The solution was cooled down on ice and BSA was added to a final concentration 2 mg/mL. The solution was stored in

aliquots at -20°C and warmed to RT before use. After blocking, the embryos were washed once with PBT. The solution was exchanges for 250 µL of antibody solution and the embryos were incubated at RT for 2 hrs. The antibody solution was prepared by addition of 1.5 mg of amphioxus powder (ground up adult amphioxus) to 400 µL of PBT and heated to 70°C for 30 min. 50 µL of BSA (20 mg/mL), 50 µL of sheep serum, and 0.5 µL of antibody (Roche Diagnostics) were added and the solution was mixed well, heated to 37°C, and stored at overnight 4°C. The solution was centrifuged shortly and the supernatant was transferred to 1 mL of PBT containing 2 mg/mL BSA and 50 µL of sheep serum. Aliquots of the antibody solution were stored at -20°C and reused up to three times for the same probe as long as they were preserved at 4°C after defrosting them once. Incubation of the embryos with antibody solution was followed by three washes with PBT for 15 minutes each. The embryos were washed three times with freshly prepared APT for 10 min each. The APT was subsequently exchanged with 500 µL of stain solution and the embryos were transferred to a sterile 24 well cell culture microplate. The plates were stored in the dark and the staining process was monitored frequently. The staining was stopped by taking off the stain solution and adding 1 mL of PBT. After washing two more times with PBT the embryos were fixed in 4% PFA at 4°C overnight. The 4% PFA was exchanged for PBT three times and finally 100% glycerol was added to each well of the plate. The embryos were left at -4°C for at least one week to clear out before photographs were taken.

3.18.4 Photographic documentation

The embryos were analyzed with a MZ8 light microscope (Leica) and the expression patterns were subsequently documented using a LSM 510 laser scanning microscope (Carl Zeiss) and the AxioVision Image Viewer software from Carl Zeiss (http://www.zeiss.de/viewer). Images were edited using the Adobe Photoshop® program.

3.19 Tissue processing and preparation for sectioning

For closer examination under the light microscope, the tissue specimens were sectioned into thin sections. In particular, cross-sections were prepared from the embryos to permit analysis of staining of individual cells. To accomplish this, the tissues were embedded in LR Gold®, an acrylic resin. The specimens are fragile, porous, and very delicate, so they must be permeated with an appropriate material for thin sectioning.

3.19.1 Rinsing, specimen orientation, and dehydration

After the specimens were fixed in PFA, they were rinsed 2-3 times in PBT buffer for a total period of 10-20 minutes to remove all residual fixatives. The primary reason for this is to minimize possible reaction between the fixative and the dehydration agent.

In order to properly orient the specimens during embedding, so that sections can be cut in a known plane, the specimens were pre-embedded in 1% agar blocks. This step also ensured that enough embryo specimens are included in a section. 5 mL of 45°C warm 2% agar was added to the same volume of rinsed embryo specimen in a 1.5 mL tube. After solidification of the agar, the block was released from the tube and cut into two or three pieces with a clean razor blade on a microscopy slide. Unlike most resins used for embedding, acrylic resins like LR Gold® tolerate small proportions of water and are at least partially (up to 10%) miscible with water. Still, all the free water from the fixed and rinsed specimens was replaced with a suitable organic solvent before infiltration of the embedding medium. Therefore, the agar blocks were passed through a series of solutions of ascending concentrations of ethanol at RT: 25% ethanol for 10 min, 50% ethanol for 10 min, 75% ethanol for 10 min, 90% ethanol for 10 min, and three times 100% ethanol for 15 min.

3.19.2 Infiltration, embedding, and polymerization

A complete and uniform penetration of tissue specimens by the embedding medium is accomplished through infiltration and embedding. Infiltration involves gradual and continuous replacement of the dehydration reagent with an embedding medium, and embedding consists of a complete impregnation of the interstices of a tissue specimen with the medium. Embedding must precede sectioning because tissues are not sufficiently rigid to be cut into thin sections without the additional support of a resin matrix.

The agar blocks were infiltrated in a mixture of ethanol and LR Gold® (1:1) for two hours at RT, followed by two infiltration steps in pure LR Gold® at 4°C overnight. One more infiltration step was performed in LR Gold® with 0.1% benzil, which acts as a catalyst, at 4°C overnight. After changing the solution for fresh LR Gold® with 0.1% benzil, the specimens were embedded in gelatine capsules, placed under a 300 W lamp, and polymerized at 4°C for three days. The polymerized, cylindrical blocks obtained from the capsules were left for one week and cut with a diamond knife (Delaware Diamond Knives) using an Ultracut E ultramicrotome (Reichert-Jung). The sections were placed on microscope slides with a drop of 100% glycerol, covered with large cover slips, and examined as described in section 3.18.4.

4 RESULTS

4.1 Sequence analysis

The four contigs that resulted from the analysis of a database of sequence traces from JGI's *B. floridae* sequencing project (see section 3.6) provided a basis for primer design. The first primer set, 5'_GSP1 and 5'_NGSP1, was designed for the first matching region of contig 5 (see Table 3-2) and a 1,875 bp long DNA fragment was obtained by 5'RACE PCR and sequenced. Secondly, two additional primers, ExonB_FOR and BfChd_REV_C, were designed for the first matching region of contig 5 and the second matching region of contig 3/4, respectively. A PCR reaction using cDNA as a template produced an 850 bp long DNA fragment, which was sequenced and used to design a third primer set, GSP2 and NGSP2, for 3'RACE PCR. This second RACE PCR produced a 1,501 bp long DNA fragment with a poly-A sequence at one end. The RACE product was sequenced, too, showing an overlap of 514 bp with the 850 bp long DNA fragment. Finally, two primers, BfChdFW10 and BfChdREV7, that are located at the very 5' end and 3' end of the 5'RACE DNA fragment and the 3'RACE DNA fragment, respectively, were used in PCR to amplify a DNA fragment, which was cloned and sequenced.

4.1.1 Nucleotide and amino acid sequences

The cDNA of the amphioxus ortholog of the *Chordin* gene is 3,709 bp long and has canonical polyadenylation signal (AAUAAA) near its 3' end. The 5' and 3' UTRs are 137 and 617 bp long, respectively. The transcript is made up of 26 exons. The longest open reading frame encodes a putative protein of 984 amino acids with a signal sequence comprising the 18 N-termial amino acids as predicted by the TMpred program (Hofmann and Stoffel 1993). The protein further contains four internal repeats of 58 to 73 residues comprising ten cysteine residues at conserved positions. Five possible N-glycosylation sites (NXS/T) can be found within the protein sequence (Figure 4-1).

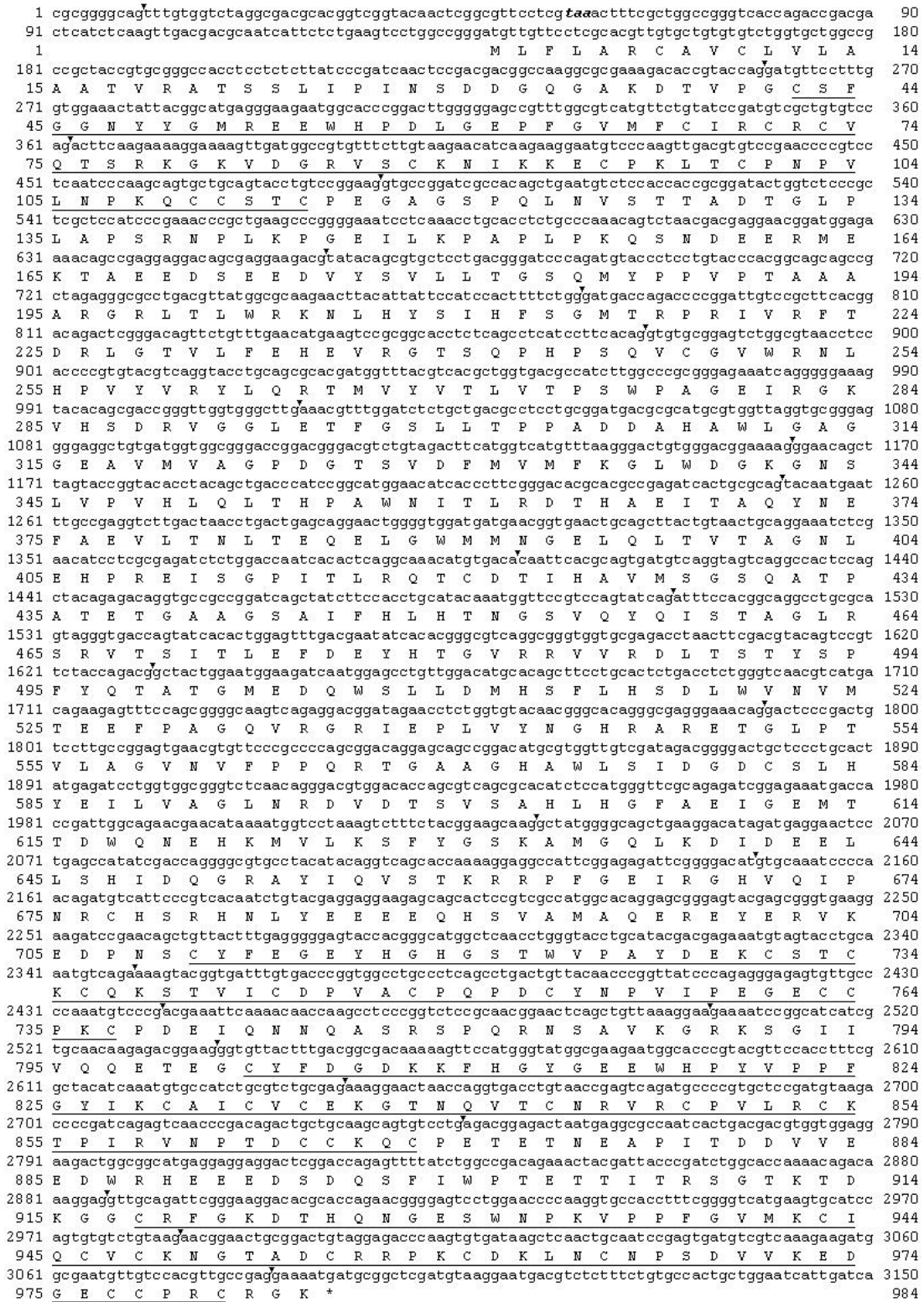
1 cgcggggcagtttgtggtctaggcgacgcacggtcggtacaactcggcgttcctcgtaaactttcgctggccgggtcaccagaccgacga 90
91 ctcatctcaagttgacgacgcaatcattctctgaagtcctggccgggatgttgttcctcgcacgttgtgctgtgtgtctggtgctggccg 180
1 M L F L A R C A V C L V L A 14
181 ccgctaccgtgcgggccacctcctctcttatcccgatcaactccgacgacggccaaggcgcgaaagacaccgtaccaggatgttcctttg 270
15 A A T V R A T S S L I P I N S D D G Q G A K D T V P G C S F 44
271 gtggaaactattacggcatgagggaagaatggcacccggacttgggggagccgtttggcgtcatgttctgtatccgatgtcgctgtgtcc 360
45 G G N Y Y G M R E E W H P D L G E P F G V M F C I R C R C V 74
361 agacttcaagaaaaggaaaagttgatggccgtgtttcttgtaagaacatcaagaaggaatgtcccaagttgacgtgtccgaaccccgtcc 450
75 Q T S R K G K V D G R V S C K N I K K E C P K L T C P N P V 104
451 tcaatcccaagcagtgctgcagtacctgtccggaaggtgccggatcgccacagctgaatgtctccaccaccgcggatactggtctcccgc 540
105 L N P K Q C C S T C P E G A G S P Q L N V S T T A D T G L P 134
541 tcgctccatcccgaaacccgctgaagcccggggaaatcctcaaacctgcacctctgcccaaacagtctaacgacgaggaacggatggaga 630
135 L A P S R N P L K P G E I L K P A P L P K Q S N D E E R M E 164
631 aaacagccgaggaggacagcgaggaagacgtatacagcgtgctcctgacgggatcccagatgtaccctcctgtacccacggcagcagccg 720
165 K T A E E D S E E D V Y S V L L T G S Q M Y P P V P T A A A 194
721 ctagagggcgcctgacgttatggcgcaagaacttacattattccatccacttttctgggatgaccagaccccggattgtccgcttcacgg 810
195 A R G R L T L W R K N L H Y S I H F S G M T R P R I V R F T 224
811 acagactcgggacagttctgtttgaacatgaagtccgcggcacctctcagcctcatccttcacaggtgtgcggagtctggcgtaacctcc 900
225 D R L G T V L F E H E V R G T S Q P H P S Q V C G V W R N L 254
901 accccgtgtacgtcaggtacctgcagcgcacgatggtttacgtcacgctggtgacgccatcttggcccgcgggagaaatcaggggggaaag 990
255 H P V Y V R Y L Q R T M V Y V T L V T P S W P A G E I R G K 284
991 tacacagcgaccgggttggtgggcttgaaacgtttggatctctgctgacgcctcctgcggatgacgcgcatgcgtggttaggtgcgggag 1080
285 V H S D R V G G L E T F G S L L T P P A D D A H A W L G A G 314
1081 gggaggctgtgatggtggcgggaccggacgggacgtctgtagacttcatggtcatgtttaagggactgtgggacggaaaaggaacagct 1170
315 G E A V M V A G P D G T S V D F M V M F K G L W D G K G N S 344
1171 tagtaccggtacacctacagctgacccatccggcatggaacatcacccttcgggacacgcacgccgagatcactgcgcagtacaatgaat 1260
345 L V P V H L Q L T H P A W N I T L R D T H A E I T A Q Y N E 374
1261 ttgccgaggtcttgactaacctgactgagcaggaactggggtggatgatgaacggtgaactgcagcttactgtaactgcaggaaatctcg 1350
375 F A E V L T N L T E Q E L G W M M N G E L Q L T V T A G N L 404
1351 aacatcctcgcgagatctctggaccaatcacactcaggcaaacatgtgacacaattcacgcagtgatgtcaggtagtcaggccactccag 1440
405 E H P R E I S G P I T L R Q T C D T I H A V M S G S Q A T P 434
1441 ctacagagacaggtgccgccggatcagctatcttccacctgcatacaaatggttccgtccagtatcagatttccacggcaggcctgcgca 1530
435 A T E T G A A G S A I F H L H T N G S V Q Y Q I S T A G L R 464
1531 gtagggtgaccagtatcacactggagtttgacgaatatcacacgggcgtcaggcgggtggtgcgagacctaacttcgacgtacagtccgt 1620
465 S R V T S I T L E F D E Y H T G V R R V V R D L T S T Y S P 494
1621 tctaccagacggctactggaatggaagatcaatggagcctgttggacatgcacagcttcctgcacctctgacctctgggtcaacgtcatga 1710
495 F Y Q T A T G M E D Q W S L L D M H S F L H S D L W V N V M 524
1711 cagaagagtttccagcggggcaagtcagaggacggatagaacctctggtgtacaacgggcacagggcgagggaaacaggactcccgactg 1800
525 T E E F P A G Q V R G R I E P L V Y N G H R A R E T G L P T 554
1801 tccttgccggagtgaacgtgttcccgccccagcggacaggagcagccggacatgcgtggttgtcgatagacggggactgctccctgcact 1890
555 V L A G V N V F P P Q R T G A A G H A W L S I D G D C S L H 584
1891 atgagatcctggtggcgggtctcaacagggacgtggacaccagcgtcagcgcacatctccatgggttcgcagagatcggagaaatgacca 1980
585 Y E I L V A G L N R D V D T S V S A H L H G F A E I G E M T 614
1981 ccgattggcagaacgaacataaaatggtcctaaagtctttctacggaagcaaggctatggggcagctgaaggacatagatgaggaactcc 2070
615 T D W Q N E H K M V L K S F Y G S K A M G Q L K D I D E E L 644
2071 tgagccatatcgaccaggggcgtgcctacatacaggtcagcaccaaaaggaggccattcggagagattcggggacatgtgcaaatcccca 2160
645 L S H I D Q G R A Y I Q V S T K R R P F G E I R G H V Q I P 674
2161 acagatgtcattcccgtcacaatctgtacgaggaggaagagcagcactccgtcgccatggcacaggagcgggagtacgagcgggtgaagg 2250
675 N R C H S R H N L Y E E E E Q H S V A M A Q E R E Y E R V K 704
2251 aagatccgaacagctgttacttttgaggggggagtaccacgggcatggctcaacctgggtacctgcatacgacgagaaatgtagtacctgca 2340
705 E D P N S C Y F E G E Y H G H G S T W V P A Y D E K C S T C 734
2341 aatgtcagaaaagtacggtgatttgtgacccggtggcctgccctcagcctgactgttacaacccggttatcccagagggagagtgttgcc 2430
K C Q K S T V I C D P V A C P Q P D C Y N P V I P E G E C C 764
2431 ccaaatgtcccgacgaaattcaaaacaaccaagcctcccggtctccgcaacggaactcagctgttaaaggaagaaaatccggcatcatcg 2520
735 P K C P D E I Q N N Q A S R S P Q R N S A V K G R K S G I I 794
2521 tgcaacaagagacggaagggtgttacttttgacggcgacaaaaagttccatgggtatggcgaagaatggcacccgtacgttccacctttcg 2610
795 V Q Q E T E G C Y F D G D K K F H G Y G E E W H P Y V P P F 824
2611 gctacatcaaatgtgccatctgcgtctgcgagaaaggaactaaccaggtgacctgtaaccgagtcagatgccccgtgctccgatgtaaga 2700
825 G Y I K C A I C V C E K G T N Q V T C N R V R C P V L R C K 854
2701 ccccgatcagagtcaacccgacagactgctgcaagcagtgtcctgagacggagactaatgaggcgccaatcactgacgacgtggtggagg 2790
855 T P I R V N P T D C C K Q C P E T E T N E A P I T D D V V E 884
2791 aagactggcggcatgaggaggaggactcggaccagagttttatctggccgacagaaactacgattacccgatctggcaccaaaacagaca 2880
885 E D W R H E E E D S D Q S F I W P T E T T I T R S G T K T D 914
2881 aaggaggttgcagattcgggaaggacacgcaccagaacggggagtcctggaaccccaaggtgccacctttcggggtcatgaagtgcatcc 2970
915 K G G C R F G K D T H Q N G E S W N P K V P P F G V M K C I 944
2971 agtgtgtctgtaagaacggaactgcggactgtaggagacccaagtgtgataagctcaactgcaatccgagtgatgtcgtcaaagaagatg 3060
945 Q C V C K N G T A D C R R P K C D K L N C N P S D V V K E D 974
3061 gcgaatgttgtccacgttgccgaggaaaatgatgcggctcgatgtaaggaatgacgtctctttctgtgccactgctggaatcattgatca 3150
975 G E C C P R C R G K * 984
3151 gcggtgtgaggaggggtgattctctgtactatgacttccactgccaacagcaatgtttcatatgttctctcacatgtaacgaatagttg 3240
3241 gaaacaccttatgtaactgttttatactcaagttttaccctctccgaaacatcttcaagagggccttgcatgtatccccctcaagctacgt 3330
3331 gaagatagcatactaaatgtatatgatgttagataactaataagacacaccggtcccatacattcgtagtaacttgctagatgctctcag 3420
3421 catgacattacggtttctaccttgagttgggtgtttgcctgtaaaatcttcatcaagtgtctctatttttgtctcacctaattattattga 3510
3511 tggacagtagatagcgagccacacttttgacagtttgttatcttggtcacctttatgcgtgccatgcacaaagcgattgattgtgagtga 3600
3601 taacaatgatgacaaatgacaagcgtaaaacatattgattttatttattccattagtagacgactatacaataaattgatatttcacaaa 3690
3691 aaaaaaaaaaaaaaaaaaa 3709

Figure 4-1. Nucleotide and deduced amino acid sequence of the amphioxus Chordin cDNA.

The in-frame stop codon preceding the presumed translational start site is shown in bold and italics as is the canonical polyadenylation signal. An asterisk indicates the stop codon at the 3' end of the longest ORF. Upside down triangles represent the intron positions. The four internal cysteine-rich repeats are underlined.

4.1.2 Protein alignment

The spacing between the cysteine-rich (CR) repeats of the amphioxus Chordin protein resembles that of homologous Chordin proteins in other species: One CR-repeat (CR1) is located in the N-terminus and the three others (CR2 to CR4) are located in tandem at the C-terminus of the protein. These CR-repeats are also known as von Willebrandt factor type C (vWC) domains. First, vWC domains are mainly defined by a consensus of ten cysteines. Second, a conserved glycine and an aromatic residue, often tryptophan, are typically found between the first pair of cysteine residues. Third, the motifs $C_2XXC_3XC_4$ and $C_8C_9XXC_{10}$, located in the middle and at the C-terminal end of the repeat, are also highly conserved (O'Leary et al. 2004). Each CR repeat of the amphioxus Chordin was clearly identified as a vWC domain by multiple sequence alignment meeting all three conditions (Figure 4-2). vWC domains are well conserved between different species and also occur in a variety of extracellular proteins other than Chordin (Abreu et al. 2002).

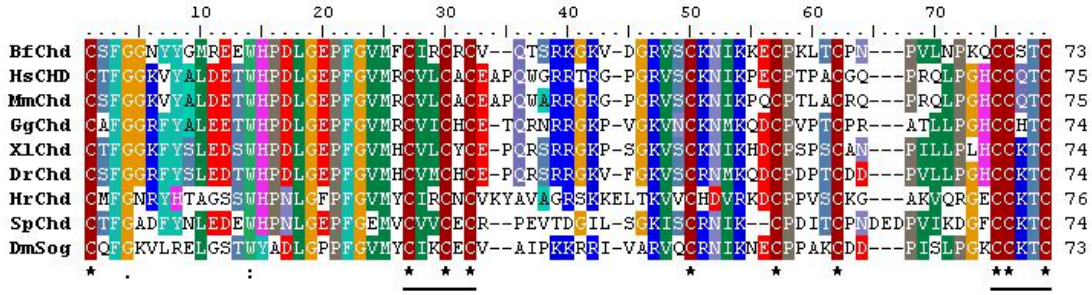

Figure 4-2. Multiple sequence alignment of the first CR repeat of selected Chordin proteins.

The alignment was generated with the CLUSTAL W program (Thompson et al. 1994). The conserved cysteines are marked by asterisks. The conserved glycine and tryptophan residues between the first two cysteines are marked by "." and ":", respectively. The conserved motifs $C_2XXC_3XC_4$ and $C_8C_9XXC_{10}$ are underlined. For database accession numbers see Table 2-17. Bf, *Branchiostoma floridae*; Dm, *Drosophila melanogaster*; Dr, *Danio rerio*; Gg, *Gallus gallus*; Hr, *Halocynthia roretzi*; Hs, *Homo sapiens*; Mm, *Mus musculus*; Sp, *Strongylocentrotus purpuratus*; Xl, *Xenopus laevis*.

4.1.3 Intron/exon organization

The Ensembl website contains annotation on selected eukaryotic genomes (Hubbard et al. 2005). Sequence data were collected and intron positions in coding sequences of Chordin homologs determined for *D. melanogaster*, *C. intestinalis*, and *H. sapiens*. The intron position for amphioxus Chordin were obtained by blasting its cDNA against the WGS sequence data from *B. floridae* sequencing project in the trace archives of the NCBI. Detailed alignment evaluation was used to correctly identify the homologous intron positions (Figure 4-3).

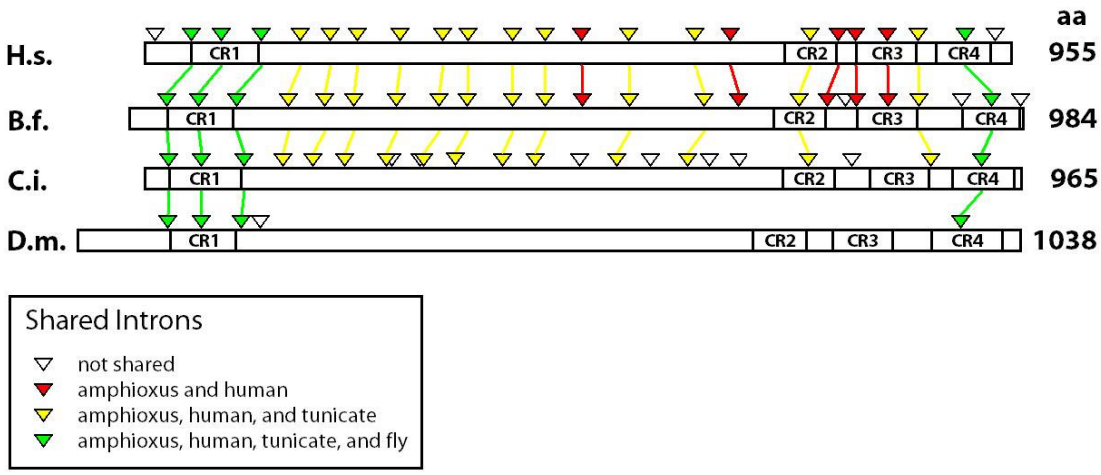

Figure 4-3. Intron positions of Chordin proteins from selected species.

The number of amino acids in each protein is indicated on the right. Shared introns are connected by colored lines. Each protein contains four CR repeats (CR1-CR4). Abbreviations are used as in Figure 4-2.

The number of introns in the coding region of *Chordin* homologs varies from five in *Drosophila* to a high of 24 in amphioxus. Human and ascidian *Chordin* have both 23 introns. The intron positions are highly conserved among the three deuterostome Chordin genes, with 21 shared between human and amphioxus and 16 shared between human and *Ciona*, and between amphioxus and *Ciona*. Only four introns are shared between human, amphioxus, *Ciona* and *Drosophila*. *Ciona* has the highest number of unique introns that are not shared reflecting the high degree of genomic divergence in this species.

4.1.4 Phylogenetic analysis

A multiple sequence alignment served as the basis for tree calculations. The full-length protein sequence of amphioxus Chordin was aligned with homologous protein sequences from other species using the multiple sequence alignment program CLUSTAL W (Thompson et al. 1994). The CR domains and the regions in between those were separately re-aligned. A phylogenetic tree generated with a maximum likelihood approach and 1000 bootstrap replicates using the TREE-PUZZLE program (Schmidt et al. 2002) clearly places amphioxus Chordin in the context of the Chordin protein family (Figure 4-4).

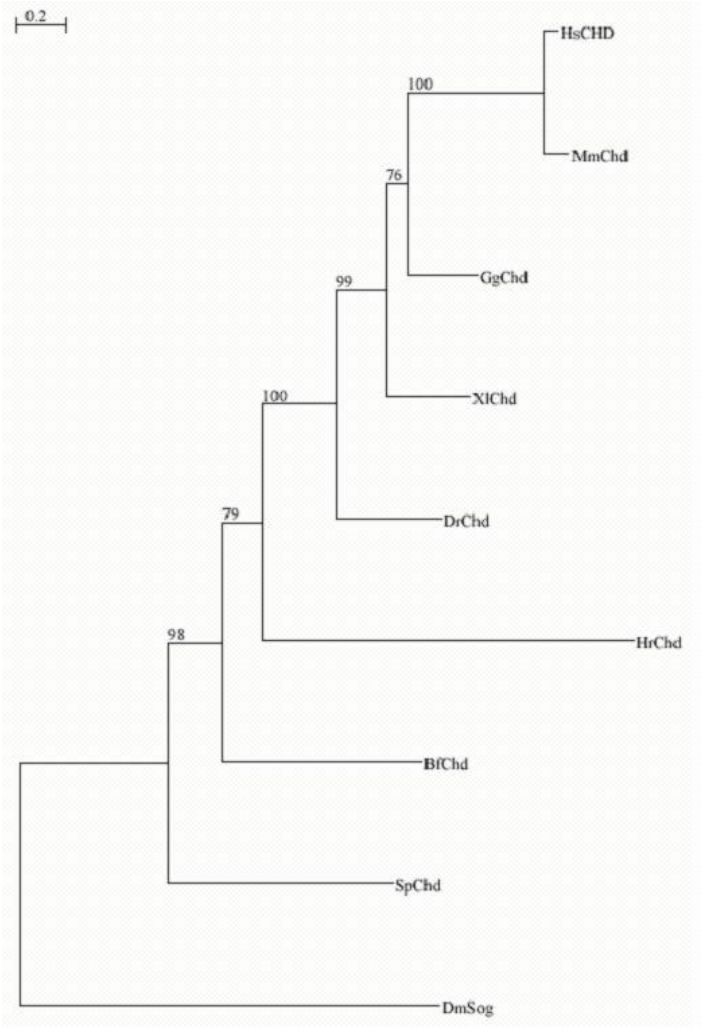

Figure 4-4: Phylogenetic tree of selected Chordin proteins from different species.

The values at the branching points are bootstrap percentages. Sequence distance is indicated at the top as the number of substitutions per site. DmSog is displayed as the outgroup. Abbreviations are used as in Figure 4-2.

The tree has a very strong bootstrap support for the vertebrate (100%) and chordate (98%) clade. However, different from the commonly accepted phylogeny based on morphological characters, the ascidian ortholog is closer to the vertebrate Chordin proteins than the amphioxus ortholog. This branching order is supported by a bootstrap support of 79% and 98% for the ascidian-vertebrate and amphioxus-(ascidian + vertebrate) branches, respectively. Notably, the branch length of ascidian Chordin is very long compared to the branch lengths of the other deuterostome Chordin proteins indicating the high sequence divergence for this protein. The Chordin homolog Sog from *D. melanogaster* is displayed as the outgroup.

4.2 Developmental expression

Chordin expression during amphioxus development was analyzed by whole mount *in situ* hybridization. A piece spanning the most 5' region of the gene was used as probe. For the other genes the cloned full-length cDNAs served as templates.

4.2.1 Expression of Chordin in untreated embryos

Transcripts of amphioxus *Chordin* were detected at the midgastrula stage (Figure 4-5A, B), strongly in the hypoblast of the dorsal blastopore, which will form the notochord and the overlying ectoderm, which will form neural tissue. The dorsal blastopore is thought to induce both the formation of neuroectoderm and influences anteroposterior neural patterning. By the late gastrula stage when the neural folds begin to form, the expression continues in the axial mesoderm, the presumptive notochord domain (Figure 4-5C-E). In the early neurula stage, when the epidermis has largely roofed over the neural plate expression of amphioxus *Chordin* is prominent in the entire notochord and in the overlying floor plate, which forms the bottom of the neural tube (Figure 4-5F-H). As neurulation proceeds and the embryo elongates, the expression domains within the notochord and floor plate stay strong (Fig. 4-5I-K). By the midneurula stage, the expression of amphioxus *Chordin* becomes down regulated in the posterior cells of the neural plate and starts to fade from the anterior region of the notochord. As a result the *Chordin* expression domains in the neural tube and in the notochord do not overlay each other. *Chordin*

expression in the neural tube is restricted in ventral and lateral regions of the neural plate (Figure4-5L-N). Later in the mid-neurula, only cells of the notochord in a region at the posterior end of the embryo, the tailbud, and of the anterior half of the nerve cord still show expression (Figure 4-5O-R). However, the signal from the neural cells has lost intensity at this stage of development. In later neurula stages, expression completely fades within one hour (between 17.3 hrs and 18.3 hrs) from these remaining domains and transcripts are no longer detectable.

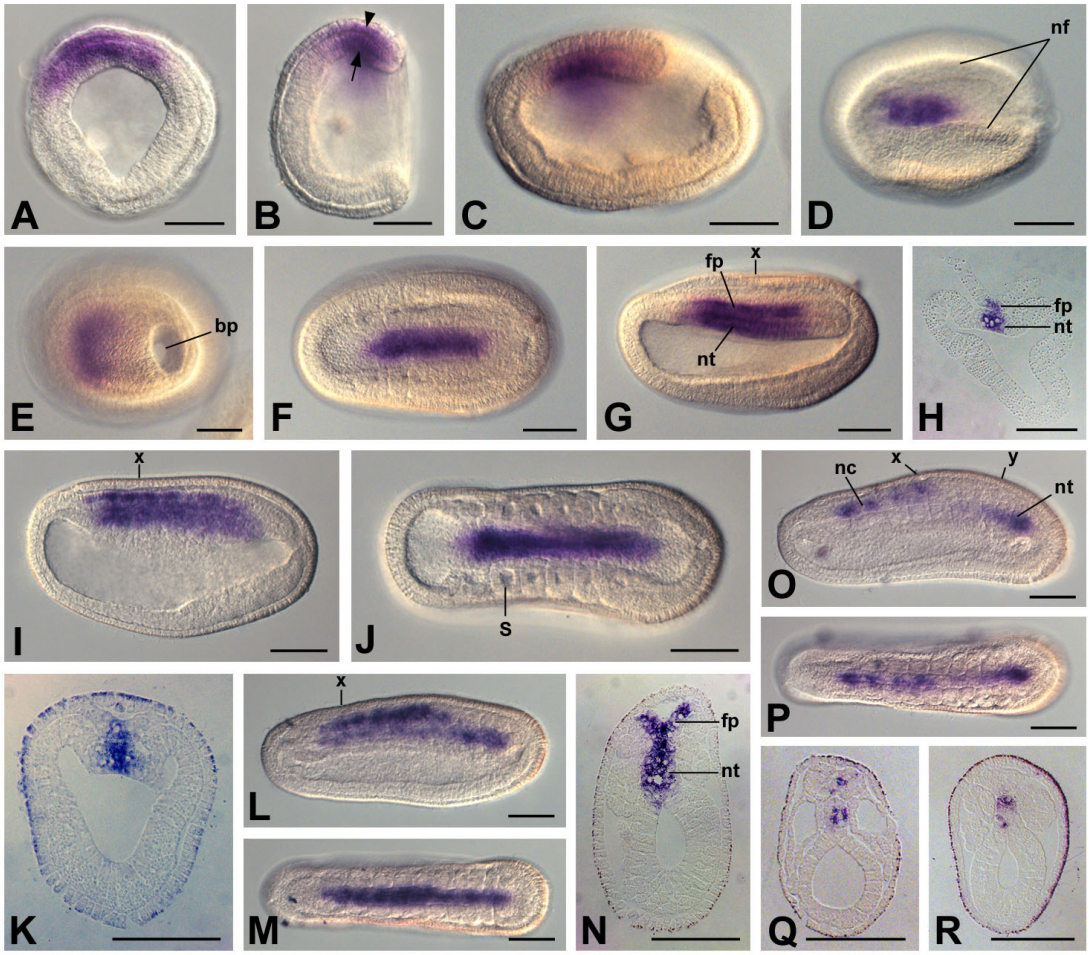

Figure 4-5. Embryonic and larval expression of amphioxus Chordin in *B. floridae* in whole mounts.

For side and dorsal view of whole mounts anterior is towards the left. Scale is 50 µM. (A) Blastopore view of 6 hrs embryo with expression in hypoblast of the dorsal blastopore and in the overlying ectoderm. Dorsal side is up. (B) Side view of the embryo in (A). (C) Side view of 8.3 hrs embryo with expression in the axial mesoderm (presumptive notochord) but not in the ectoderm. (D) Tilted dorsal view of the embryo in (C) with the forming neural folds and expression in the axial mesoderm. (E) Dorsal view of the embryo in (C). (F) Dorsal view of 10 hrs embryo with expression in the axial mesoderm and floor plate. (G) Side view of the embryo in (F). (H) Cross-section through level x of the embryo in (G) with expression in the notochord and the floor plate. (I) Side view of 14 hrs embryo with expression in the

notochord and floor plate. (J) Dorsal view of the embryo in (I). (K) Cross-section through level x of the embryo in (I) with expression in the notochord and floor plate. (L) Side view of 17.3 hrs embryo with weak expression in the notochord, more strong expression in the posterior notochord, and strongest expression in the anterior half of the forming nerve cord. (M) Dorsal view of the embryo in (L). (N) Cross-section through level X of the embryo in (L) with expression in the notochord and floor plate. (O) Side view of 18 hrs embryo with expression in the posterior region of the notochord and weaker expression in the anterior half of the nerve cord. (P) Dorsal view of the embryo in (O). (Q) Cross section through level x in (O) with expression in the notochord and nerve cord. (R) Cross section through level y in (O) with expression in the notochord.

4.2.2 Expression of Chordin in LiCl-treated embryos

In amphioxus embryos that were raised in seawater containing 50 mM of lithium chloride the expression of amphioxus *Chordin* in midgastrula-stage embryos shifts towards the animal pole of the embryo and is only visible in the epiblast (Figure 4-6A, B). The ectoderm in these embryos does not properly invaginate through the edges of the blastopore. Through this the embryos become bell-shaped by the end of gastrulation with strong expression of *Chordin* in the ectoderm of the animal half of the embryo (Figure 4-6C, D).

Embryos that were treated with 300 mM of lithium chloride for 20 minutes during late blastula stages have an approximately normal appearance during gastrulation and the cells of the dorsal margin of the blastopore expresses amphioxus *Chordin* within the epi- and hypoblast. Later on the development some embryos do not properly elongate and the neural folds do not form, to roof over the embryo (Figure 4-6G, H). Other embryos show more elongation and neural fold formation but the neural folds fail to close over the embryo and the blastopore remains open (Figure 4-6I, J). The expression of *Chordin* in these embryos is detectable in the axial dorsal mesoderm and in the overlying ectoderm.

Embryos that were treated with 500 mM of lithium chloride have a delayed gastrula phenotype and show strong expression of *Chordin* within the epi- and hypoblast of the dorsal blastopore (Figure 4-6K). As these embryos neurulate they fail to properly elongate which can be seen by the compressed axial mesoderm, which is marked by the expression of *Chordin*. In addition, a protrusion forms from the ectoderm at one side of the blastopore (Figure 4-6L).

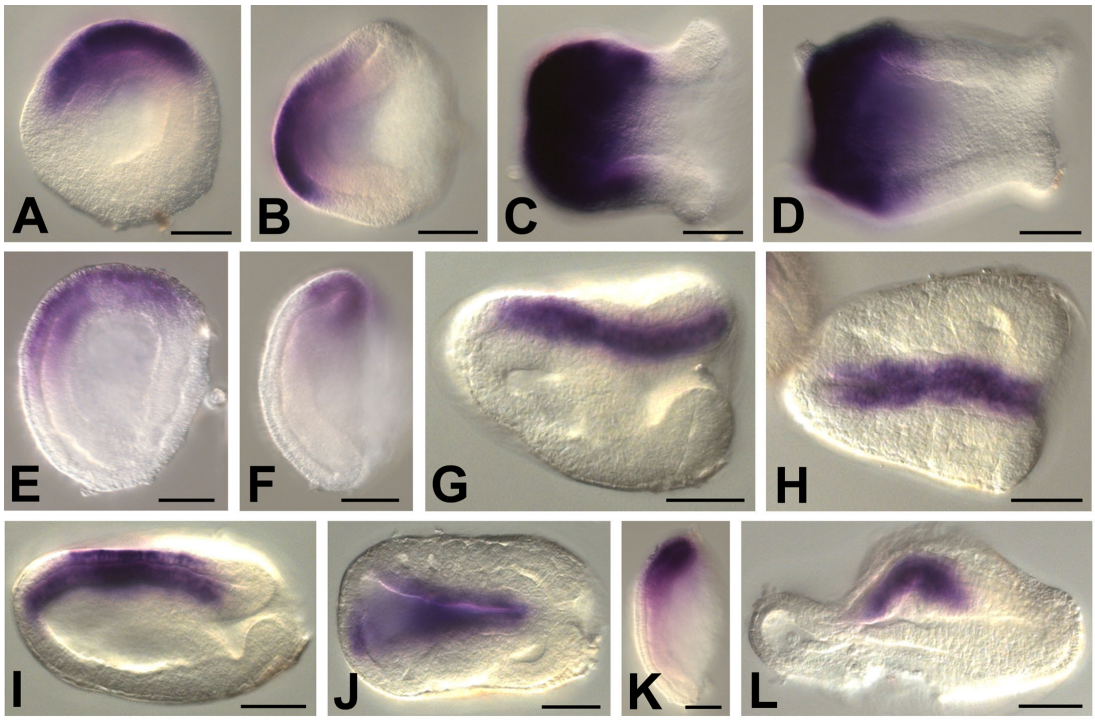

Figure 4-6. Spatial distribution of Chordin in lithium chloride treated B. floridae in whole mounts.

For side and dorsal view of whole mounts anterior is towards the left. Scale is 50 µM. (A)-(D) treated with 50 mM if lithium chloride continuously; (E)-(J) and (K)-(L) treated pulsed with 300 mM and 500 mM of lithium chloride, respectively. (A) Dorsal view on blastopore of 6 hrs embryo with expression in the epiblast at the animal pole. (B) Side view of the embryo in (A). The surface ectoderm does not properly invaginate. (C) Side view of 10.5 hrs embryo with strong expression in the ectoderm of the animal half. The surface ectoderm is bent outwards around the blastopore. (D) Embryo of the same stage as in C with less strong phenotype. (E) Blastopore view of 6 hrs embryo with expression in the epi- and hypoblast of the dorsal blastopore. (F) Side view of the embryo in (E). (G) Side view of 13 hrs embryo with expression in the dorsal mesoderm. Neural folds have not roofed over the neural plate and blastopore is open. (H) Dorsal view of the embryo in (G). (I) Side view of 13 hrs embryo with expression in the dorsal mesoderm and the overlying ectoderm. The blastopore is open. (J) Dorsal view of the embryo in (I). The neural folds have begun to roof over the neural plate but have not closed anteriorly. (K) Side view of 6 hrs embryo with expression in the dorsal blastopore. (L) Side view of 13 hrs embryo with expression in the compressed axial mesoderm.

4.2.3 Expression of downstream targets of β-catenin and/or D-V patterning genes up to late gastrulation

To estimate how early the dorsoventral axis is established in the amphioxus embryo, we analyzed the spatial distribution of genes that are supposedly downstream of the maternal β-catenin signal and/or are involved in D-V axis specification. We chose

the following eight genes: the organizer genes *goosecoid*, *Chordin*, *Dickkopf*, and *lefty* which are all downstream of the β-catenin signal and whose products partially antagonize BMP2/4 and Wnt8 which promote ventral fates. *SoxB1* and *SoxB2* are early neural specific genes and *FoxQ2* exclusively marks the anterior ectoderm during early stages of development.

FoxQ2, which marks the anterior ectoderm consistently during early gastrulation, is expressed from the blastula stage on (4.5 hrs) marking the entire ectoderm up to the onset of gastrulation (5.5 hrs). During gastrulation its expression becomes restricted to the dorsal-anterior ectoderm (6.0 hrs). The neural specific-genes, *SoxB1* and *SoxB2,* become expressed in the ectoderm roughly at the same time (5.5 hrs). Both genes mark the neural ectoderm but *SoxB2* also marks anterior ectoderm, in a region reminiscent of *FoxQ2* expression. By the end of gastrulation (8.5 hrs) *SoxB1* marks the dorsal ectoderm and involuting mesendoderm while *SoxB2* is only marking dorsal ectoderm. After a broad distribution throughout the embryo *goosecoid* becomes strongly expressed at the dorsal one-third of the mesendodermal cells at the midblastula stage (4.5 hrs) before the onset of gastrulation. As gastrulation proceeds (6 hrs) *goosecoid* expression marks the axial dorsal mesoderm from which the notochord will arise. An asymmetric expression of *Chordin* can be observed in the early blastula (3.5 hrs) at the dorsal side of the mesendoderm and adjacent ectoderm. The dorsal expression of *Chordin* persists throughout development. *Bmp2/4* is ubiquitously expressed at the blastula stage but becomes confined to the flattening endodermal plate at the onset of gastrulation (5.5 hrs). During later stages of gastrulation *Bmp2/4* marks the entire hypoblast with strongest expression in the regions where the presomitic grooves will form. *Dickkopf* expression is most strongly in the nuclei of cells on the dorsal part of the mesendoderm at the early blastula stage (3.5 hrs) but then forms a ring around the blastopore that is approximately three cells wide (5.5 hrs). During later gastrula stages *Dickkopf* expression becomes restricted to the dorsal and ventral sides of the blastopore. At the midblastula stage *Wnt8* is expressed in the ectoderm adjacent to the mesendoderm (4.5 hrs). During gastrulation *Wnt8* expression circumvents the blastopore (6.0 hrs) and, as cells move inside the embryo, marks the paraxial mesoderm from which the somites will arise (8.5 hrs). Finally, *lefty* expression becomes confined to the dorsal

ectoderm at the blastula stage (4.5 hrs) and shows a conspicuous left/right asymmetry at the gastrula stage (6.0 hrs) with expression extending more towards the left in the ectoderm. During late gastrula stages (8.5 hrs) the dorsal mesoderm, in addition to the dorsal ectoderm, expresses *lefty*.

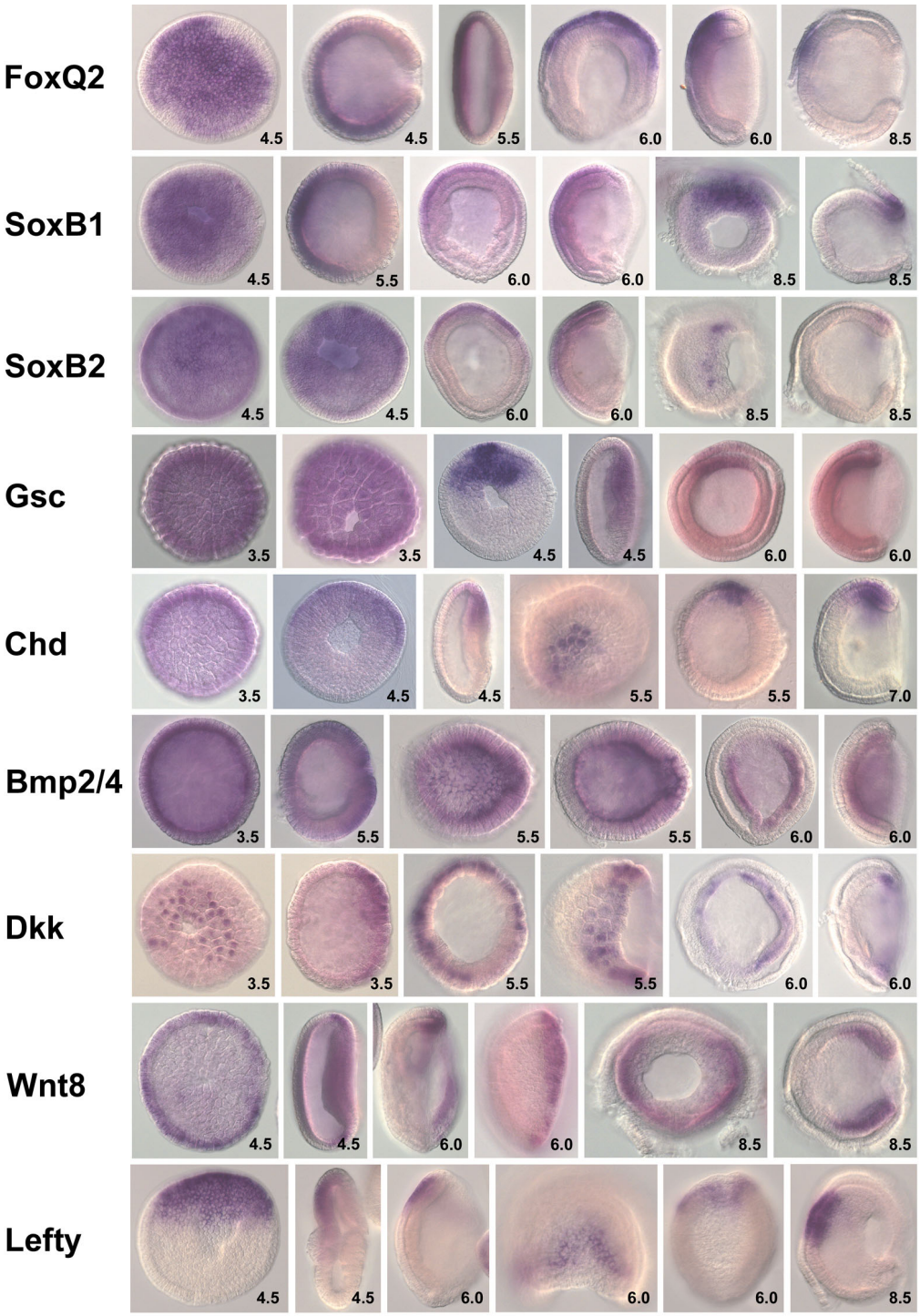

Figure 4-7. Spatial distribution of developmental genes involved in D-V patterning and/or neural specification up to the late gastrula stage.

Thus, the amphioxus embryo shows asymmetric expression before the onset of gastrulation for *goosecoid*, *Chordin*, *Dickkopf*, *lefty* and *Wnt8*. While the organizer-specific genes are being expressed on the dorsal side of the embryo, indicating that a considerable amount of D-V polarity becomes defined by those genes before the onset of gastrulation. *Wnt8* expression is restricted to the posterior ectoderm adjacent to the mesendoderm. This latter expression shows that an A-P polarity exists in the early embryo before the onset of gastrulation.

4.2.4 Effect of LiCl treatments on downstream targets of β-catenin and/or D-V patterning genes

We extracted RNA from untreated embryos at the midgastrula stage and from treated embryos at the midgastrula stage that were either subjected to a lower concentration of lithium chloride continuously during development or to a higher concentration for 20 minutes at the late blastula stage. This RNA was reverse transcribed and subjected to QPCR analysis for the following ten genes: *β-catenin*, *Wnt8*, *goosecoid*, *Chordin*, *Bmp2/4*, *Noggin*, *SoxB1*, *FoxQ2*, *Sox1/2/3*, and *Dickkopf*. We first analyzed the expression level of the ten genes in comparison to the expression level of cytoplasmic *β-actin*, a housekeeping gene with a constant expression level that we also used to normalize our data (Figure 4-8).

In untreated embryos the *Bmp2/4* expression level is about 25% of that of *β-actin*, whereas the *Chordin* expression level is much lower with only 6-7%. The expression level of another BMP antagonist *Noggin* is less than 0.01% of the expression level of *β-actin*. The expression levels of the neural-specific genes differ markedly: the *Sox1/2/3* expression level is as high as the expression level of the housekeeping gene and the expression level of *SoxB1* is only 0.5%. *goosecoid* and *Wnt8* expression levels are both about 30% and the *Dickkopf* expression level much lower at 7%. The expression level of *FoxQ2* is at 70% and that of *β-catenin* at 2-3%.

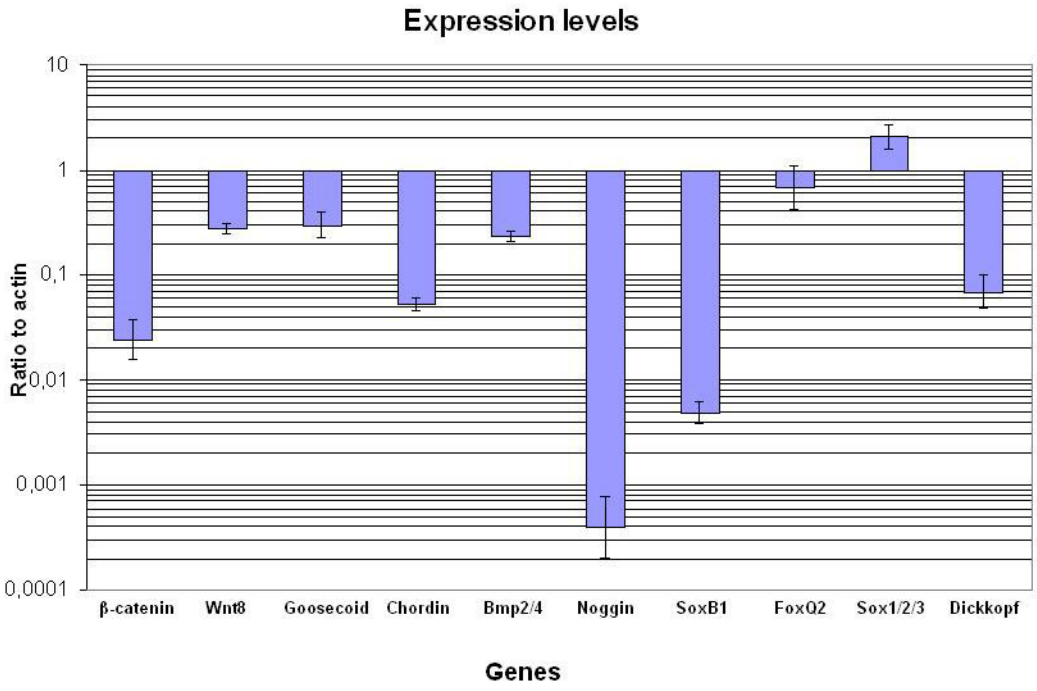

Figure 4-8. Differences in levels of expression of ten genes in comparison to a house keeping gene in midgastrula stage embryos.

The blue bars display the fold-difference of expression levels in comparison to the expression level of the housekeeping gene (cytoplasmic *β-actin*). A log scale is used to display the fold-differences on the y-axis.

Second, we analyzed the expression levels of the ten genes in lithium-treated embryos and compared them to the expression levels in untreated embryos (Figure 4-9). Lithium is known to upregulate Wnt signaling by inhibiting GSK3β, thereby freeing β-catenin from degradation and allowing its translocation into the nucleus.

The expression level of *FoxQ2* in continuously treated embryos is reduced by more than 80% and confirms that the continuous treatment posteriorizes the embryos. The change in expression level is not as significant for the pulsed treated embryos, where *FoxQ2* expression is reduced by only 30%. The expression of the neural specific gene, *Sox1/2/3*, in continuously treated embryos is about 30% of its expression in untreated embryos, indicating that the neural domain is reduced as previously proposed by Holland et al. (2005). There is little difference in expression level between normal and pulsed-treated embryos. Only a minor change in the expression level of the second neural promoting factor, *SoxB1*, which is expressed at a very low level in comparison to *Sox1/2/3*, is observed in continuously treated embryos.

Consistently, the expression level of *Bmp2/4* in continuously treated embryos is more than doubled, which points at an enlargement of the non-neural ectoderm at the expense of neural ectoderm. The expression of *Dickkopf* is more than four-fold upregulated in the continuously treated embryos suggesting that a negative feed-back loop of Wnt signaling might exist that inhibits canonical Wnt pathway via the activation of *Dickkopf*. The expression level of *Chordin* is less than 70% and 50% of its normal expression in continuously treated embryos and pulsed-treated embryos, respectively. The downregulation of this neural inducing/maintaining factor might be another reason for the reduction of neural tissue. In continuously treated embryos *Wnt8* expression is reduced to 60%, whereas *goosecoid* expression is slightly enhanced. Due to high error values the gene expression levels of *β-catenin* and *Noggin* are insignificant. In conclusion, the pulsed lithium treatment did not produce as significant changes in gene expression levels as the continuous lithium treatment.

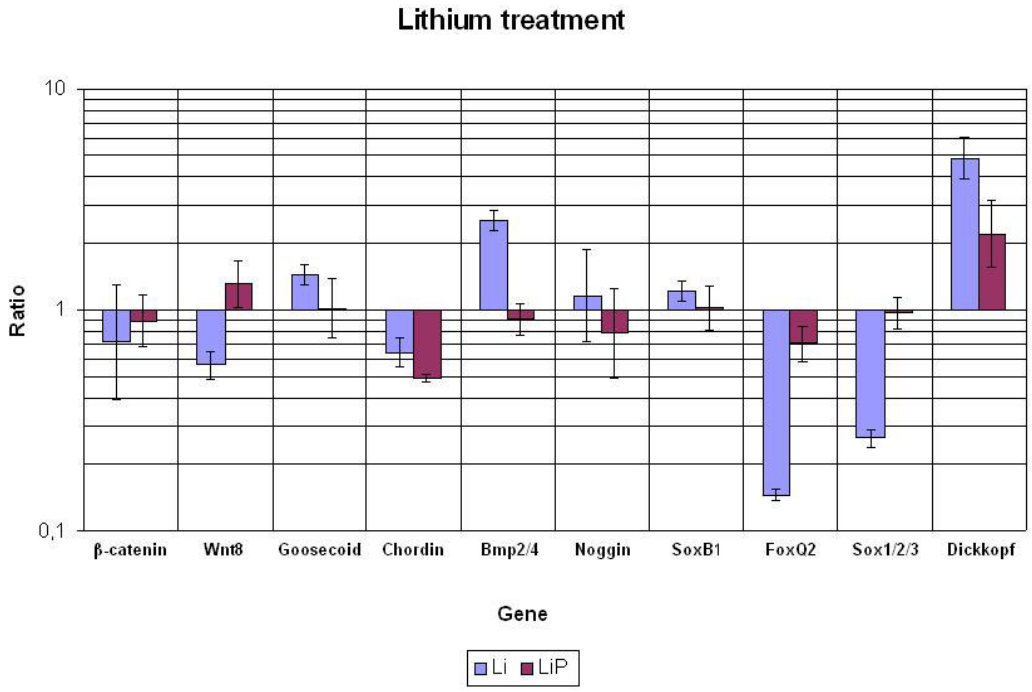

Figure 4-9. Differences in levels of expression of ten genes in lithium treated embryos in comparison to untreated embryos at the mid-gastrula stage.

The bars display the fold difference in expression level in lithium treated in comparison to untreated embryos. The blue bars indicate continuous treatment and the red bars indicate pulsed treatment. The error is displayed as the one-time standard deviation. The x-axis shows the names of genes analyzed. A log scale is used to display the fold-differences on the y-axis.

5 DISCUSSION

5.1 An amphioxus ortholog of Chordin

The *Chordin* gene was described for the first time in *Xenopus* more than ten years ago (Sasai et al. 1994). At about the same time the gene *Short Gastrulation* was described in *Drosophila* (Francois et al. 1994) and both were found to be homologs of one another (Francois and Bier 1995). Since then this gene has been reported from diverse metazoans, including birds, mice and humans (Streit et al. 1998; Bachiller et al. 2000; Millet et al. 2001).

The *Chordin* homolog of amphioxus was cloned by RACE PCR using the shotgun genomic reads from the ongoing *B. floridae* sequencing project (Gibson-Brown et al. 2003) at the JGI (Joint Genome Institute). The cDNA sequence for amphioxus *Chordin* comprised an open reading frame of 984 amino acids. Analysis of this protein revealed that it contained four cysteine-rich (CR) domains, mainly defined by the presence of ten cysteine residues at conserved positions. The spatial distribution of these CR-repeats within the protein was characteristic for Chordin: One CR repeat is located at the amino-terminus, while the other three are located near the carboxyl-terminus. We next analyzed the genomic organization of the coding sequence. While the intron positions in the coding sequences were being highly conserved between amphioxus and human (21 shared introns), the ascidian ortholog shared only 16 introns with both amphioxus and human. In addition, the coding region of the ascidian ortholog contained the highest number of unique introns (those that could not be found in the orthologous coding regions of the other species) reflecting its high divergence at the level of genomic organization. In contrast, the coding region in *D. melanogaster* was marked by extensive intron loss (Figure 4.3).

In a maximum likelihood-based phylogenetic analysis the amphioxus ortholog was clearly placed within the Chordin protein family. Although in our tree the ascidian ortholog was closer to vertebrate Chordin proteins than the amphioxus ortholog we conclude that long-branch attraction biases due the high sequence divergence of the

ascidian ortholog have caused this result. This point of view is corroborated by the comparably long branch lengths for the ascidian and *D. melanogaster* orthologs. Both species are regarded as genetically highly divergent model organism (Adams et al. 2000; Dehal et al. 2002). In conclusion, the isolated amphioxus gene is a true *Chordin* ortholog as judged by its protein domain architecture and phylogenetic analysis. In fact, its genomic organization resembles the vertebrate *Chordin* more than the ascidian or the *Drosophila Chordin*.

5.2 Chordin expression complements Bmp2/4 expression in amphioxus

The dorsal expression of *Chordin* in amphioxus complements the ventral expression of *Bmp2/4* in patterning of the ectoderm and mesoderm. Such a "competing" patterning system becomes initially obvious at the early gastrula stage where *Bmp2/4* has withdrawn from all cells to only mesendodermal cells at the site of invagination. At the same time *Chordin* expression localizes in the dorsal mesendoderm and adjacent ectoderm. At the very early neurula stage when the neural plate begins to form, *Chordin* expression can be detected in the axial mesoderm and in the overlying dorsal ectoderm and *Bmp2/4* expression becomes downregulated in the prospective neural plate and adjacent ectoderm that forms the neural folds. However, expression of *Bmp2/4* remains strong in the presomitic grooves of the mesoderm while it is absent from the dorsal axial mesoderm. The BMP-Chordin competing system seems to be also involved in the patterning of mesoderm in amphioxus.

In later development the expression of *Chordin* in cells of the posterior notochord in the region of the tail bud, still complements *Bmp2/4* expression which remains detectable in the adjacent most posterior paraxial mesoderm that also is part of the tail bud-like growth zone. Therefore, the BMP2/4-Chordin system might be acting in the posterior zone of the elongating embryo, similarly to its proposed function in the zebrafish (Miller-Bertoglio et al. 1997): to function within the tail organizing center to maintain correct dorsoventral polarity of the extending body axis.

5.3 The role of Chordin during neural tissue formation

First, *Chordin* is expressed in prospective neural tissue (the dorsal ectoderm at the midgastrula stage), second in the organizer, that induces the neural plate, and notochord, and third in the developing nerve cord itself. This pattern of expression suggests that Chordin in amphioxus has a neural inducing capacity during early gastrulation and later on acts to maintain the induced fates in the neural domain by the inhibition of BMP. Chordin acts by binding to BMPs in the extracellular space preventing them from binding to their cognate receptors (Yamamoto and Oelgeschlager 2004). In *Drosophila* the mount of neurogenic ectoderm from which the CNS derives is regulated by a dorsal-ventral system of secreted molecules of which Sog and Dpp play fundamental roles (Ferguson and Anderson 1992; Wharton et al 1993; Francois et al. 1994). The same signaling system also acts in vertebrates not only to pattern the ectoderm but also to pattern the mesoderm (Dosch et al. 1997; Nikaido 1997). The default model has become the dominating concept of neural induction in vertebrates (reviewed by Munoz-Sanjuan and Brivanlou 2002).

The expression domains of *Xenopus Chordin* and its amphioxus ortholog are comparably similar before gastrulation being expressed dorsally in the preorganizer region that has recently been referred to as the BCNE centre in *Xenopus* (Kuroda et al. 2004). Descendants of the BCNE centre cells give rise to the anterior CNS, floor plate and notochord. In *Xenopus*, the entire BCNE centre cells express *Chordin* shortly after the midblastula transition, but at the early gastrula stage only the mesendodermal descendants (future prechordal plate; notochord) express *Chordin* and the ectodermal descendants (anterior CNS; neural tube) are devoid of *Chordin* expression (Kuroda et al. 2004). Except for a transient expression in the anterior CNS *Chordin* expression is never observed within prospective neural tissue in developing vertebrates (Sasai et al. 1994; Schulte-Merker at al. 1997; Streit at al. 1998).

Before gastrulation amphioxus *Chordin* is expressed in the dorsal mesendoderm and adjacent ectoderm. More strikingly, expression can be detected in both the hypoblast

of the dorsal blastopore (presumptive notochord) and in the overlying ectoderm (presumptive neural tissue) at the midgastrula stage. Therefore, Chordin might induce neural tissue or render tissue to respond to neural inducing signals in amphioxus from the midblastula stage on. During later gastrula stages *Chordin* expression disappears from the ectoderm but continues in the axial mesoderm. At this point Chordin signals from the presumptive notochord region could help fine-tuning the dorsoventral pattern of the neural plate by inhibiting BMP signals at the edges of the neural plate. At the early neurula stage the notochord still shows expression for *Chordin* and, in addition, expression can be detected in the neural tube. This latter expression in the developing nerve cord cannot be found in vertebrates and, most likely, helps to maintain the neural state of the induced tissue that shows strong expression up to the late neurula sage.

In ascidians Chordin-BMP antagonism has not been linked to the specification of neural induction but rather to the specification of sensory pigment cells at the beginning of gastrulation (Darras and Nishida 2001). However, *Chordin* expression can be detected at the blastula stage (64 cell stage) in precursor cells of the notochord, the brain-stem, and the spinal cord. Also, precursors of mesenchyme cells, muscle cells, and some cells that are not yet restricted in their fates show expression for *Chordin*. During later stages of development up to the tail bud stage mainly cells of the nervous system and some other tissues still express *Chordin* (Satou et al. 2005). These data from ascidians, together with the data from amphioxus presented in this thesis, suggest that all chordates have used *Chordin* to antagonize Bmp signals within neural tissue (probably to maintain neural identity) and that vertebrates have lost this neural expression domain of *Chordin* during evolution. Thus, vertebrates might only use Chordin to induce neural tissue. This also might be due to the fact that vertebrates have evolved additional ways to maintain neural identity within induced tissues and so a localized neural expression became dispensable during vertebrate evolution (e.g. multiple Sox genes). The explanation that the last common ancestor of chordates never expressed *Chordin* in its neural tissue, while neural specific *Chordin* expression has been evolving independently in ascidians and cephalochordates, is not parsimonious and will be rejected.

Although current models in ascidians and in the chick deemphasize a role for BMP regulation during neural tissue formation (Wilson and Edlund 2001; Bertrand et al. 2003; Stern 2002, 2004), the expression pattern of *Chordin* in amphioxus stresses the central role of BMP inhibition by Chordin and other BMP antagonizing molecules in the specification of neural tissue during chordate development.

5.4 Embryonic polarity and Chordin expression in LiCl-treated embryos

We studied the expression of *Chordin* in embryos that were treated continuously with a lower concentration of lithium chloride (50 mM) and in embryos that were pulsed treated with a lower (300 mM) and with a higher (500 mM) concentration for 20 minutes during late blastula stages.

Embryos that were constantly treated with a lower concentration of lithium chloride resulted in exogastrulae, an effect that has recently been reported by others (Holland et al. 2005) and can also be observed in similarly treated sea urchin embryos (Cameron and Davidson 1997). The exogastrulae were characterized by the failure of the surface ectoderm to properly invaginate. Instead, the ectoderm curled up at the edges of the blastopore creating a bell-shaped phenotype. Chordin is expressed in what appears to be the outer layer for the 6 hrs embryos. As Chordin marks the dorsal ectoderm and mesoderm, it could mean that this layer is a mixture of ectoderm and mesoderm (undifferentiated outer layer?) or that the mesoderm expression is lost. It could also be argued that the embryos became radial symmetric by the treatment. However, it has been shown that similarly treated embryos can result in "cap-shaped embryos" with a radial symmetric appearance that express *Hnf-3* on the dorsal and ventral sides indicating that polarity exists in these embryos (Yasui et al. 2002). Although their hat-shaped phenotype differs from our bell-shaped phenotype, we cannot rule out the possibility that D-V polarity exist in our embryos at the level of gene expression making our first assumption of posteriorization more likely.

Pulsed treatments with lower concentrations resulted in a gastrula phenotype with a normal appearance. Effects of the treatment became obvious during late

gastrula/early neurula when the embryos failed to elongate and retained a widely open blastopore. A notochord and a neural plate that both expressed Chordin were present but the neural folds did not form or failed to close over the embryo. All in all these embryos seemed to be delayed in their developmental program. Pulsed treatments with higher concentrations produced embryos that initially gastrulated normal but then did not properly elongate, which could be clearly seen by the compressed expression of *Chordin* in the axial domain. The embryos developed into flattened gastrula with an open blastopore. It has previously been proposed that this "cap shaped" phenotype produced by lithium treatment is devoid of dorsal structures, such as a notochord and/or a neural plate (Yasui et al. 2002; Holland et al. 2005). We observe that cells express *Chordin* in this phenotype and conclude that the only cells that do so must be precursors of the notochord or neural plate. The former seems more likely as an ectodermal sheet of cells that does not show expression can be seen above the *Chordin* expressing cells.

5.5 D-V polarity in amphioxus before the onset of gastrulation

The amphioxus embryo shows a considerable amount of D-V polarity at the gene expression level before the onset of gastrulation. In particular, this D-V polarity becomes evident through an asymmetric expression of organizer-specific genes that are expressed dorsally in the embryo. Although the organizer has been implicated as the driving force to promote dorsal identity during gastrulation in vertebrates (Spemann and Mangold 1924; Harland and Gerhart 1997) its products seem to function earlier in the amphioxus embryo to initiate D-V polarity, just before the formation of an organizer-equivalent structure. Transplantation experiments have provided support for an organizer in amphioxus (Tung et al. 1962).

More recently, a revised fate map of *Xenopus laevis* (Lane and Sheets 2002) has been compared to the ascidian and the expression domains of organizer-specific genes been surveyed (Kourakis and Smith 2005). Under the revised fate map, anterior somites arise near the organizer and posterior somites opposite to the organizer.

Blood islands develop vegetally to the somite forming mesoderm and anterior identity is defined by the vicinity to the organizer. Dorsal-ventral is reassigned as animal-vegetal, whereas somites map nearer to the animal pole and blood island nearer to the vegetal pole. As a consequence the fate maps of *Xenopus* and the ascidian are more alike and suggest a common generalized fate map for all chordates. Because ascidian orthologs of organizer-specific genes are not expressed similarly to vertebrates it has been suggested that those genes became deployed for that function in the lineage leading to vertebrates and cephalochordates, after its divergence from the tunicate lineage. Based on the expression of the amphioxus organizer genes we conclude that amphioxus possess an organizer during gastrulation, although the expression pattern of *Dickkopf* disagrees with this conclusion. Dickkopf has been implicated in head development in higher vertebrates (Glinka et al. 1998). Since amphioxus lacks an elaborate head in comparison to vertebrates its deployment as an organizer-specific gene might have happened in the lineage leading to animals with a more developed heads, such as craniates. Expression data on *Dickkopf* orthologs from agnathans might clarify this issue in the future. We assume that that the organizer has more of a permissive role than an instructive one during amphioxus development because orthologs of vertebrate organizer-specific genes start to function before this structure has actually formed.

5.6 Downstream targets of β-catenin are affected by lithium treatment

In continuously treated embryos the expression of the anterior ectodermal marker *FoxQ2* became significantly downregulated confirming that the treatment has produced posteriorized phenotypes (see section 5.4). The enhancement of Wnt signaling through lithium in these embryos reduced the *Chordin* expression level and increased the level of *Bmp2/4* indicating that non-neural ectoderm was enlarged at the expense of neural ectoderm. This assumption was corroborated by the finding that the expression level of the neural specific marker gene *Sox1/2/3* became significantly reduced by the treatment. *Sox1/2/3* has previously been proposed to be

the amphioxus ortholog of the *SoxB1* class of genes (Holland et al. 2000). However, in the working group "Evolution and Development" a closer amphioxus ortholog of the *SoxB1* class of genes has been identified, referred to as *SoxB1* hereafter, which was not affected by the lithium chloride treatment. This could be explained by the fact that *Sox1/2/3* might be specifically expressed in tissue whereas *SoxB1* acts as a neural promoting factor allowing cells to respond to neural inducing signals. Accordingly, *SoxB1* expression in the ectoderm at the midgastrula stage is more expanded than *Sox1/2/3* expression indicating that *SoxB1* acts in a less restricted domain. Thus, the *Sox1/2/3* gene might have been the result of a gene duplication event specific to the cephalochordate lineage. The increase of *Dickkopf* expression, a secreted inhibitor of the Wnt signaling pathway, in lithium treated embryos suggests that *Dickkopf* might be induced by the elevated levels of nuclear β-catenin through lithium. It has recently been shown that this negative feedback loop regulates the Wnt/ β-catenin signaling pathway, a mechanism that is lost in colon cancer (Gonzalez-Sancho et al. 2005).

6 REFERENCES

IHGSC (2004). Finishing the euchromatic sequence of the human genome. *Nature* **431**, 931-45.

Adams, M. D. Celniker, S. E. Holt, R. A. Evans, C. A. Gocayne, J. D. Amanatides, P. G. Scherer, S. E. Li, P. W. Hoskins, R. A. Galle, R. F. et al. (2000). The genome sequence of Drosophila melanogaster. *Science* **287**, 2185-95.

Agius, E., Oelgeschlager, M., Wessely, O., Kemp, C. and De Robertis, E. M. (2000). Endodermal Nodal-related signals and mesoderm induction in Xenopus. *Development* **127**, 1173-83.

Altschul, S. F., Gish, W., Miller, W., Myers, E. W. and Lipman, D. J. (1990). Basic local alignment search tool. *J Mol Biol* **215**, 403-10.

Alvarez Martinez, C. E., Binato, R., Gonzalez, S., Pereira, M., Robert, B. and Abdelhay, E. (2002). Characterization of a Smad motif similar to Drosophila mad in the mouse Msx 1 promoter. *Biochem Biophys Res Commun* **291**, 655-62.

Arendt, D. and Nubler-Jung, K. (1994). Inversion of dorsoventral axis? *Nature* **371**, 26.
Attisano, L. and Wrana, J. L. (2002). Signal transduction by the TGF-beta superfamily. *Science* **296**, 1646-7.

Bachiller, D., Klingensmith, J., Kemp, C., Belo, J. A., Anderson, R. M., May, S. R., McMahon, J. A., McMahon, A. P., Harland, R. M., Rossant, J. et al. (2000). The organizer factors Chordin and Noggin are required for mouse forebrain development. *Nature* **403**, 658-61.

Barth, K. A., Kishimoto, Y., Rohr, K. B., Seydler, C., Schulte-Merker, S. and Wilson, S. W. (1999). Bmp activity establishes a gradient of positional information throughout the entire neural plate. *Development* **126**, 4977-87.

Belo, J. A., Bouwmeester, T., Leyns, L., Kertesz, N., Gallo, M., Follettie, M. and De Robertis, E. M. (1997). Cerberus-like is a secreted factor with neutralizing activity expressed in the anterior primitive endoderm of the mouse gastrula. *Mech Dev* **68**, 45-57.

Benchabane, H. and Wrana, J. L. (2003). GATA- and Smad1-dependent enhancers in the Smad7 gene differentially interpret bone morphogenetic protein concentrations. *Mol Cell Biol* **23**, 6646-61.

Benton, M. J. (2004). Vertebrate Palaeontology. Oxford: Blackwell Science.

Bertrand, V., Hudson, C., Caillol, D., Popovici, C. and Lemaire, P. (2003). Neural tissue in ascidian embryos is induced by FGF9/16/20, acting via a combination of maternal GATA and Ets transcription factors. *Cell* **115**, 615-27.

Biehs, B., Francois, V. and Bier, E. (1996). The Drosophila short gastrulation gene prevents Dpp from autoactivating and suppressing neurogenesis in the neuroectoderm. *Genes Dev* **10**, 2922-34.

Blair, J. E. and Hedges, S. B. (2005). Molecular phylogeny and divergence times of deuterostome animals. *Mol Biol Evol* **22**, 2275-84.

Bonfield, J. K., Smith, K. and Staden, R. (1995). A new DNA sequence assembly program. *Nucleic Acids Res* **23**, 4992-9.

Borson, N. D., Salo, W. L. and Drewes, L. R. (1992). A lock-docking oligo(dT) primer for 5' and 3' RACE PCR. *PCR Methods Appl* **2**, 144-8.

Bourlat, S. J., Nielsen, C., Lockyer, A. E., Littlewood, D. T. and Telford, M. J. (2003). Xenoturbella is a deuterostome that eats molluscs. *Nature* **424**, 925-8.

Bouwmeester, T., Kim, S., Sasai, Y., Lu, B. and De Robertis, E. M. (1996). Cerberus is a head-inducing secreted factor expressed in the anterior endoderm of Spemann's organizer. *Nature* **382**, 595-601.

Brannon, M., Gomperts, M., Sumoy, L., Moon, R. T. and Kimelman, D. (1997). A beta-catenin/XTcf-3 complex binds to the siamois promoter to regulate dorsal axis specification in Xenopus. *Genes Dev* **11**, 2359-70.

Brauckmann, S. and Gilbert, S. F. (2004). Sucking in the gut: A brief history of early studies on gastrulation. In *Gastrulation: From Cells to Embryo*, (ed. S. C. D.), pp. 1-20. Cold Spring Harbor: Cold Spring Harbor Laboratory Press.

Brugger, S. M., Merrill, A. E., Torres-Vazquez, J., Wu, N., Ting, M. C., Cho, J. Y., Dobias, S. L., Yi, S. E., Lyons, K., Bell, J. R. et al. (2004). A phylogenetically conserved cis-regulatory module in the Msx2 promoter is sufficient for BMP-dependent transcription in murine and Drosophila embryos. *Development* **131**, 5153-65.

Cameron, C. B., Garey, J. R. and Swalla, B. J. (2000). Evolution of the chordate body plan: new insights from phylogenetic analyses of deuterostome phyla. *Proc Natl Acad Sci U S A* **97**, 4469-74.

Cameron, R. A. and Davidson, E. H. (1997). LiCl perturbs ectodermal veg1 lineage allocations in Strongylocentrotus purpuratus embryos. *Dev Biol* **187**, 236-9.

Castresana, J., Feldmaier-Fuchs, G., Yokobori, S., Satoh, N. and Paabo, S. (1998). The mitochondrial genome of the hemichordate Balanoglossus carnosus and the evolution of deuterostome mitochondria. *Genetics* **150**, 1115-23.

Chang, C., Holtzman, D. A., Chau, S., Chickering, T., Woolf, E. A., Holmgren, L. M., Bodorova, J., Gearing, D. P., Holmes, W. E. and Brivanlou, A. H. (2001). Twisted gastrulation can function as a BMP antagonist. *Nature* **410**, 483-7.

Chen, J.-Y., Dzik, J., Edgecombe, G. D., Ramsköld, L. and Zhou, G.-Q. (1995). A possible Early Cambrian chordate. *Nature* **377**, 720-722.

Chen, J.-Y., Huang, D.-Y. and Li, C.-W. (1999). An early Cambrian craniate-like chordate. *Nature* **402**, 518-522.

Chomczynski, P. (1993). A reagent for the single-step simultaneous isolation of RNA, DNA and proteins from cell and tissue samples. *Biotechniques* **15**, 532-4, 536-7.

Chomczynski, P. and Sacchi, N. (1987). Single-step method of RNA isolation by acid guanidinium thiocyanate-phenol-chloroform extraction. *Anal Biochem* **162**, 156-9.

Conklin, E. G. (1932). The embryology of amphioxus. *J Morphol* **54**, 69-151.

Conway Morris, S. (1982). Atlas of the Burgess Shale. London: Palaeontological Association.

Darras, S. and Nishida, H. (2001). The BMP/CHORDIN antagonism controls sensory pigment cell specification and differentiation in the ascidian embryo. *Dev Biol* **236**, 271-88.

De Robertis, E. M., Larrain, J., Oelgeschlager, M. and Wessely, O. (2000). The establishment of Spemann's organizer and patterning of the vertebrate embryo. *Nat Rev Genet* **1**, 171-81.

De Robertis, E. M. and Sasai, Y. (1996). A common plan for dorsoventral patterning in Bilateria. *Nature* **380**, 37-40.

de Rosa, R., Grenier, J. K., Andreeva, T., Cook, C. E., Adoutte, A., Akam, M., Carroll, S. B. and Balavoine, G. (1999). Hox genes in brachiopods and priapulids and protostome evolution. *Nature* **399**, 772-6.

Dehal, P., Satou, Y., Campbell, R. K., Chapman, J., Degnan, B., De Tomaso, A., Davidson, B., Di Gregorio, A., Gelpke, M., Goodstein, D. M. et al. (2002). The draft genome of Ciona intestinalis: insights into chordate and vertebrate origins. *Science* **298**, 2157-67.

Delaune, E., Lemaire, P. and Kodjabachian, L. (2005). Neural induction in Xenopus requires early FGF signalling in addition to BMP inhibition. *Development* **132**, 299-310.

Dosch, R., Gawantka, V., Delius, H., Blumenstock, C. and Niehrs, C. (1997). Bmp-4 acts as a morphogen in dorsoventral mesoderm patterning in Xenopus. *Development* **124**, 2325-34.

Duboc, V., Rottinger, E., Besnardeau, L. and Lepage, T. (2004). Nodal and BMP2/4 signaling organizes the oral-aboral axis of the sea urchin embryo. *Dev Cell* **6**, 397-410.

Duboule, D. (1994). Temporal colinearity and the phylotypic progression: a basis for the stability of a vertebrate Bauplan and the evolution of morphologies through heterochrony. *Dev Suppl*, 135-42.

Dumeril, A. M. C. (1806). Zoologie analytique, ou methode naturelle de classification des aimaux. Didot, Paris.

Eldar, A., Dorfman, R., Weiss, D., Ashe, H., Shilo, B. Z. and Barkai, N. (2002). Robustness of the BMP morphogen gradient in Drosophila embryonic patterning. *Nature* **419**, 304-8.

Fainsod, A., Deissler, K., Yelin, R., Marom, K., Epstein, M., Pillemer, G., Steinbeisser, H. and Blum, M. (1997). The dorsalizing and neural inducing gene follistatin is an antagonist of BMP-4. *Mech Dev* **63**, 39-50.

Feinberg, A. P. and Vogelstein, B. (1983). A technique for radiolabeling DNA restriction endonuclease fragments to high specific activity. *Anal Biochem* **132**, 6-13.

Felsenstein, J. (1992). Estimating effective population size from samples of sequences: a bootstrap Monte Carlo integration method. *Genet Res* **60**, 209-20.

Ferguson, E. L. (1996). Conservation of dorsal-ventral patterning in arthropods and chordates. *Curr Opin Genet Dev* **6**, 424-31.

Ferguson, E. L. and Anderson, K. V. (1992). Decapentaplegic acts as a morphogen to organize dorsal-ventral pattern in the Drosophila embryo. *Cell* **71**, 451-61.

Ferrier, D. E. and Holland, P. W. (2001). Ancient origin of the Hox gene cluster. *Nat Rev Genet* **2**, 33-8.

Finnerty, J. R. and Martindale, M. Q. (1998). The evolution of the Hox cluster: insights from outgroups. *Curr Opin Genet Dev* **8**, 681-7.

Finnerty, J. R., Pang, K., Burton, P., Paulson, D. and Martindale, M. Q. (2004). Origins of bilateral symmetry: Hox and dpp expression in a sea anemone. *Science* **304**, 1335-7.

Flood, P. R., Guthrie, D. M. and Banks, J. R. (1969). Paramyosin muscle in the notochord of Amphioxus. *Nature* **222**, 87-8.

Forey, P. and Janvier, P. (1993). Agnathans and the origin of jawed vertebrates. *Nature* **361**, 129-134.

Forey, P. L. (1984). more reflections on agnathan-gnathostome relationships. *J Vert Paleo* **4**, 330-343.

Francois, V. and Bier, E. (1995). Xenopus chordin and Drosophila short gastrulation genes encode homologous proteins functioning in dorsal-ventral axis formation. *Cell* **80**, 19-20.

Francois, V., Solloway, M., O'Neill, J. W., Emery, J. and Bier, E. (1994). Dorsal-ventral patterning of the Drosophila embryo depends on a putative negative growth factor encoded by the short gastrulation gene. *Genes Dev* **8**, 2602-16.

Frohman, M. A., Dush, M. K. and Martin, G. R. (1988). Rapid production of full-length cDNAs from rare transcripts: amplification using a single gene-specific oligonucleotide primer. *Proc Natl Acad Sci U S A* **85**, 8998-9002.

Furlong, R. F. and Holland, P. W. (2002). Bayesian phylogenetic analysis supports monophyly of ambulacraria and of cyclostomes. *Zoolog Sci* **19**, 593-9.

Garcia Abreu, J., Coffinier, C., Larrain, J., Oelgeschlager, M. and De Robertis, E. M. (2002). Chordin-like CR domains and the regulation of evolutionarily conserved extracellular signaling systems. *Gene* **287**, 39-47.

Garstang, W. (1894). Preliminary note on a new theory of the phylogeny of the chordata. *Zool Anzeiger* **22**, 122–125.

Garstang, W. (1928). The morphology of the Tunicata. *Quart J Microscop Sci* **72**, 51-189.

Gerard, G. F., Fox, D. K., Nathan, M. and D'Alessio, J. M. (1997). Reverse transcriptase. The use of cloned Moloney murine leukemia virus reverse transcriptase to synthesize DNA from RNA. *Mol Biotechnol* **8**, 61-77.

Gerhart, J. (2000). Inversion of the chordate body axis: are there alternatives? *Proc Natl Acad Sci U S A* **97**, 4445-8.

Gerhart, J., Lowe, C. and Kirschner, M. (2005). Hemichordates and the origin of chordates. *Curr Opin Genet Dev* **15**, 461-7.

Germain, S., Howell, M., Esslemont, G. M. and Hill, C. S. (2000). Homeodomain and winged-helix transcription factors recruit activated Smads to distinct promoter elements via a common Smad interaction motif. *Genes Dev* **14**, 435-51.

Gibson-Brown, J. J., Osoegawa, K., McPherson, J. D., Waterston, R. H., De Jong, P. J., Rokhsar, D. S. and Holland, L. Z. (2003). A proposal to sequence the amphioxus genome

submitted to the Joint Genome Institute of the US Department of Energy. *J Exp Zoolog B Mol Dev Evol* **300**, 5-22.

Giribet, G., Distel, D. L., Polz, M., Sterrer, W. and Wheeler, W. C. (2000). Triploblastic relationships with emphasis on the acoelomates and the position of Gnathostomulida, Cycliophora, Plathelminthes, and Chaetognatha: a combined approach of 18S rDNA sequences and morphology. *Syst Biol* **49**, 539-62.

Gonzalez-Sancho, J. M., Aguilera, O., Garcia, J. M., Pendas-Franco, N., Pena, C., Cal, S., Garcia de Herreros, A., Bonilla, F. and Munoz, A. (2005). The Wnt antagonist DICKKOPF-1 gene is a downstream target of beta-catenin/TCF and is downregulated in human colon cancer. *Oncogene* **24**, 1098-103.

Gregory, T. R. (2005). Animal Genome Size Database. http://www.genomesize.com/. Last accessed 30.11.2005.

Hall, T. A. (1999). BioEdit: a user-friendly biological sequence alignment editor and analysis program for Windows 95/98/NT. *Nucleic Acids Symp* **Ser. 41**, 95-98.

Hansen, C. S., Marion, C. D., Steele, K., George, S. and Smith, W. C. (1997). Direct neural induction and selective inhibition of mesoderm and epidermis inducers by Xnr3. *Development* **124**, 483-92.

Harada, Y., Okai, N., Taguchi, S., Tagawa, K., Humphreys, T. and Satoh, N. (2000). Developmental expression of the hemichordate otx ortholog. *Mech Dev* **91**, 337-9.

Hari, L., Brault, V., Kleber, M., Lee, H. Y., Ille, F., Leimeroth, R., Paratore, C., Suter, U., Kemler, R. and Sommer, L. (2002). Lineage-specific requirements of beta-catenin in neural crest development. *J Cell Biol* **159**, 867-80.

Harland, R. and Gerhart, J. (1997). Formation and function of Spemann's organizer. *Annu Rev Cell Dev Biol* **13**, 611-67.

Hawley, S. H., Wunnenberg-Stapleton, K., Hashimoto, C., Laurent, M. N., Watabe, T., Blumberg, B. W. and Cho, K. W. (1995). Disruption of BMP signals in embryonic Xenopus ectoderm leads to direct neural induction. *Genes Dev* **9**, 2923-35.

Heid, C. A., Stevens, J., Livak, K. J. and Williams, P. M. (1996). Real time quantitative PCR. *Genome Res* **6**, 986-94.

Hemmati-Brivanlou, A., Kelly, O. G. and Melton, D. A. (1994). Follistatin, an antagonist of activin, is expressed in the Spemann organizer and displays direct neuralizing activity. *Cell* **77**, 283-95.

Hemmati-Brivanlou, A. and Melton, D. (1997). Vertebrate embryonic cells will become nerve cells unless told otherwise. *Cell* **88**, 13-7.

Henningfeld, K. A., Rastegar, S., Adler, G. and Knochel, W. (2000). Smad1 and Smad4 are components of the bone morphogenetic protein-4 (BMP-4)-induced transcription complex of the Xvent-2B promoter. *J Biol Chem* **275**, 21827-35.

Hillier, L. and Green, P. (1991). OSP: a computer program for choosing PCR and DNA sequencing primers. *PCR Methods Appl* **1**, 124-8.

Hinman, V. F., Nguyen, A. T., Cameron, R. A. and Davidson, E. H. (2003). Developmental gene regulatory network architecture across 500 million years of echinoderm evolution. *Proc Natl Acad Sci U S A* **100**, 13356-61.

Hofmann, K. and Stoffel, W. (1993). TMbase - A database of membrane spanning proteins segments. In *Biol Chem*, vol. 374 (ed.: Hoppe-Seyler.

Holland, L. Z. and Holland, N. D. (2001). Evolution of neural crest and placodes: amphioxus as a model for the ancestral vertebrate? *J Anat* **199**, 85-98.

Holland, L. Z., Holland, P. W. H. and Holland, N. D. (1996). Revealing homologies between body parts of distantly related animals by in situ hybridization to developmental genes: Amphioxus versus vertebrates. In *Molecular Zoology: Advances, Strategies, and Protocols*, (ed. J. D. Ferraris and S. R. Palumbi), pp. 267-282; 473-483. New York: Wiley-Liss.

Holland, L. Z., Laudet, V. and Schubert, M. (2004). The chordate amphioxus: an emerging model organism for developmental biology. *Cell Mol Life Sci* **61**, 2290-308.

Holland, L. Z., Panfilio, K. A., Chastain, R., Schubert, M. and Holland, N. D. (2005). Nuclear beta-catenin promotes non-neural ectoderm and posterior cell fates in amphioxus embryos. *Dev Dyn* **233**, 1430-43.

Holland, L. Z., Schubert, M., Holland, N. D. and Neuman, T. (2000). Evolutionary conservation of the presumptive neural plate markers AmphiSox1/2/3 and AmphiNeurogenin in the invertebrate chordate amphioxus. *Dev Biol* **226**, 18-33.

Holland, L. Z. and Yu, J. K. (2004). Cephalochordate (amphioxus) embryos: procurement, culture, and basic methods. *Methods Cell Biol* **74**, 195-215.

Holland, N. D. (2003). Early central nervous system evolution: an era of skin brains? *Nat Rev Neurosci* **4**, 617-27.

Holland, N. D. and Chen, J. (2001). Origin and early evolution of the vertebrates: new insights from advances in molecular biology, anatomy, and palaeontology. *Bioessays* **23**, 142-51.

Holland, N. D. and Holland, L. Z. (1993). Embryos and larvae of invertebrate deuterostomes. In *Essential Development Biology: an Experimental Approach*, (ed. C. Stern and P. W. H. Holland), pp. 21-32. Oxford: I.R.L. Press.

Holland, N. D. and Holland, L. Z. (1999). Amphioxus and the utility of molecular genetic data for hypothesizing body part homologies between distantly related animals. *Amer Zool* **39**, 630-640.

Holland, P. W. and Garcia-Fernandez, J. (1996). Hox genes and chordate evolution. *Dev Biol* **173**, 382-95.

Holland, P. W., Garcia-Fernandez, J., Williams, N. A. and Sidow, A. (1994). Gene duplications and the origins of vertebrate development. *Dev Suppl*, 125-33.

Holley, S. A. and Ferguson, E. L. (1997). Fish are like flies are like frogs: conservation of dorsal-ventral patterning mechanisms. *Bioessays* **19**, 281-4.

Holley, S. A., Jackson, P. D., Sasai, Y., Lu, B., De Robertis, E. M., Hoffmann, F. M. and Ferguson, E. L. (1995). A conserved system for dorsal-ventral patterning in insects and vertebrates involving sog and chordin. *Nature* **376**, 249-53.

Hubbard, T., Andrews, D., Caccamo, M., Cameron, G., Chen, Y., Clamp, M., Clarke, L., Coates, G., Cox, T., Cunningham, F. et al. (2005). Ensembl 2005. *Nucleic Acids Res* **33**, D447-53.

Hudson, C., Darras, S., Caillol, D., Yasuo, H. and Lemaire, P. (2003). A conserved role for the MEK signalling pathway in neural tissue specification and posteriorisation in the invertebrate chordate, the ascidian Ciona intestinalis. *Development* **130**, 147-59.

Huxley, T. H. (1874). On the classification of the animal kingd. *J Linn Soc Lond* **12**, 199-226.

Janvier, P. (1999). Catching the first fish. *Nature* **402**, 21-22.

Karaulanov, E., Knochel, W. and Niehrs, C. (2004). Transcriptional regulation of BMP4 synexpression in transgenic Xenopus. *Embo J* **23**, 844-56.

Kellogg, D. E., Rybalkin, I., Chen, S., Mukhamedova, N., Vlasik, T., Siebert, P. D. and Chenchik, A. (1994). TaqStart Antibody: "hot start" PCR facilitated by a neutralizing monoclonal antibody directed against Taq DNA polymerase. *Biotechniques* **16**, 1134-7.

Klein, P. S. and Melton, D. A. (1996). A molecular mechanism for the effect of lithium on development. *Proc Natl Acad Sci U S A* **93**, 8455-9.

Kourakis, M. J. and Smith, W. C. (2005). Did the first chordates organize without the organizer? *Trends Genet* **21**, 506-10.

Kowalevsky, A. O. (1867). Die Entwickelungsgeschichte des Amphioxus lanceolatus. *Mem Acad Sci St Petersb* **7th Ser 11**, 1-17.

Kozmik, Z., Holland, N. D., Kalousova, A., Paces, J., Schubert, M. and Holland, L. Z. (1999). Characterization of an amphioxus paired box gene, AmphiPax2/5/8: developmental expression patterns in optic support cells, nephridium, thyroid-like structures and pharyngeal gill slits, but not in the midbrain-hindbrain boundary region. *Development* **126**, 1295-304.

Kuraku, S., Hoshiyama, D., Katoh, K., Suga, H. and Miyata, T. (1999). Monophyly of lampreys and hagfishes supported by nuclear DNA-coded genes. *J Mol Evol* **49**, 729-35.

Kuroda, H., Wessely, O. and De Robertis, E. M. (2004). Neural induction in Xenopus: requirement for ectodermal and endomesodermal signals via Chordin, Noggin, beta-Catenin, and Cerberus. *PLoS Biol* **2**, E92.

Lacalli, T. (2003). Evolutionary biology: Body plans and simple brains. *Nature* **424**, 263-4.

Lane, M. C. and Sheets, M. D. (2002). Rethinking axial patterning in amphibians. *Dev Dyn* **225**, 434-47.

Larabell, C. A., Torres, M., Rowning, B. A., Yost, C., Miller, J. R., Wu, M., Kimelman, D. and Moon, R. T. (1997). Establishment of the dorso-ventral axis in Xenopus embryos is presaged by early asymmetries in beta-catenin that are modulated by the Wnt signaling pathway. *J Cell Biol* **136**, 1123-36.

Larrain, J., Bachiller, D., Lu, B., Agius, E., Piccolo, S. and De Robertis, E. M. (2000). BMP-binding modules in chordin: a model for signalling regulation in the extracellular space. *Development* **127**, 821-30.

Larrain, J., Oelgeschlager, M., Ketpura, N. I., Reversade, B., Zakin, L. and De Robertis, E. M. (2001). Proteolytic cleavage of Chordin as a switch for the dual activities of Twisted gastrulation in BMP signaling. *Development* **128**, 4439-47.

Laurent, M. N., Blitz, I. L., Hashimoto, C., Rothbacher, U. and Cho, K. W. (1997). The Xenopus homeobox gene twin mediates Wnt induction of goosecoid in establishment of Spemann's organizer. *Development* **124**, 4905-16.

Lemaire, P., Garrett, N. and Gurdon, J. B. (1995). Expression cloning of Siamois, a Xenopus homeobox gene expressed in dorsal-vegetal cells of blastulae and able to induce a complete secondary axis. *Cell* **81**, 85-94.

Liem, K. F., Jr., Tremml, G. and Jessell, T. M. (1997). A role for the roof plate and its resident TGFbeta-related proteins in neuronal patterning in the dorsal spinal cord. *Cell* **91**, 127-38.

Liem, K. F., Jr., Tremml, G., Roelink, H. and Jessell, T. M. (1995). Dorsal differentiation of neural plate cells induced by BMP-mediated signals from epidermal ectoderm. *Cell* **82**, 969-79.

Linker, C. and Stern, C. D. (2004). Neural induction requires BMP inhibition only as a late step, and involves signals other than FGF and Wnt antagonists. *Development* **131**, 5671-81.

Logan, C. Y., Miller, J. R., Ferkowicz, M. J. and McClay, D. R. (1999). Nuclear beta-catenin is required to specify vegetal cell fates in the sea urchin embryo. *Development* **126**, 345-57.

Loh, E. Y., Elliott, J. F., Cwirla, S., Lanier, L. L. and Davis, M. M. (1989). Polymerase chain reaction with single-sided specificity: analysis of T cell receptor delta chain. *Science* **243**, 217-20.

Lowe, C. J., Wu, M., Salic, A., Evans, L., Lander, E., Stange-Thomann, N., Gruber, C. E., Gerhart, J. and Kirschner, M. (2003). Anteroposterior patterning in hemichordates and the origins of the chordate nervous system. *Cell* **113**, 853-65.

Maisey, J. G. (1984). Heads and tails: a chordate phylogeny. *Cladistics* **2**, 201-256.

Mallatt, J. and Chen, J. Y. (2003). Fossil sister group of craniates: predicted and found. *J Morphol* **258**, 1-31.

Mallatt, J. and Sullivan, J. (1998). 28S and 18S rDNA sequences support the monophyly of lampreys and hagfishes. *Mol Biol Evol* **15**, 1706-18.

Marques, G., Musacchio, M., Shimell, M. J., Wunnenberg-Stapleton, K., Cho, K. W. and O'Connor, M. B. (1997). Production of a DPP activity gradient in the early Drosophila embryo through the opposing actions of the SOG and TLD proteins. *Cell* **91**, 417-26.

Maxam, A. M. and Gilbert, W. (1977). A new method for sequencing DNA. *Proc Natl Acad Sci U S A* **74**, 560-4.

Metschnikoff, E. (1869). Ueber die Systematische Stellung von Balanoglossus. *Zool Anz* **4**, 139-143, 153-157.

Miller-Bertoglio, V. E., Fisher, S., Sanchez, A., Mullins, M. C. and Halpern, M. E. (1997). Differential regulation of chordin expression domains in mutant zebrafish. *Dev Biol* **192**, 537-50.

Miller, J. R., Rowning, B. A., Larabell, C. A., Yang-Snyder, J. A., Bates, R. L. and Moon, R. T. (1999). Establishment of the dorsal-ventral axis in Xenopus embryos coincides with the dorsal enrichment of dishevelled that is dependent on cortical rotation. *J Cell Biol* **146**, 427-37.

Millet, C., Lemaire, P., Orsetti, B., Guglielmi, P. and Francois, V. (2001). The human chordin gene encodes several differentially expressed spliced variants with distinct BMP opposing activities. *Mech Dev* **106**, 85-96.

Miya, T., Morita, K., Suzuki, A., Ueno, N. and Satoh, N. (1997). Functional analysis of an ascidian homologue of vertebrate Bmp-2/Bmp-4 suggests its role in the inhibition of neural fate specification. *Development* **124**, 5149-59.

Moon, R. T. and Kimelman, D. (1998). From cortical rotation to organizer gene expression: toward a molecular explanation of axis specification in Xenopus. *Bioessays* **20**, 536-45.

Morrison, T. B., Weis, J. J. and Wittwer, C. T. (1998). Quantification of low-copy transcripts by continuous SYBR Green I monitoring during amplification. *Biotechniques* **24**, 954-8, 960, 962.

Müller, W. (1873). Über die Hypobranchialrinne der Tunicaten und deren Vorhandensein bei Amphoxus und den Cyklostomen. *Jena Z Med Naturw* **7**, 327-332.

Mullis, K., Faloona, F., Scharf, S., Saiki, R., Horn, G. and Erlich, H. (1986). Specific enzymatic amplification of DNA in vitro: the polymerase chain reaction. *Cold Spring Harb Symp Quant Biol* **51 Pt 1**, 263-73.

Munoz-Sanjuan, I. and A, H. B. (2001). Early posterior/ventral fate specification in the vertebrate embryo. *Dev Biol* **237**, 1-17.

Munoz-Sanjuan, I. and Brivanlou, A. H. (2002). Neural induction, the default model and embryonic stem cells. *Nat Rev Neurosci* **3**, 271-80.

Munoz-Sanjuan, I. and Brivanlou, A. H. (2004). Modulation of BMP signaling during vertebrate gastrulation. In *Gastrulation: From Cells to Embryo*, (ed. C. D. Stern), pp. 475-490. Cold Spring Harbor: Cold Spring Harbor Laboratory Press.

Nguyen, V. H., Trout, J., Connors, S. A., Andermann, P., Weinberg, E. and Mullins, M. C. (2000). Dorsal and intermediate neuronal cell types of the spinal cord are established by a BMP signaling pathway. *Development* **127**, 1209-20.

Nielsen, C. (1998). Origin and evolution of animal life cycles. *Biol Rev* **73**, 125-155.

Nikaido, M., Tada, M., Saji, T. and Ueno, N. (1997). Conservation of BMP signaling in zebrafish mesoderm patterning. *Mech Dev* **61**, 75-88.

Nubler-Jung, K. and Arendt, D. (1994). Is ventral in insects dorsal in vertebrates? A history of embryological arguments favouring axis inversion in chordate ancestors. *Roux's Arch Dev Biol* **203**, 357-366.

O'Leary, J. M., Hamilton, J. M., Deane, C. M., Valeyev, N. V., Sandell, L. J. and Downing, A. K. (2004). Solution structure and dynamics of a prototypical chordin-like cysteine-rich repeat (von Willebrand Factor type C module) from collagen IIA. *J Biol Chem* **279**, 53857-66.

Oda, H., Wada, H., Tagawa, K., Akiyama-Oda, Y., Satoh, N., Humphreys, T., Zhang, S. and Tsukita, S. (2002). A novel amphioxus cadherin that localizes to epithelial adherens junctions has an unusual domain organization with implications for chordate phylogeny. *Evol Dev* **4**, 426-34.

Oelgeschlager, M., Larrain, J., Geissert, D. and De Robertis, E. M. (2000). The evolutionarily conserved BMP-binding protein Twisted gastrulation promotes BMP signalling. *Nature* **405**, 757-63.

Pallas, P. S. (1774). Limax lanceolatus: descriptio Limacis lanceolaris. In Spicilegia Zoologica, quibus novae imprimus et obscurae animalium species iconibus, descriptionibus. **10**, 19. Table 1, Figs. 11a, 11b.

Panopoulou, G. and Poustka, A. J. (2005). Timing and mechanism of ancient vertebrate genome duplications -- the adventure of a hypothesis. *Trends Genet* **21**, 559-67.

Panopoulou, G. D., Clark, M. D., Holland, L. Z., Lehrach, H. and Holland, N. D. (1998). AmphiBMP2/4, an amphioxus bone morphogenetic protein closely related to Drosophila decapentaplegic and vertebrate BMP2 and BMP4: insights into evolution of dorsoventral axis specification. *Dev Dyn* **213**, 130-9.

Pearce, J. J., Penny, G. and Rossant, J. (1999). A mouse cerberus/Dan-related gene family. *Dev Biol* **209**, 98-110.

Pfaffl, M. W. (2004). Quantification Strategies in Real-Time PCR. In *A to Z of Quantitative PCR*, (ed. S. A. Bustin), pp. 87-120. La Jolla: International University Line.

Philippe, H., Lartillot, N. and Brinkmann, H. (2005). Multigene analyses of bilaterian animals corroborate the monophyly of Ecdysozoa, Lophotrochozoa, and Protostomia. *Mol Biol Evol* **22**, 1246-53.

Piccolo, S., Agius, E., Lu, B., Goodman, S., Dale, L. and De Robertis, E. M. (1997). Cleavage of Chordin by Xolloid metalloprotease suggests a role for proteolytic processing in the regulation of Spemann organizer activity. *Cell* **91**, 407-16.

Piccolo, S., Sasai, Y., Lu, B. and De Robertis, E. M. (1996). Dorsoventral patterning in Xenopus: inhibition of ventral signals by direct binding of chordin to BMP-4. *Cell* **86**, 589-98.

Plachov, D., Chowdhury, K., Walther, C., Simon, D., Guenet, J. L. and Gruss, P. (1990). Pax8, a murine paired box gene expressed in the developing excretory system and thyroid gland. *Development* **110**, 643-51.

Poss, S. G. and Boschung, H. T. (1996). Lancelets (Cephalochordata: Branchiostomatidae): How many species are valid? *Isr J Zool* **42**, 13-66.

Roeser, T., Stein, S. and Kessel, M. (1999). Nuclear beta-catenin and the development of bilateral symmetry in normal and LiCl-exposed chick embryos. *Development* **126**, 2955-65.

Ross, J. J., Shimmi, O., Vilmos, P., Petryk, A., Kim, H., Gaudenz, K., Hermanson, S., Ekker, S. C., O'Connor, M. B. and Marsh, J. L. (2001). Twisted gastrulation is a conserved extracellular BMP antagonist. *Nature* **410**, 479-83.

Saiki, R. K., Gelfand, D. H., Stoffel, S., Scharf, S. J., Higuchi, R., Horn, G. T., Mullis, K. B. and Erlich, H. A. (1988). Primer-directed enzymatic amplification of DNA with a thermostable DNA polymerase. *Science* **239**, 487-91.

Saint-Hillaire, G. E. (1822). Considerations generales sur la vertebre. *Mem du Mus Hist Nat* **9**, 89-119.

Saitou, N. and Nei, M. (1987). The neighbor-joining method: a new method for reconstructing phylogenetic trees. *Mol Biol Evol* **4**, 406-25.

Sanger, F., Nicklen, S. and Coulson, A. R. (1977). DNA sequencing with chain-terminating inhibitors. *Proc Natl Acad Sci U S A* **74**, 5463-7.

Sasai, Y., Lu, B., Steinbeisser, H. and De Robertis, E. M. (1995). Regulation of neural induction by the Chd and Bmp-4 antagonistic patterning signals in Xenopus. *Nature* **376**, 333-6.

Sasai, Y., Lu, B., Steinbeisser, H., Geissert, D., Gont, L. K. and De Robertis, E. M. (1994). Xenopus chordin: a novel dorsalizing factor activated by organizer-specific homeobox genes. *Cell* **79**, 779-90.

Satou, Y., Kawashima, T., Shoguchi, E., Nakayama, A. and Satoh, N. (2005). An integrated database of the ascidian, Ciona intestinalis: towards functional genomics. *Zoolog Sci* **22**, 837-43.

Schaeffer, B. (1987). Deuterostome monophyly and phylogeny. *Evol Biol* **21**.

Schafer, E. A. (1874). Some teachings of development. *Q J Microsc Sci* **20**, 202-218.

Schmidt, H. A., Strimmer, K., Vingron, M. and von Haeseler, A. (2002). TREE-PUZZLE: maximum likelihood phylogenetic analysis using quartets and parallel computing. *Bioinformatics* **18**, 502-4.

Schulte-Merker, S., Lee, K. J., McMahon, A. P. and Hammerschmidt, M. (1997). The zebrafish organizer requires chordino. *Nature* **387**, 862-3.

Scott, I. C., Blitz, I. L., Pappano, W. N., Maas, S. A., Cho, K. W. and Greenspan, D. S. (2001). Homologues of Twisted gastrulation are extracellular cofactors in antagonism of BMP signalling. *Nature* **410**, 475-8.

Sears, L. E., Moran, L. S., Kissinger, C., Creasey, T., Perry-O'Keefe, H., Roskey, M., Sutherland, E. and Slatko, B. E. (1992). CircumVent thermal cycle sequencing and alternative manual and automated DNA sequencing protocols using the highly thermostable VentR (exo-) DNA polymerase. *Biotechniques* **13**, 626-33.

Sheng, G., dos Reis, M. and Stern, C. D. (2003). Churchill, a zinc finger transcriptional activator, regulates the transition between gastrulation and neurulation. *Cell* **115**, 603-13.

Shimeld, S. M. and Holland, N. D. (2005). Amphioxus molecular biology: insights into vertebrate evolution and developmental mechanisms. *Can J Zool* **83**, 90-100.

Shu, D.-G., Conway Morris, S. and Zhang, X.-L. (1996). A Pikaia-like chordate from the Lower Cambrian of China. *Nature* **384**, 157-158.

Shu, D. (2003). A palaeontological perspective of vertebrate origins. *Chinese Sci Bull* **48**, 725-735.

Shu, D., Luo, H., Conway Morris, S., Zhang, X., Hu, S., Chen, L., Han, J., Zhu, M., Li, Y. and Chen, L. (1999). Lower Cambrian vertebrates from south China. *Nature* **402**, 42-46.

Shu, D., Zhang, X. and Chen, L. (1996). Reinterpretation of Yunnanozoon as the earliest known hemichordate. *Nature* **380**, 428-430.

Shu, D. G., Chen, L., Han, J. and Zhang, X. L. (2001). An Early Cambrian tunicate from China. *Nature* **411**, 472-3.

Shu, D. G., Morris, S. C., Han, J., Chen, L., Zhang, X. L., Zhang, Z. F., Liu, H. Q., Li, Y. and Liu, J. N. (2001). Primitive deuterostomes from the Chengjiang Lagerstatte (Lower Cambrian, China). *Nature* **414**, 419-24.

Shu, D. G., Morris, S. C., Han, J., Zhang, Z. F. and Liu, J. N. (2004). Ancestral echinoderms from the Chengjiang deposits of China. *Nature* **430**, 422-8.

Shu, D. G., Morris, S. C., Han, J., Zhang, Z. F., Yasui, K., Janvier, P., Chen, L., Zhang, X. L., Liu, J. N., Li, Y. et al. (2003). Head and backbone of the Early Cambrian vertebrate Haikouichthys. *Nature* **421**, 526-9.

Smith, W. C. and Harland, R. M. (1992). Expression cloning of noggin, a new dorsalizing factor localized to the Spemann organizer in Xenopus embryos. *Cell* **70**, 829-40.

Smith, W. C., McKendry, R., Ribisi, S., Jr. and Harland, R. M. (1995). A nodal-related gene defines a physical and functional domain within the Spemann organizer. *Cell* **82**, 37-46.

Spemann, H. and Mangold, H. (1924). Über Induktion von Embryonalanlagen durch Implantation artfremder Organisatoren. *Roux's Arch EntwMech Org* **100**, 599-638.

Stachel, S. E., Grunwald, D. J. and Myers, P. Z. (1993). Lithium perturbation and goosecoid expression identify a dorsal specification pathway in the pregastrula zebrafish. *Development* **117**, 1261-74.

Steida, L. (1873). Studien über den Amphioxus lanceolatus. *Mem Acad Imp Sci St Petersb* **Ser. VII**, 1-70.

Stern, C. D. (2002). Induction and initial patterning of the nervous system - the chick embryo enters the scene. *Curr Opin Genet Dev* **12**, 447-51.

Stern, C. D. (2004). Neural Induction. In *Gastrulation: From Cells to Embryo*, (ed. C. D. Stern), pp. 419-432. Cold Spring Harbor: Cold Spring Harbor Laboratory Press.

Stern, C. D. (2005). Neural induction: old problem, new findings, yet more questions. *Development* **132**, 2007-21.

Stock, D. W. and Whitt, G. S. (1992). Evidence from 18S ribosomal RNA sequences that lampreys and hagfishes form a natural group. *Science* **257**, 787-9.

Stokes, M. D. and Holland, N. D. (1998). The lancelet: also known as 'amphioxus', this curious creature has returned to the limelight as a player in the phylogenetic history of the vertebrates. *Am Sci* **86**, 552-560.

Streit, A., Berliner, A. J., Papanayotou, C., Sirulnik, A. and Stern, C. D. (2000). Initiation of neural induction by FGF signalling before gastrulation. *Nature* **406**, 74-8.

Streit, A., Lee, K. J., Woo, I., Roberts, C., Jessell, T. M. and Stern, C. D. (1998). Chordin regulates primitive streak development and the stability of induced neural cells, but is not sufficient for neural induction in the chick embryo. *Development* **125**, 507-19.

Streit, A. and Stern, C. D. (1999). Establishment and maintenance of the border of the neural plate in the chick: involvement of FGF and BMP activity. *Mech Dev* **82**, 51-66.

Streit, A. and Stern, C. D. (1999). Mesoderm patterning and somite formation during node regression: differential effects of chordin and noggin. *Mech Dev* **85**, 85-96.

Strimmer, K. and Haeseler von, A. (1996). A quartet puzzling: a quartet maximum likelihood method for reconstructing tree topologies. *Mol Biol Evol* **13**, 964-969.

Taguchi, S., Tagawa, K., Humphreys, T. and Satoh, N. (2002). Group B sox genes that contribute to specification of the vertebrate brain are expressed in the apical organ and ciliary bands of hemichordate larvae. *Zoolog Sci* **19**, 57-66.

Takacs, C. M., Moy, V. N. and Peterson, K. J. (2002). Testing putative hemichordate homologues of the chordate dorsal nervous system and endostyle: expression of NK2.1 (TTF-1) in the acorn worm Ptychodera flava (Hemichordata, Ptychoderidae). *Evol Dev* **4**, 405-17.

Takahashi, S., Yokota, C., Takano, K., Tanegashima, K., Onuma, Y., Goto, J. and Asashima, M. (2000). Two novel nodal-related genes initiate early inductive events in Xenopus Nieuwkoop center. *Development* **127**, 5319-29.

Takezaki, N., Figueroa, F., Zaleska-Rutczynska, Z. and Klein, J. (2003). Molecular phylogeny of early vertebrates: monophyly of the agnathans as revealed by sequences of 35 genes. *Mol Biol Evol* **20**, 287-92.

Thompson, J. D., Higgins, D. G. and Gibson, T. J. (1994). CLUSTAL W: improving the sensitivity of progressive multiple sequence alignment through sequence weighting, position-specific gap penalties and weight matrix choice. *Nucleic Acids Res* **22**, 4673-80.

Tiso, N., Filippi, A., Pauls, S., Bortolussi, M. and Argenton, F. (2002). BMP signalling regulates anteroposterior endoderm patterning in zebrafish. *Mech Dev* **118**, 29-37.

Tung, T. C., Wu, S. C. and Tung, Y. Y. F. (1962). Experimental studies on the neural induction in amphioxus. *Sci Sin* **11**, 805-820.

Turbeville, J. M., Schulz, J. R. and Raff, R. A. (1994). Deuterostome phylogeny and the sister group of the chordates: evidence from molecules and morphology. *Mol Biol Evol* **11**, 648-55.

Varga, A. C. and Wrana, J. L. (2005). The disparate role of BMP in stem cell biology. *Oncogene* **24**, 5713-21.

Venkatesh, T. V., Holland, N. D., Holland, L. Z., Su, M. T. and Bodmer, R. (1999). Sequence and developmental expression of amphioxus AmphiNk2-1: insights into the evolutionary origin of the vertebrate thyroid gland and forebrain. *Dev Genes Evol* **209**, 254-9.

Venter, J. C. Adams, M. D. Myers, E. W. Li, P. W. Mural, R. J. Sutton, G. G. Smith, H. O. Yandell, M. Evans, C. A. Holt, R. A. et al. (2001). The sequence of the human genome. *Science* **291**, 1304-51.

Wada, H. and Satoh, N. (1994). Details of the evolutionary history from invertebrates to vertebrates, as deduced from the sequences of 18S rDNA. *Proc Natl Acad Sci U S A* **91**, 1801-4.

Weinstein, D. C. and Hemmati-Brivanlou, A. (1999). Neural induction. *Annu Rev Cell Dev Biol* **15**, 411-33.

Wharton, K. A., Ray, R. P. and Gelbart, W. M. (1993). An activity gradient of decapentaplegic is necessary for the specification of dorsal pattern elements in the Drosophila embryo. *Development* **117**, 807-22.

Whittaker, J. R. (1997). Cephalochordates, the Lancelets. In *Embryology: Constructing the Organism*, (ed. S. F. Gilbert and A. M. Raunio), pp. 365-381. Sunderland: Sinauer Associates.

Wicht, H. and Lacalli, T. C. (2005). The nervous system of amphioxus: structure, development, and evolutionary significance. *Can J Zool* **83**, 122-150.

Wikramanayake, A. H., Hong, M., Lee, P. N., Pang, K., Byrum, C. A., Bince, J. M., Xu, R. and Martindale, M. Q. (2003). An ancient role for nuclear beta-catenin in the evolution of axial polarity and germ layer segregation. *Nature* **426**, 446-50.

Wilkinson, D. G. and Nieto, M. A. (1993). Detection of messenger RNA by in situ hybridization to tissue sections and whole mounts. *Methods Enzymol* **225**, 361-73.

Wilson, L. and Maden, M. (2005). The mechanisms of dorsoventral patterning in the vertebrate neural tube. *Dev Biol* **282**, 1-13.

Wilson, S. I. and Edlund, T. (2001). Neural induction: toward a unifying mechanism. *Nat Neurosci* **4 Suppl**, 1161-8.

Wilson, S. I., Graziano, E., Harland, R., Jessell, T. M. and Edlund, T. (2000). An early requirement for FGF signalling in the acquisition of neural cell fate in the chick embryo. *Curr Biol* **10**, 421-9.

Winchell, C. J., Sullivan, J., Cameron, C. B., Swalla, B. J. and Mallatt, J. (2002). Evaluating hypotheses of deuterostome phylogeny and chordate evolution with new LSU and SSU ribosomal DNA data. *Mol Biol Evol* **19**, 762-76.

Xu, R. H., Kim, J., Taira, M., Zhan, S., Sredni, D. and Kung, H. F. (1995). A dominant negative bone morphogenetic protein 4 receptor causes neuralization in Xenopus ectoderm. *Biochem Biophys Res Commun* **212**, 212-9.

Yamaguchi, Y. and Shinagawa, A. (1989). Marked alteration at midblastula transition in the effect of lithium on formation of the larval body plan of Xenopus laevis. *Dev Growth Differ* **31**, 531-541.

Yamamoto, Y. and Oelgeschlager, M. (2004). Regulation of bone morphogenetic proteins in early embryonic development. *Naturwissenschaften* **91**, 519-34.

Yasui, K., Li, G., Wang, Y., Saiga, H., Zhang, P. and Aizawa, S. (2002). beta-Catenin in early development of the lancelet embryo indicates specific determination of embryonic polarity. *Dev Growth Differ* **44**, 467-75.

Yost, C., Torres, M., Miller, J. R., Huang, E., Kimelman, D. and Moon, R. T. (1996). The axis-inducing activity, stability, and subcellular distribution of beta-catenin is regulated in Xenopus embryos by glycogen synthase kinase 3. *Genes Dev* **10**, 1443-54.

Zhang, W., Yatskievych, T. A., Cao, X. and Antin, P. B. (2002). Regulation of Hex gene expression by a Smads-dependent signaling pathway. *J Biol Chem* **277**, 45435-41.

Zimmerman, L. B., De Jesus-Escobar, J. M. and Harland, R. M. (1996). The Spemann organizer signal noggin binds and inactivates bone morphogenetic protein 4. *Cell* **86**, 599-606.

Zrzavy, J., Mihulka, S., Kepka, P., Bezdek, A. and Tietz, D. (1998). Phylogeny of the metazoa based on morphology and 18S ribosomal DNA evidence. *Cladistics* **14**, **249-285**.

7 APPENDIX

7.1 Abbreviations

AP	alkaline phosphatase
A-P	anterior-posterior
BCIP	5-bromo-4-chloro-3-indolyl phosphate
BCNE	Blastula Chordin and Noggin Expression Center
BLAST	basic local alignment search tool
BMP	bone morphogenetic protein
bp	base pair
BSA	bovine serum albumin
cDNA	complementary DNA
CNS	central nervous system
CR	cysteine-rich
dATP	deoxyadenosine triphosphate
DC	direct current
dCTP	deoxycytidine triphosphate
dd	double distilled
DEPC	diethyl pyrocarbonate
dGTP	deoxyguanosine triphosphate
DIG	digoxigenin
DNA	deoxyribonucleic acid
DNase	deoxyribonuclease
dNTP	deoxyribonucleotide triphosphate
ddNTP	dideoxyribonucleotide triphosphate
Dpp	decapentaplegic
DTT	DL-Dithiothreitol
dTTP	deoxythymidine triphosphate
dUTP	deoxyuridine triphosphate

D-V	dorsal-ventral
EDTA	ethylenediaminetetraacetic acid
FGF	fibroblast growth factor
g	unit of acceleration due to the earth's gravity (9.806 65 m/s²)
GSK3β	glycogen synthase-kinase-3β
HCl	hydrochloric acid
HEPES	4-(2-Hydroxyethyl)piperazine-1-ethane sulfonic acid
kb	kilo base pairs
LiCl	lithium chloride
LEF	lymphocyte enhancer factor-1
M	molar
MCS	multiple cloning site
MgCl	magnesium chloride
M-MLV	Moloney Murine Leukemia Virus
mRNA	messenger RNA
NaOH	sodium hydroxyl solution
NBT	nitro blue tetrazolium chloride
OD	opitcal density
ORF	open reading frame
PCI	phenol:chloroform:isoamylalcohol
PCR	polymerase chain reaction
PFA	paraformaldehyde
QPCR	quantitative “real-time” PCR
RA	retinoic acid
RACE	rapid amplification of cDNA ends
RNA	ribonucleic acid
RNase	ribonuclease
rpm	rounds per minute
rRNA	ribosomal RNA
RT	room temperatur
SDS	sodium dodecyl sulfate

Shh	sonic hedgehog
Sog	Short Gastrulation
TCF	T-cell factor
TRIS	tris-(hydroxymethyl)-aminomethane
Tsg	Twisted Gastrulation
UTR	untranslated region
UV	ultraviolet
V	volt
WMISH	whole-mount *in situ* hybridization
X-Gal	bromo-4-chloro-indoxyl-ß-D-galactoside
Xnr	*Xenopus* nodal-related protein

7.2 Glossary

alecithal Having little or no yolk: an alecithal egg.

alignment Refers to the procedure of comparing two or more sequences by looking for a series of individual characters or character patterns that are in the same order in the sequences. Of the two types of alignment, local or global, a local alignment is generally the most useful.

animal pole The position on the oocyte and embryo in which the meiotic reduction divisions occur, and that will give rise to the anterior region of the adult body plan.

animal-vegetal axis The body axis in the oocyte and embryo that runs from the animal to the vegetal pole.

archenteron The primitive gut that forms during embryogenesis at gastrulation.

bilateral symmetry The presence of two similar sides with definite upper and lower surfaces, and anterior and posterior ends.

bilateria A phylogenetic subdivision of animals that is characterized by left-right symmetry along the primary body axis at some stage of the life cycle. They include acoelomorphs, protostomes and deuterostomes.

BLAST A computer program that identifies homologous (similar) genes in different organisms, such as human, fruit fly, or nematode.

blastoderm The layer of cells of the blastula.

blastomere An early embryonic cell that is derived from the cleavage of a fertilized egg.

blastopore The slit-like or circular invagination on the surface of animal embryos, through which the mesoderm and endoderm move inside the embryo at gastrulation.

blastula The stage of animal development that follows the early cleavage programme but precedes gastrulation.

bootstrap analysis A method for testing how well a particular dataset fits a model. For example, the validity of the branch arrangement in a predicted phylogenetic tree can be tested by resampling columns in a multiple sequence alignment to create many new alignments. The appearance of a particular branch in trees generated from these resampled sequences can then be measured.

branch length In sequence analysis the number of sequence changes along a particular branch of a phylogenetic tree.

cell autonomous If the activity of a gene has effects only in the cells that express it, its function is said to be cell autonomous; if it causes effects in cells other than (or in addition to) those expressing it, its function is cell non-autonomous.

clade A lineage of organisms or alleles that comprises an ancestor and all its descendants.

chordamesoderm The area of mesoderm that forms the notochord.

cnidarians Radially symmetrical animals that have sac-like bodies with only one opening. They include jellyfish, corals, hydra and anemones.

common-mediator Smad (co-Smad) A class of Smad proteins that forms hetero-oligomeric complexes with activated R-Smads, and appears essential for R-Smad function.

contig A set of clones that can be assembled into a linear order.

ctenophores Biradially symmetrical hermaphroditic solitary marine animals resembling jellyfishes having for locomotion eight rows of cilia arranged like teeth in a comb.

derived Evolved to a state that is distinct from the primitive condition.

deuterostome A bilaterian animal in which the mouth forms as a secondary opening, separate from the blastopore. Deuterostomes include chordates, hemichordates and echinoderms.

dipleurula-type larvae A deuterostome larval type with a perforated ciliary band.

direct development A developmental strategy in which embryogenesis generates a juvenile adult without the formation of an intervening larval form.

epiblast The outer layer of a blastula that gives rise to the ectoderm after gastrulation.

expect value (E) In a database similarity search, the probability that an alignment score as good as the one found between a query sequence and a database sequence would be found in as many comparisons between random sequences as was done to find the matching sequence.

gastrula The stage of animal development during which the formation of distinct germ layers occurs; that is, gastrulation.

gastrulation The process during which cells move from the outer regions of the embryo to the inside, to give rise to the endodermal (gut) and mesodermal (for example, muscle and blood) germ-layer derivatives; the cells that remain on the surface of the embryo give rise to the ectodermal derivatives (skin and nervous system).

holoblastic cleavage Cleavage in which the entire egg separates into individual blastomeres.

hypoblast The layer of the blastula that lies inside the embryo (differently used in amniote embryos).

inhibitory Smad (I-Smad) A class of Smad proteins that antagonizes the activity of the co-Smad/R-Smad complexes.

long-branch attraction bias An effect that can be observed when two distantly related sequences are grouped together in a phylogenetic analysis although the true topology supports a more distant grouping. This is due to convergent evolution in distantly related sequences, as even two random sequences would show up the same nucleotide in 1/4 of the sites. For random protein sequences the

number of identical positions would be 1/20 whereas the number of similar positions is certainly higher.

maximum parsimony The minimum number of evolutionary steps required to generate the observed variation in a set of sequences, as found by comparison of the number of steps in all possible phylogenetic trees.

maximum likelihood (phylogeny, alignment) The most likely outcome (tree or alignment), given a probabilistic model of evolutionary change in DNA sequences.

metazoan A multicellular animal.

neighbor-joining method Clusters alike pairs within a group of related objects (e.g. genes with similar sequences) to create a tree whose branches reflect the degrees of difference among the objects.

neurulation The process in which the ectoderm of the future brain and spinal cord develops folds and forms the neural tube.

neural crest Cells at the dorsal midline of the vertebrate neural tube, which undergo an epithelial-to-mesenchymal transition and migrate to many locations, contributing to the development of a wide variety of structures, including the peripheral nervous system and craniofacial features, therefore essentially enabling a second wave of development.

oral-aboral axis The body axis that runs from the oral side to the side that is opposite the oral. The term is used in animals that do not have an obvious anterior-posterior axis.

organizer A small dorsal region of the blastopore of a vertebrate gastrula-stage embryo that has a remarkable capacity to organize a complete embryonic body plan.

orthologs Genes in two organisms that share a common ancestor and originated by speciation.

outgroup taxon A closely related taxon that is used for comparison; for example, to infer the ancestral versus the derived state of character evolution.

paralogs Genes in the same organism that have evolved from gene duplication, usually with a subsequent, sometimes subtle, divergence of function.

paraxial mesoderm A subpopulation of the mesoderm that lies on both sides of the neural tube, which gives rise to the somites.

pharyngeal gill slits Perforations in the wall of the pharynx near the digestive tract. As fish develop, these slits give rise to gills, which in land-based vertebrates such as humans, they close and disappear.

protostome A bilaterian animal in which the mouth develops before the anus during embryogenesis. Protostomes include arthropods, molluscs and worms.

radial symmetry The presence of multiple planes of mirror symmetry running through the longitudinal axis.

receptor-mediated Smad (R-Smad) A class of Smad proteins that are phosphorylated and activated by different activated type I receptors for TGF-b family ligands.

somites Mesodermal balls of cells adjacent to the neural tube that will differentiate into the muscle, vertebrae and dermis.

stem group All fossils more closely related to a particular crown group than to any other, but more basal than its most basal member.

tail bud Located at the extreme posterior tip of the embryo the tail bud generates the posterior portions of the notochord, somites and neural tube during amphioxus and vertebrate development.

tornaria larva A hemichordate, acorn-worm larva with distinct ciliary bands.

vegetal pole The position in the oocyte and embryo which is on the opposite side of the animal pole and generally gives rise to the gut.